



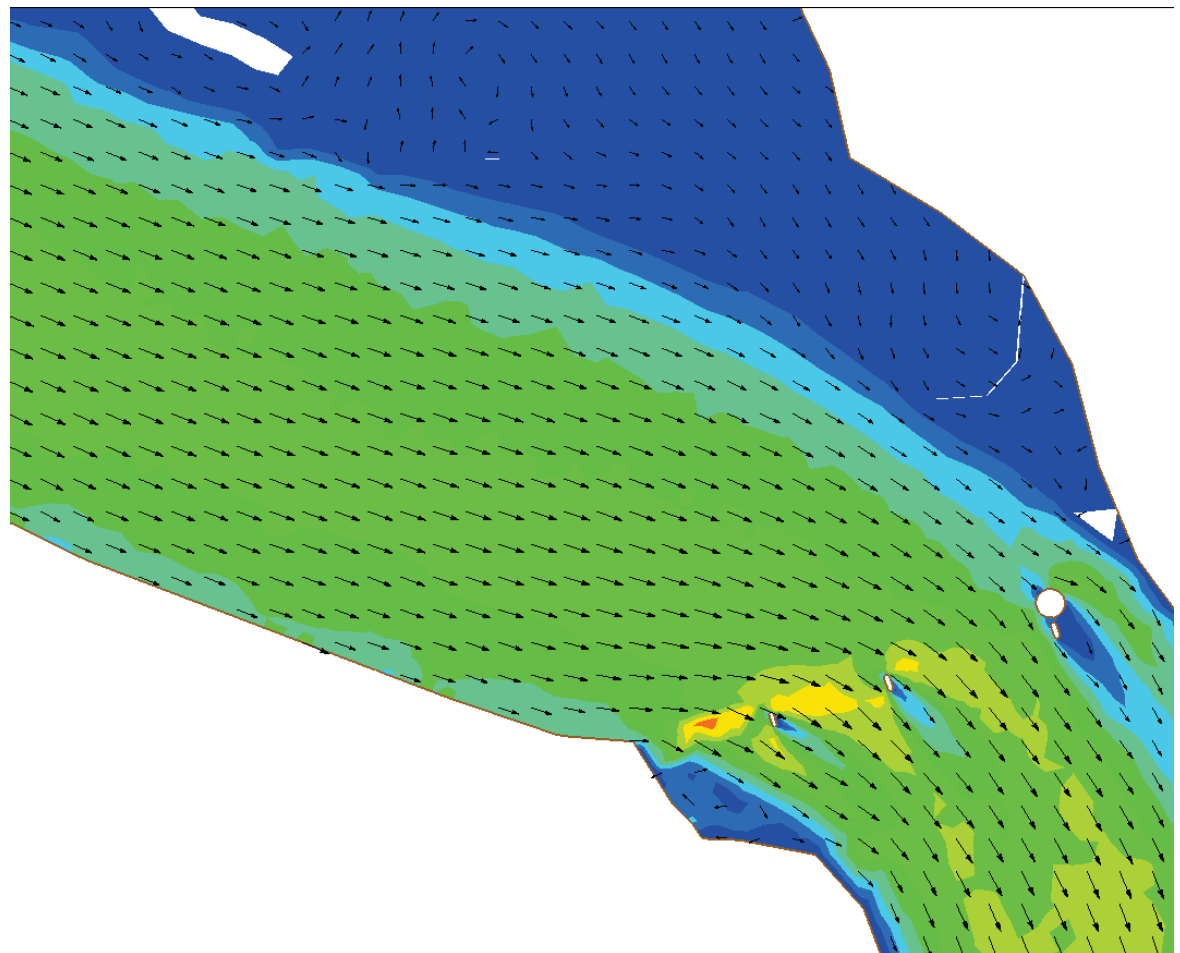
**US Army Corps
of Engineers®**
Engineer Research and
Development Center

ERDC
INNOVATIVE SOLUTIONS
for a safer, better world

Jackson Bar Training Structure Study

Jeremy A. Sharp and Steve H. Scott

May 2015



The US Army Engineer Research and Development Center (ERDC) solves the nation's toughest engineering and environmental challenges. ERDC develops innovative solutions in civil and military engineering, geospatial sciences, water resources, and environmental sciences for the Army, the Department of Defense, civilian agencies, and our nation's public good. Find out more at www.erdc.usace.army.mil.

To search for other technical reports published by ERDC, visit the ERDC online library at <http://acwc.sdp.sirsi.net/client/default>.

Jackson Bar Training Structure Study

Jeremy A. Sharp and Steve H. Scott

*Coastal and Hydraulics Laboratory
U.S. Army Engineer Research and Development Center
3909 Halls Ferry Road
Vicksburg, MS 39180-6199*

Final report

Approved for public release; distribution is unlimited.

Abstract

Three proposed alternatives intended to reduce shoaling at Jackson Bar, AL, were investigated. A two-dimensional hydrodynamic and sediment model was used to simulate hydraulic conditions at Jackson Bar, located on the Black Warrior-Tombigbee Waterway (BWT) in the vicinity of Jackson, AL. Jackson Bar, a sand bar, is located on the left descending bank upstream of a railroad bridge. Located in a bend in the BWT at Jackson, AL, the railroad bridge presents a navigation hazard. Annual dredging provides the clearance necessary for tows to properly align with the bridge pass. The hydrodynamic model was validated with gage data from the U.S. Geological Survey 02470050 Tombigbee River at Steamplant near Leroy, AL, gage (Leroy Gage), a previously constructed HEC-2 model, and a previously constructed WES physical model from 1987. Three alternatives were modeled in an attempt to reduce shoaling/eliminate dredging at Jackson Bar by using one or more river training structures (e.g., bendway weirs, dikes, kickers). A three-fold screening approach was applied to determine the feasibility of each alternative. The selected alternative was a variation of Plan D that used a kicker and transverse dikes.

DISCLAIMER: The contents of this report are not to be used for advertising, publication, or promotional purposes. Citation of trade names does not constitute an official endorsement or approval of the use of such commercial products. All product names and trademarks cited are the property of their respective owners. The findings of this report are not to be construed as an official Department of the Army position unless so designated by other authorized documents.

DESTROY THIS REPORT WHEN NO LONGER NEEDED. DO NOT RETURN IT TO THE ORIGINATOR.

Contents

Abstract	ii
Figures and Tables.....	v
Preface	ix
Unit Conversion Factors	x
1 Introduction.....	1
2 Background.....	4
2.1 Navigation	4
2.2 Dredging.....	4
2.3 1987 Physical model study.....	6
3 Field Data	8
4 Modeling Approach	13
5 Model Development	15
5.1 Boundary Conditions	15
5.1.1 Hydrodynamic.....	15
5.1.2 Sediment load	16
5.2 Mesh construction	19
5.2.1 Bathymetry data.....	19
5.2.2 Mesh materials	19
5.2.3 Upstream and downstream limits.....	21
5.2.4 Bed gradation.....	21
5.3 Implementation of AEC Power Plant.....	22
6 Validation	24
6.1 Leroy Gage	24
6.2 Model-to-model comparison	25
6.2.1 HEC-2 slope	27
6.2.2 1987 WES physical model (PM).....	31
6.3 Sediment validation.....	35
6.4 Comparison of the AEC Power Plant existing conditions model	35
7 Alternatives	41
7.1 Plan B	41
7.2 Plan C	43
7.3 Plan D	44
7.4 Additional plans	45

8 Results	47
8.1 Existing conditions models	47
8.1.1 <i>Existing conditions model</i>	47
8.1.2 <i>AEC existing conditions model</i>	47
8.2 Plan B	51
8.3 Plan C	58
8.4 Plan D	65
8.5 Plan D AEC Power Plant.....	70
8.6 Deposition at AEC Power Plant	78
9 Discussion	80
9.1 Plan B	81
9.2 Plan C	82
9.3 Plan D	83
9.4 Plan D AEC Power Plant variation	84
9.5 Alternative selection	85
9.5.1 <i>Dredging</i>	85
9.5.2 <i>Velocity</i>	85
9.5.3 <i>Volume of rock for each plan</i>	86
10 Recommendations.....	87
10.1 Recommended alternative implementation.....	87
10.2 Future analysis.....	87
10.3 Monitoring.....	88
10.4 Concerns	88
References	89
Appendix	91

Report Documentation Page

Figures and Tables

Figures

Figure 1. Site and vicinity map for Jackson Bar, AL	1
Figure 2. November 2003 dredge cut at Jackson Bar, with RM shown in black.	2
Figure 3. Tow sail lines relative to the Norfolk Southern railroad bridge piers near Jackson, AL.....	5
Figure 4. Left pier, cell, and fender structure intended to protect against vessel impacts, looking upstream at the Norfolk Southern railroad bridge near Jackson, AL.....	5
Figure 5. 1983–2012 dredging data for Jackson Bar, AL.....	6
Figure 6. 1987 WES physical model study of the Jackson Bar Reach.....	7
Figure 7. Upstream location of field samples collected from the bed.....	8
Figure 8. Midreach location of field samples collected from the bed.....	9
Figure 9. Downstream location of field samples collected from the bed.....	10
Figure 10. Bed sample gradations for sample locations in the vicinity of Jackson Bar, AL, on 11 November 2012.....	11
Figure 11. Location of river gages and Jackson Bar near site, Jackson, AL	16
Figure 12. Discharge at the Coffeeville Gage and gage height at the Leroy Gage for 20 November 2003–11 May 2004.	17
Figure 13. Coffeeville Gage flood frequency curve.....	17
Figure 14. Estimated total sand concentration as a function of discharge at the Coffeeville Gage for 20 November 2003–11 May 2004.	18
Figure 15. Estimated total silt concentration as a function of discharge at the Coffeeville Gage for 20 November 2003–11 May 2004.	18
Figure 16. Material number and location for the Jackson Bar 2004 existing-conditions model.	20
Figure 17. Collected sample bed gradations (11 November 2012) compared to model input gradation in the Jackson Bar vicinity.	22
Figure 18. AEC Power Plant existing conditions model with the six mooring cells for the AEC loading terminal near Jackson, AL	23
Figure 19. Validation plot of Leroy field data vs. simulated data, 172-day hydrograph.	25
Figure 20. Simulated base data vs. Leroy Gage field data, 172-day hydrograph.	25
Figure 21. Cross-section comparison between the AdH and 1987 WES PM bathymetry 573 ft upstream of the Norfolk Southern railroad bridge.	26
Figure 22. Cross-section comparison between the AdH model and 1987 WES PM bathymetry 2,610 feet upstream of the Norfolk Southern railroad bridge.	27
Figure 23. HEC-2 and AdH frequency profile for 20,000 ft ³ /sec.	28
Figure 24. HEC-2 and AdH frequency profile for 40,000 ft ³ /sec.....	29
Figure 25. HEC-2 and AdH frequency profile for 60,000 ft ³ /sec.....	29
Figure 26. HEC-2 and AdH frequency profile for 60,000 ft ³ /sec.	30
Figure 27. HEC 2 slopes compared to AdH slopes.	31
Figure 28. Conveyance potential for normal depth in AdH and the 1987 WES PM.	32

Figure 29. 20,000 ft ³ /sec flow comparison for the AdH model and the 1987 WES PM.	33
Figure 30. 40,000 ft ³ /sec flow comparison for the AdH model and the 1987 WES PM.	33
Figure 31. 60,000 ft ³ /sec flow comparison for the AdH model and the 1987 WES PM.	34
Figure 32. 100,000 ft ³ /sec flow comparison for the AdH model and the 1987 WES PM.	34
Figure 33. 140,000 ft ³ /sec flow comparison for the AdH model and the 1987 WES PM.	35
Figure 34. Temporal accumulation of deposition in the 2004 dredge cut in the Jackson Bar, AL, vicinity.	36
Figure 35. Flux line locations in the model.	37
Figure 36. Flux downstream of Norfolk Southern railroad bridge.	38
Figure 37. Existing conditions minus AEC existing conditions velocity during the peak hydrograph flow at day 87 (red: AEC less; blue: AEC more).	39
Figure 38. Bed shear AEC existing conditions minus existing conditions (red: AEC more; blue: AEC less).	40
Figure 39. Plan B bathymetry with training structure alignment and channel layout.	42
Figure 40. Plan C bathymetry with training structure alignment and channel layout.	43
Figure 41. Plan D bathymetry with training structure alignment and channel layout.	45
Figure 42. Existing conditions deposition (feet) at the end of the simulation, Jackson Bar.	48
Figure 43. Existing conditions velocities (feet/second) at peak flow, day 87.	48
Figure 44. Existing conditions maximum bed shear stress, in pascals.	49
Figure 45. AEC existing conditions deposition (feet) at the end of the hydrograph, Jackson Bar.	49
Figure 46. AEC existing conditions velocities (feet/second) at peak flow, day 87.	50
Figure 47. AEC existing conditions maximum bed shear stress, in pascals.	50
Figure 48. Plan B_2 deposition (feet) at the end of the simulation.	51
Figure 49. Plan B_3 deposition (feet) at the end of the simulation.	52
Figure 50. Plan B_4 deposition (feet) at the end of the simulation.	52
Figure 51. Plan B deposition (feet) at the end of the simulation.	53
Figure 52. Deposition in dredge cut vs. structure elevation for Plan B alternatives.	53
Figure 53. Velocity comparisons for Plan B at the Norfolk Southern railroad bridge.	54
Figure 54. Velocity comparisons for Plan B, 2,000 ft upstream of the Norfolk Southern railroad bridge.	54
Figure 55. Plan B_2 minus existing conditions, velocity difference, feet/second (red: Plan B_2 higher; blue: Plan B_2 lower).	55
Figure 56. Plan B_3 minus existing conditions, velocity difference, feet/second (red: Plan B_3 higher; blue: Plan B_3 lower).	55
Figure 57. Plan B_4 minus existing conditions, velocity difference, feet/second (red: Plan B_4 higher; blue: Plan B_4 lower).	56
Figure 58. Plan B minus existing conditions, velocity difference, feet/second (red: Plan B higher; blue: Plan B lower).	56
Figure 59. Plan C deposition (feet) at the end of the simulation.	58
Figure 60. Plan C_4 deposition (feet) at the end of the simulation.	59
Figure 61. Plan C_3 deposition (feet) at the end of the simulation.	59
Figure 62. Plan C Kicker deposition (feet) at the end of the simulation.	60

Figure 63. Deposition in dredge cut vs. structure elevation for Plan C alternatives.....	60
Figure 64. Velocity comparisons for Plan C at the Norfolk Southern railroad bridge.....	61
Figure 65. Velocity comparisons for Plan C, 2,000 ft upstream of the Norfolk Southern railroad bridge.....	61
Figure 66. Plan C minus existing conditions, velocity difference, feet/second (red: Plan C higher; blue: Plan C lower).....	62
Figure 67. Plan C_3 minus existing conditions, velocity difference, feet/second (red: Plan C_3 higher; blue: Plan C_3 lower).....	62
Figure 68. Plan C_4 minus existing conditions, velocity difference, feet/second (red: Plan C_4 higher; blue: Plan C_4 lower).....	63
Figure 69. Plan C Kicker minus existing conditions, velocity difference, feet/second (red: Plan C higher; blue: Plan C lower).....	63
Figure 70. Plan D deposition (feet) at the end of the simulation.....	65
Figure 71. Plan D Kicker deposition (feet) at the end of the simulation.....	66
Figure 72. Velocity comparisons for Plan D at the Norfolk Southern railroad bridge.....	66
Figure 73. Plan D, 3,000 ft upstream of the Norfolk Southern railroad bridge.....	67
Figure 74. Plan D minus existing conditions, velocity difference, feet/second (red: Plan D higher; blue: Plan D lower).....	67
Figure 75. Plan D Kicker minus existing conditions, velocity difference, feet/second (red: Plan D Kicker higher; blue: Plan D Kicker lower).....	68
Figure 76. Maximum bed shear for Plan D minus existing conditions, pascals (red: Plan D higher; blue: Plan D lower).....	69
Figure 77. Maximum bed shear for Plan D Kicker minus existing conditions, pascals (red: Plan D Kicker higher; blue: Plan D Kicker lower).....	70
Figure 78. Plan D Power Plant deposition (feet) at the end of the simulation.....	71
Figure 79. Plan D 50% Dike Downstream Dike Power Plant deposition (feet) at the end of the simulation.....	72
Figure 80. Plan D Kicker Downstream Dike Power Plant deposition (feet) at the end of the simulation.....	72
Figure 81. Velocity comparisons for Plan D Power Plant at the Norfolk Southern railroad bridge.....	73
Figure 82. Velocity comparison for Plan D Power Plant, 3,000 ft upstream of the Norfolk Southern railroad bridge.....	73
Figure 83. Plan D Power Plant minus AEC existing conditions, feet/second (red: Plan D higher; blue: Plan D lower).....	74
Figure 84. Plan D 50% Dike Downstream Dike Power Plant minus AEC existing conditions, feet/second (red: Plan D higher; blue: Plan D lower).....	74
Figure 85. Plan D Kicker Downstream Dike Power Plant minus AEC existing conditions, feet/second (red: Plan D higher, blue: Plan D lower).....	75
Figure 86. Maximum bed shear for Plan D Power Plant minus AEC existing conditions, pascals (red: Plan D higher; blue: Plan D lower).....	76
Figure 87. Maximum bed shear for Plan D 50% Dike DS Dike Power Plant minus AEC existing conditions, pascals (red: Plan D higher; blue: Plan D lower).....	77
Figure 88. Maximum bed shear for Plan D Kicker DS Dike Power Plant minus AEC existing conditions, pascals (red: Plan D higher; blue: Plan D lower).....	77

Figure 89. AEC Power Plant deposition footprint (dark-blue rectangle).....	78
Figure 90. Typical deposition (feet) pattern around AEC terminal, Plan D Kicker DS Dike (red is deposition; blue is erosion).....	79
Figure 91. Percent reduction in dredging for all alternatives.	81
Figure 92. Average velocity increase above the existing conditions models.	81
Figure 93. Final recommended alternative, Plan D with the 50%-length transverse dikes.	91

Tables

Table 1. Sieve stack sizes for all bed samples taken in the vicinity of Jackson Bar, AL, on 11 November 2012.	10
Table 2. Estimated sand fraction concentration as a function of grain size and flow at the Coffeyville Gage for 20 November 2003–11 May 2004.	19
Table 3. Prescribed Manning's number for materials in the AdH models of the Jackson Bar vicinity.	21
Table 4. Statistical analysis comparison of HEC-2 and AdH model.	28
Table 5. Statistical analysis of the comparison of velocity along the thalweg between the 1987 WES PM and the AdH model....	32
Table 6. Alternative plan descriptions.	46
Table 7. Statistical analysis of velocity, in feet per second, for Plan B alternatives minus existing conditions.....	57
Table 8. Statistical analysis of velocity, in feet per second, for Plan C alternatives minus existing conditions.....	64
Table 9. Statistical analysis of velocity, in feet per second, for Plan D alternatives minus existing conditions.....	68
Table 10. Statistical analysis of velocity, in feet per second, for Plan D Power Plant alternatives minus AEC existing conditions.	75
Table 11. Deposition volumes and percent increases for the deposition footprint at the AEC power plant.	79
Table 12. Alternative deposition in dredge cut comparison.....	80
Table 13. Training structure volumes of rock.	86

Preface

This study was conducted for the U.S. Army Engineer District, Mobile (SAM), under project identification Training Structure Study for Jackson Bar. The technical monitors were Wade A. Ross and Thomas J. Beckham.

The work was performed by the River Engineering Branch of the Flood and Storm Protection Division, U.S. Army Engineer Research and Development Center (ERDC), Coastal and Hydraulics Laboratory (CHL). At the time of publication, Dr. Loren L. Wehmeyer was Chief of the River Engineering Branch; Dr. Ty V. Wamsley was Chief of the Flood and Storm Protection Division. The Deputy Director of CHL was Dr. Kevin Barry, and the Director of CHL was José E. Sánchez.

LTC John T. Tucker III was the Acting Commander of ERDC, and Dr. Jeffery P. Holland was the Director.

Unit Conversion Factors

Multiply	By	To Obtain
cubic feet	0.02831685	cubic meters
cubic yards	0.7645549	cubic meters
feet	0.3048	meters
foot-pounds force	1.355818	joules
gallons (U.S. liquid)	3.785412 E-03	cubic meters
inches	0.0254	meters
miles (nautical)	1,852	meters
miles (U.S. statute)	1,609.347	meters
pounds (force) per square foot	47.88026	pascals
tons (2,000 pounds, mass)	907.1847	kilograms
tons (2,000 pounds, mass) per square foot	9,764.856	kilograms per square meter
yards	0.9144	meters

1 Introduction

The report summarizes work performed by ERDC for SAM. The purpose of the study is to test three proposed alternatives that are intended to reduce shoaling/eliminate dredging at Jackson Bar. A two-dimensional (2D) hydrodynamic and sediment model was applied to investigate three alternatives. The model simulated hydraulic conditions at Jackson Bar, located on the Black Warrior-Tombigbee Waterway (BWT) in the vicinity of Jackson, AL. Jackson Bar, a sand bar, is located on the left descending bank southwest of Jackson, AL, and upstream of the Norfolk Southern railroad bridge (Figure 1). The railroad bridge is located in the Jackson bend, river mile (RM) 90. Navigation of this section is hazardous due to the location of the bridge relative to the bend and the accreting sand bar upstream (U.S. Army Corps of Engineers (USACE), SAM 1988).

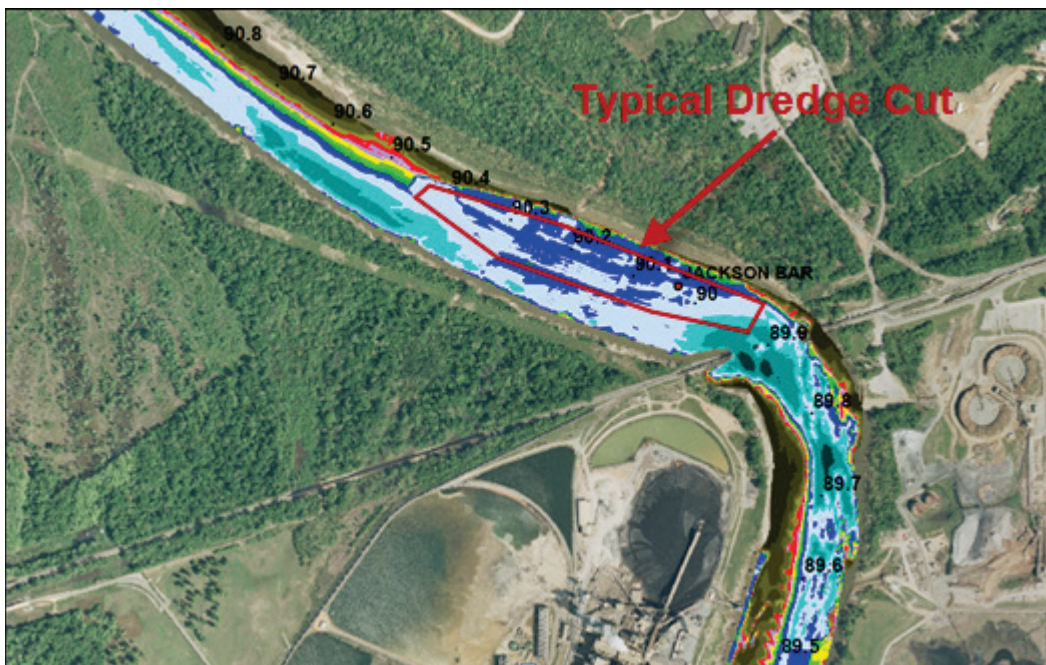
Figure 1. Site and vicinity map for Jackson Bar, AL.



Investigations performed to date have not conclusively identified plausible/realistic shoaling mitigation measures for application by SAM in the vicinity of Jackson Bar. Thus, annual dredging has been required to maintain navigation on the BWT in the vicinity of Jackson, AL. Dredging (see Figure 2 for a typical dredge cut) is becoming less favorable as a mitigation means due to three issues: disposal of material, thalweg realignment, and navigation clearance. Material is disposed in either an upland facility or in-channel. The upland facility is 1.3 miles upstream of the bridge on the right bank, requiring dredge pipe to cross the navigation

channel. Disposing in-channel, located 0.6 miles upstream of the bridge, raises the potential for recycling of the dredged material. Furthermore, in-channel disposal on the left bank accelerates the deposition on the downstream left bank. The increase in shoaling is due in part to the in-channel dredge material placement that forces the thalweg to the right bank and increases bank loss. Additionally, during dredging operations, the dredge blocks a portion of the navigation channel causing navigation complications and temporary stoppages in dredging. Fundamentally, a realignment of the thalweg is necessary to maintain usability of the channel while reducing dredging and bank loss.

Figure 2. November 2003 dredge cut at Jackson Bar, with RM shown in black.



The 2D model simulated proposed training structures intended to adjust the alignment of the thalweg. Ideally, the thalweg would be moved towards the left side of the channel, increasing bed shear stress along the Jackson Bar. The increased forcing on the bed would mobilize material that typically deposits on Jackson Bar and transport it downstream.

The numerical code applied for the study, Adaptive Hydraulics (AdH), was developed at ERDC. The AdH code can describe both saturated and unsaturated groundwater, overland flow, three-dimensional (3D) Navier-Stokes, 3D shallow water, and 2D shallow water problems (Berger et al. 2010). It can be used in a serial or multiprocessor mode on multiple platforms. AdH has the capability to dynamically refine the domain mesh in

areas where more resolution is needed at certain times due to changes in the flow or transported constituent conditions. AdH can simulate sediment transport that is coupled to bed and hydrodynamic changes. The sediment transport computations are computed in the sediment library (SEDlib) of AdH. The ability of AdH to allow the domain to wet and dry as flow conditions or tides change is suitable for shallow marsh environments, beach slopes, floodplains, etc. Supercritical and subcritical flows can be represented at the model boundaries as well as internal to the system. AdH can simulate vessel transport, bridge decks, and culvert entrances as pressure field applications. The model is being developed at CHL and has been used to model hydrodynamics in sections of the Mississippi River, tidal conditions in southern California, and vessel traffic in the Houston Ship Channel among others (Stockstill and Vaughan 2009; Stockstill et al. 2010; Martin et al. 2011; Tate et al. 2010). The code is designed to work in conjunction with the Surface Water Modeling System (SMS), a modeling package for building models, running simulations, and visualizing results.

2 Background

2.1 Navigation

Located in a bend in the BWT near Jackson, AL, the Norfolk Southern railroad bridge presents a navigation hazard. Bridges should not be located in bends (American Society of Civil Engineers 1998). In order to safely navigate the bend, down-bound tows must favor the left bank and often require a flanking maneuver to properly align with the bridge pass. Annual dredging provides the clearance that allows for tows to properly align with the bridge pass. Without annual dredging, reduction in draft, or a reduced tow configuration, the bridge pass would be un-navigable. For further complication, the bridge piers are poorly aligned with the pass. Piers are generally parallel to the flow field. Here the piers are out of alignment to the upstream current by 53° and are 20° out of alignment to the downstream current. The bridge misalignment coupled with the bridge/river bend location produces a hazardous navigation pass.

Ideally, the sail line through the pass would follow the thalweg as denoted by the red line Approximate Ideal Sail Line plotted in Figure 3. However, in the present bridge configuration, the tow would not clear the center pier. The present sail line is denoted by the blue line in Figure 3 and is called the Approximate Required Sail Line. This line allows for the proper clearance as tows pass the bridge. Under normal flow conditions, the maneuver is difficult; however, with high flow conditions, the difficulty increases substantially. Thus, SAM has protected the left-most pier with a protective cell upstream and a fender structure that encompasses the pier and ties into the cell (Figure 4).

2.2 Dredging

The Jackson Bar reach is one of the most dredged reaches on the BWT. Recurring dredging is required to mitigate the accretion of the bar into the navigation channel. The annual volume of dredging over the past 30 years (yr) has averaged approximately 144,000 cubic yards (yd^3) with only 3 yr where no dredging was conducted (1988, 2007, 2008) (Figure 5). Because it was similar to the average annual dredging volume from 1983–2012 and similar to annual dredging values throughout the late 1990s and 2000s, the year 2004 (145,084 yd^3) was selected as the representative period for simulation.

Figure 3. Tow sail lines relative to the Norfolk Southern railroad bridge piers near Jackson, AL.

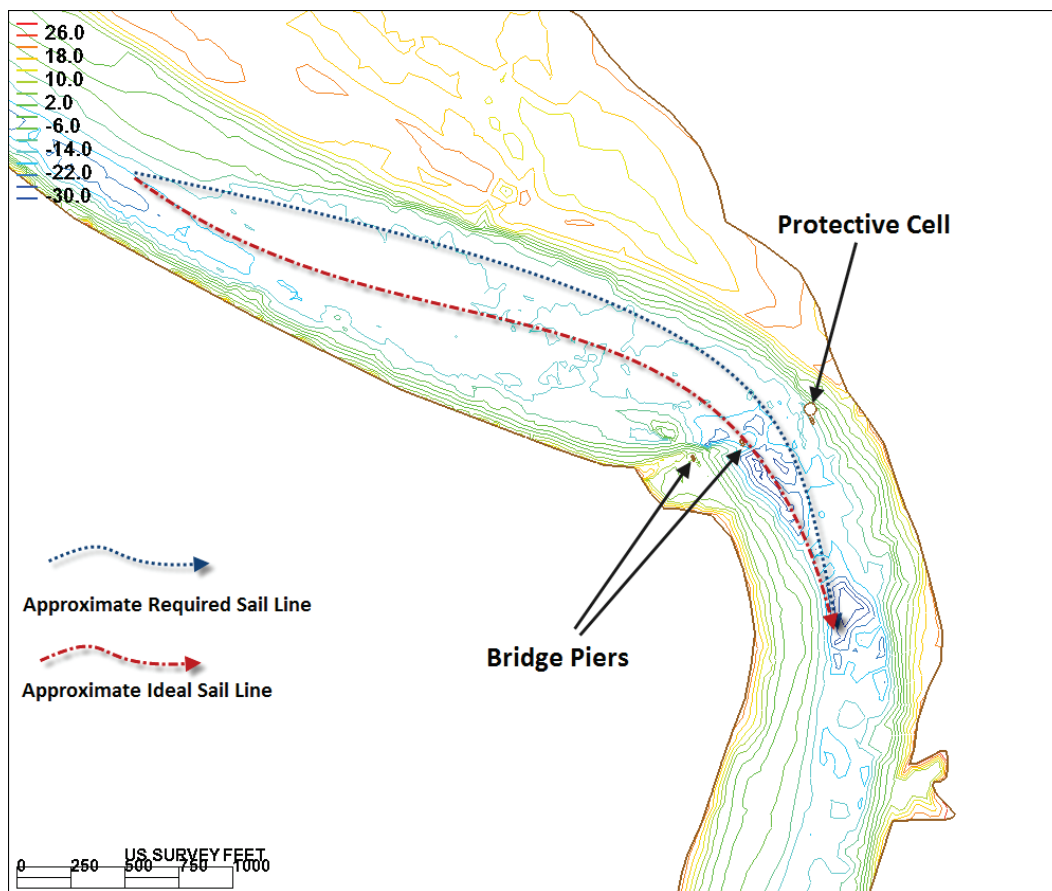
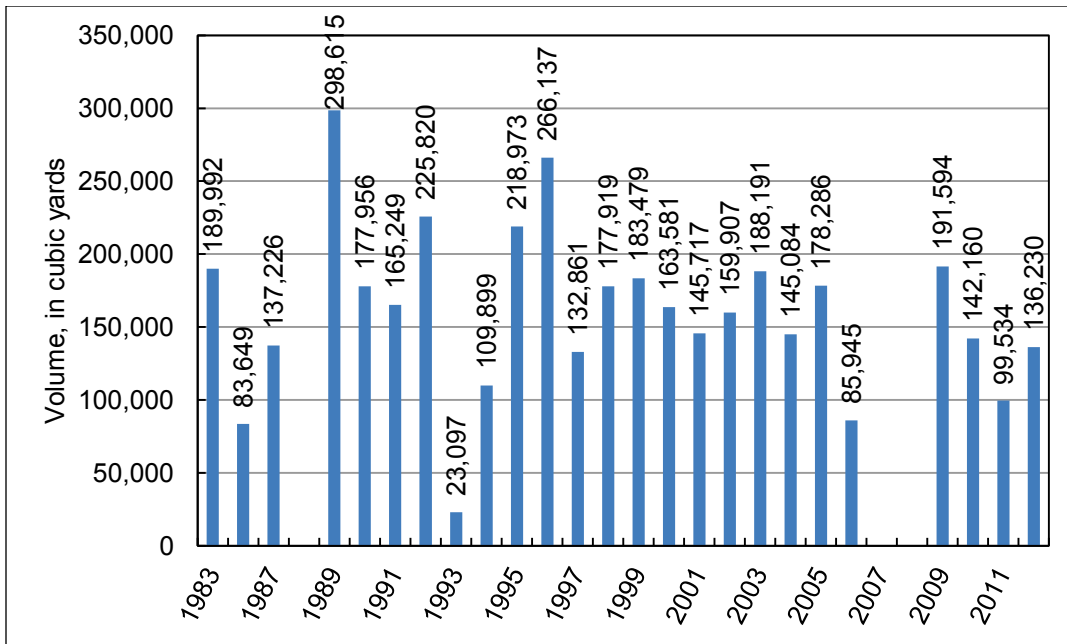


Figure 4. Left pier, cell, and fender structure intended to protect against vessel impacts, looking upstream at the Norfolk Southern railroad bridge near Jackson, AL.



Figure 5. 1983–2012 dredging data for Jackson Bar, AL.



2.3 1987 Physical model study

In January 1987, alternative channel alignments were analyzed with a physical model. The ERDC CHL (formerly Waterways Experiment Station (WES)), collaborated with SAM to analyze solutions for bridge alignment and dredging at Jackson Bar. A 1:100 scale physical model was constructed to determine the navigability of the alternative channel alignment (Figure 6). The model domain extended from RM 89.5 to 91.5 and was constructed using a 1984 bank-to-bank survey along with topographical maps for the overbank. Five river alternatives were analyzed. Each alternative evaluated realignment and training structure options.

Hydraulic conditions were simulated with flows of 20,000, 40,000, 60,000, 100,000, and 140,000 cubic feet per second (ft³/sec). The water surface elevation (WSE) for the tested flows was determined from a HEC-2 backwater model (USACE, SAM 1988). The design vessel was a six-barge, fully loaded tow. The effort showed realignment of the channel would improve navigation over the present conditions (USACE, SAM 1988). However, it proved to be too costly, and bridge protection was selected using a fender and cell on the left pier. For the purpose of this study, the physical model data were used as one aspect of the AdH model validation.

Figure 6. 1987 WES physical model study of the Jackson Bar Reach.



3 Field Data

A field data collection effort was conducted 11 November 2012. Bed samples were collected along the left and right descending bank and thalweg (Figures 7–9). Samples were collected with a grab bucket or a clam shell sampler. A total of eight transects were sampled. At each transect, three samples were collected. Additionally, a general site reconnaissance was conducted. Key system features were documented along with additional sediment samples from the in-channel disposal and the confined disposal facility (CDF).

Figure 7. Upstream location of field samples collected from the bed.

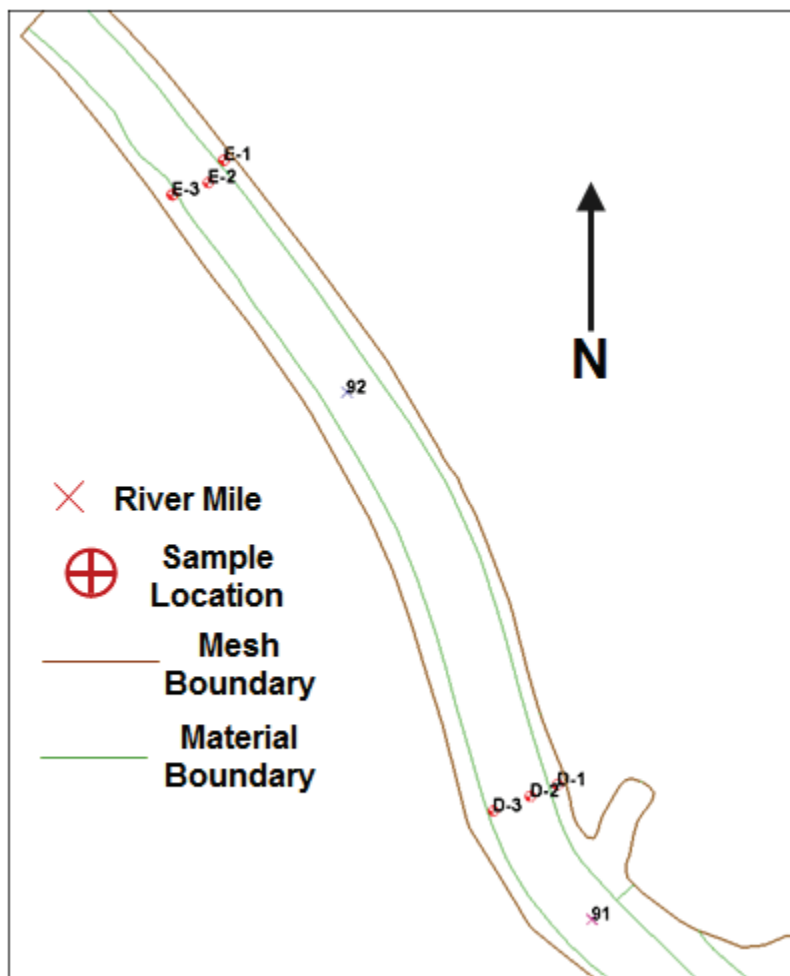
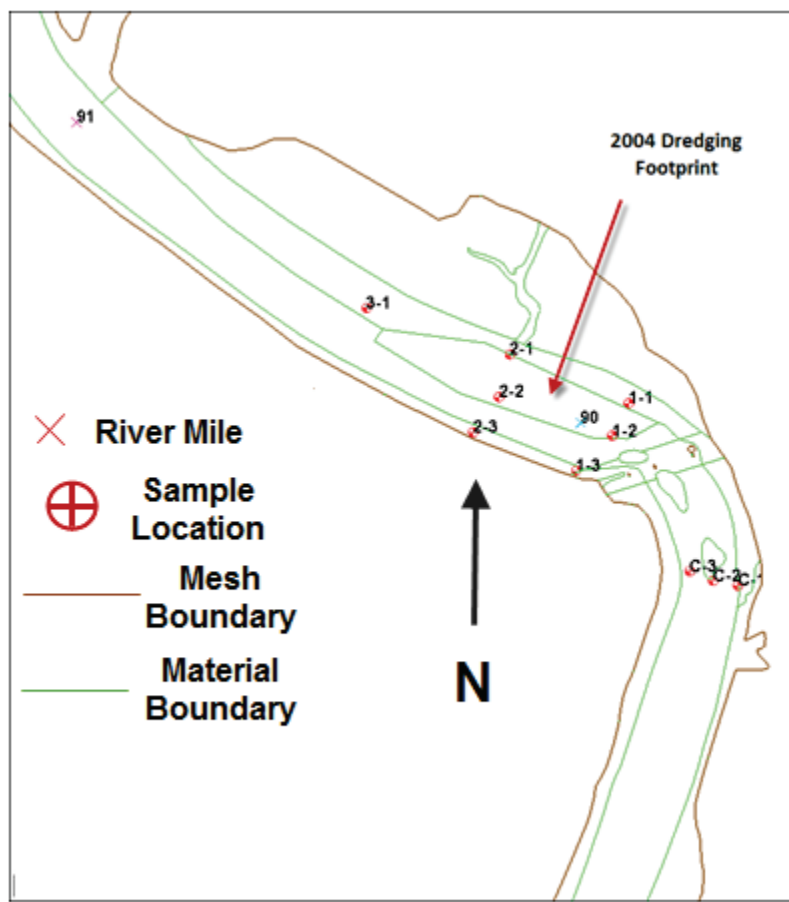


Figure 8. Midreach location of field samples collected from the bed.



Two characters identify the samples (Figures 7–9). The first character is either a letter or number. Those with letters are transects outside the dredged reach; conversely, the ones with numbers are within the dredged reach. The second character, always a number, indicates the location along the transect where the sample was taken. Numbers 1, 2, and 3 are located left bank, thalweg, and right bank, respectively. At some locations, no sample was collected due to a hard bottom. These locations yielded little bed material and are E-2, D-2, and C-2.

All bed samples were sieved to determine the material gradation (Table 1). Samples were dried prior to sieving and passed through a stack of nine sieves. Gradation curves, percent finer vs. grain size, were constructed (Figure 10). These samples provided the data necessary to define the bed composition.

Figure 9. Downstream location of field samples collected from the bed.

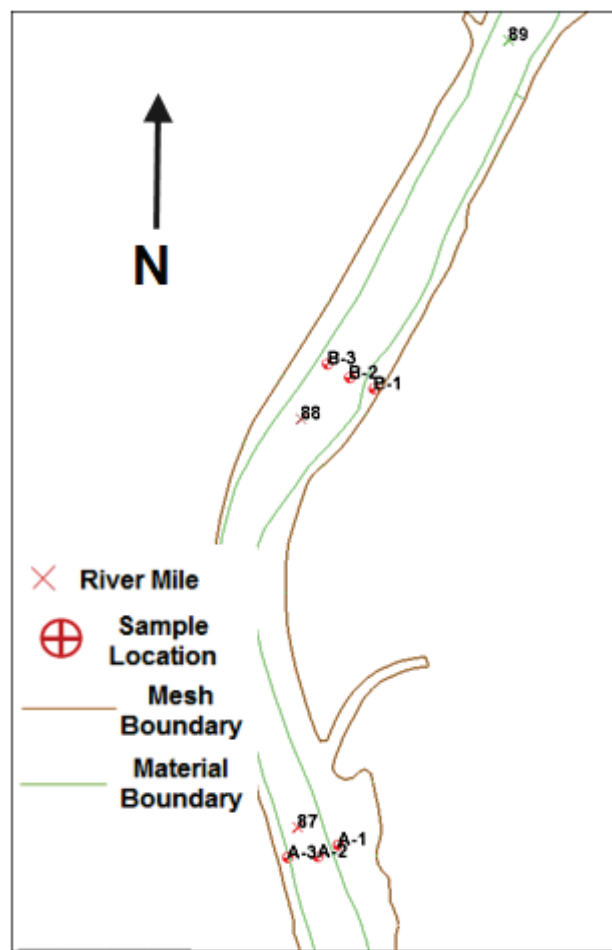
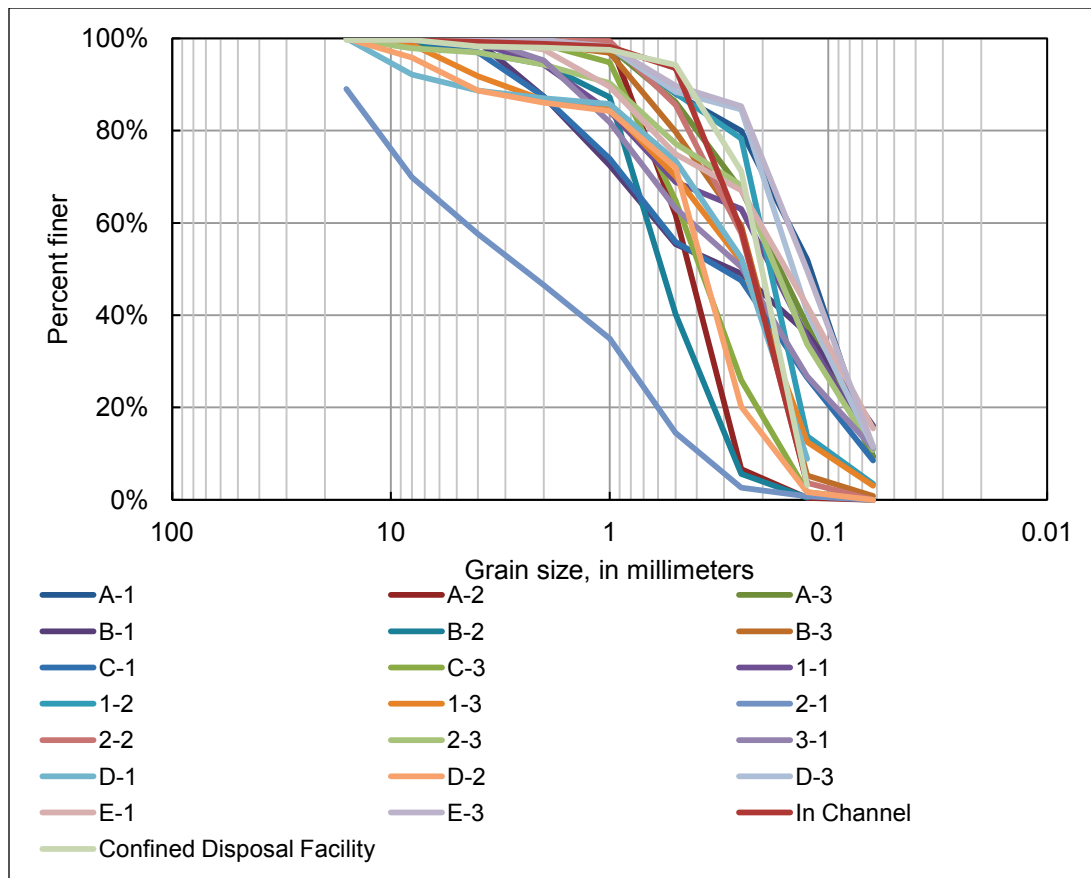


Table 1. Sieve stack sizes for all bed samples taken in the vicinity of Jackson Bar, AL, on 11 November 2012.

Sieve Size	
American Society for Testing and Materials (ASTM)	millimeters
5/8"	16
5/16"	8
5	4
10	2
18	1
35	0.5
60	0.25
120	0.125
230	0.0625
Pan (<120)	(<0.125)

Figure 10. Bed sample gradations for sample locations in the vicinity of Jackson Bar, AL, on 11 November 2012.



Relative to each other, the bed samples are closely graded with the exception of sample 2-1. Excluding sample 2-1 from the following analysis, the D₅₀ for the remaining samples ranged from 0.13–0.6 millimeters (mm). For four of these samples, the D₅₀ is classified as a medium sand while the remaining samples are classified as fine sand (Julien 2002). The D₁₀ is also a narrow range, ranging from 0.27–0.055 mm. Classified as a medium sand to course silt range (Julien 2002). Additionally, the D₉₀ ranges from 4–0.4 mm, which is a classification of fine gravel to medium sand. The narrow range of the D₉₀, D₅₀, and D₁₀ values was considered to indicate a well-graded group of samples. Thus, the gradation of the channel both longitudinally and laterally is near uniform for this reach of the river.

Sample 2-1 is the coarsest in the group of samples. It is located near center left bank of the 2004 dredge cut. The characteristics of the sample are directly related to the source of material. Located at the sample point exists a confluence of the BWT and a storm water runoff ditch from the city of Jackson. The storm water ditch passes through an abandoned

gravel pit, picking up gravel-size material and depositing it in the Jackson Bar. This sample does not represent the rest of the river, but due to the location and its coarser gradation, it presents a source for armoring Jackson Bar by creating a scour-resistant bed form.

4 Modeling Approach

The 2D models were developed with the AdH code to provide velocities, bed shear, and shoaling patterns/volumes to evaluate the effect of recommended training structures. AdH is a tool to formulate a recommended plan for training structures that will reduce shoaling at Jackson Bar. Existing conditions and three alternative plans at 100% build-out were modeled. The four simulations are the base simulations. These were a starting point from which individual structures of each alternative plan were later isolated in a separate simulation in order to identify the benefit of each structure. Thus, a total of 15 simulations were made including the 4 base simulations. Every model simulates both hydrodynamics and sediment with the same boundary conditions. The four base models represent the basic requirements necessary to show the existing shoaling and the appropriately sized structures to move the shoal.

The first base model represents the 2004 conditions and is the existing conditions model. The existing condition model is used to validate and confirm the model's formulation and domain. With limited field and historic data in the vicinity of the domain, the validation process relied on previous model studies, a HEC-2 model and the 1987 WES physical model (USACE, SAM 1988), and data from the USGS 02470050 Tombigbee River at Steamplant near Leroy, AL, gage (Leroy Gage). While not ideal, the approach was the only time- and cost-efficient means of validation. However, this does not mean that the AdH model matches the older models; rather, the authors believe that it provides sufficient evidence that the AdH model is behaving appropriately.

The remaining three base models simulated alternatives developed by ERDC CHL and SAM staff. These three models represent the 100% build-out of the structures. The 100% build-out configuration is based on the anticipated structure requirement to eliminate dredging in the 2004 Jackson Bar cut. The model bathymetry for the three base models was altered from the 2004 conditions base model to simulate the proposed dikes and bendway weir configurations. All other inputs remained the same. A complete description of all the alternatives simulated is provided in Chapter 7.

An additional evaluation of potential shoaling was conducted 4,000 ft downstream of the Norfolk Southern railroad bridge at the Alabama Electric Cooperative (AEC) power plant. The AEC power plant is located on the right bank with the power plant's waterway receiving facility. Here, coal is removed from barges to fire the plant. Analysis of the terminal required an additional existing conditions model along with a new 100% alternative model adding two more models to the four base models. Also constructed, along with the two new base models, were two models that simulated various levels of completeness from the 100% alternative model. All 13 alternative models provided an avenue of assessment for the proposed solution. Comparison between the two existing conditions models and the 13 alternative models yielded a qualitative and quantitative means of evaluating measures to reduce shoaling in the model at Jackson Bar.

5 Model Development

Model development is the numerical construction of the domain and its key features. The model is developed from several sources of data. Most of the data were provided by SAM, including bathymetry, topography, aerial imagery, bridge placement, and dredging data. For the sediment portion of the model, bed samples were collected.

Metric units are required for AdH sediment modeling. Thus, all provided SAM data were converted to metric and all 15 model outputs were generated in metric units. However, for reporting purposes, and at the request of SAM, model data were converted to United States customary units with the exception of bed shear (bed shear is most commonly reported in pascals). For model input, the horizontal geo-referenced datum was North American Datum (NAD) 1983 State Plane Alabama West Meters, and the vertical datum was National Geodetic Vertical Datum (NGVD) 1929 Meters.

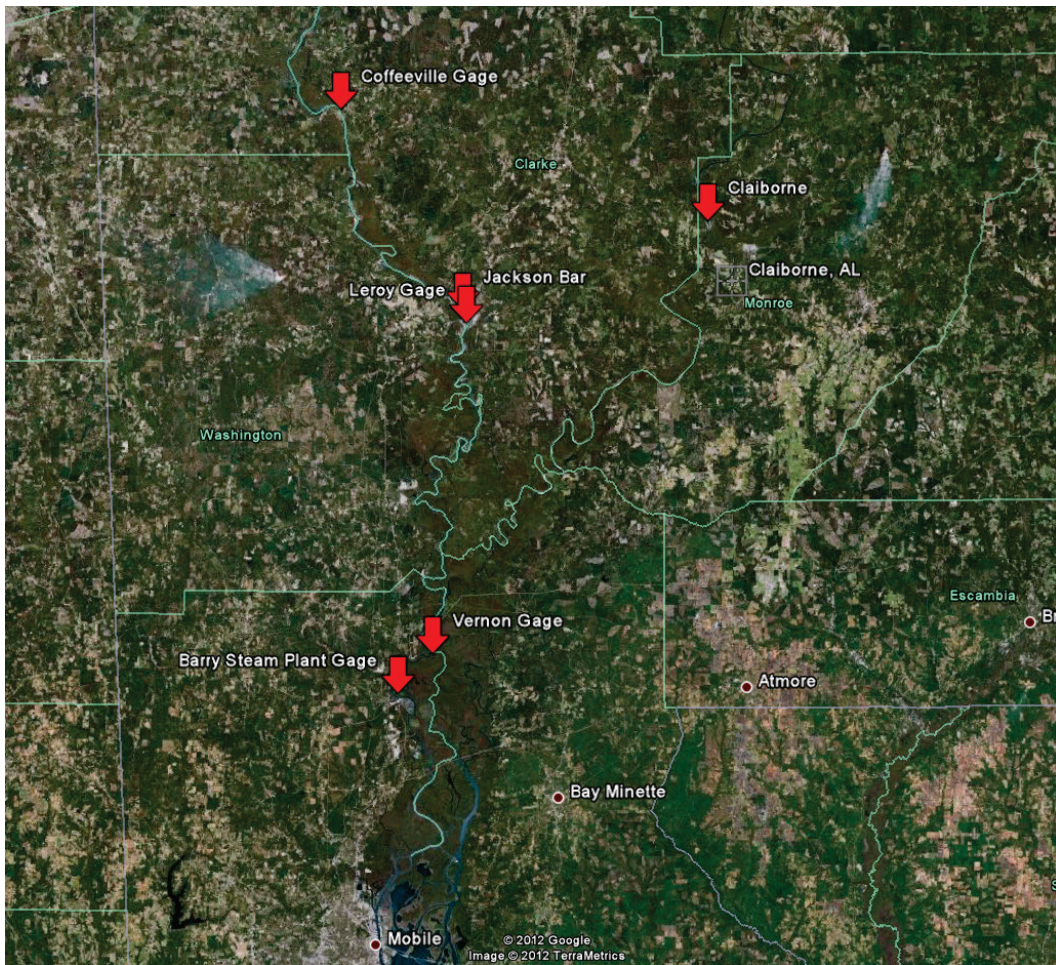
5.1 Boundary Conditions

5.1.1 Hydrodynamic

Daily data from the two closest river gages were used for the hydrodynamic boundary conditions. The upstream discharge boundary was generated from the U.S. Geological Survey (USGS) 02469762 Tombigbee R Bl Coffeeville L&D Near Coffeeville (Coffeeville Gage), and the tailwater boundary was generated from the Leroy Gage (Figure 11). Gage zero at the Leroy Gage is zero feet (ft) National Geodetic Vertical Datum NGVD 1929. Lag time from the Coffeeville Gage to the Leroy Gage is less than a day, thus a temporal adjustment was not made. Furthermore, there are no major confluences between the gages, so the flow data were used directly. The tailwater boundary was translated from the Leroy Gage, so the gage data from the Leroy Gage was adjusted down by 1 ft to correct for water surface slope.

The hydrograph covered the same time period as the dredging event of 2004. The hydrograph from 20 November 2003 to 11 May 2004 (172-day period) was selected to represent the desired dredging event of 2004. Once the hydrograph was selected, the mesh's vertical extents were chosen.

Figure 11. Location of river gages and Jackson Bar near site, Jackson, AL.



During the hydrograph, the high flow is approximately 154,000 ft³/sec (Figure 12). Based on the flood frequency curve constructed using annual peak stream flows from 1961 to 2012 (Figure 13), the high flow magnitude corresponds to a 2 yr event, typically considered the bank full flow. In the area of interest, the event corresponds to a water surface elevation of 28–30 ft. Thus, the vertical extents of the model were trimmed to this elevation.

5.1.2 Sediment load

There is no known sediment concentration data for the area of interest, so sediment concentrations were estimated. A sediment channel design code (SAM.sed), was implemented, using bed gradations (Figure 10) to calculate the approximate sediment rating curve. For the hydraulic input, a series of six steady-state flows were simulated. From these flows, SAM.sed applied the Van Rijn sediment transport function (the same transport function used

in AdH) to calculate the concentration for the representative grain sizes. The sand portion of the load is shown in Figure 14 and Table 2. For silt (0.022 and 0.04 mm) a concentration for low flows was held at 20 milligrams per liter (mg/L) and increased for the larger flows according to Figure 15.

Figure 12. Discharge at the Coffeeville Gage and gage height at the Leroy Gage for 20 November 2003–11 May 2004.

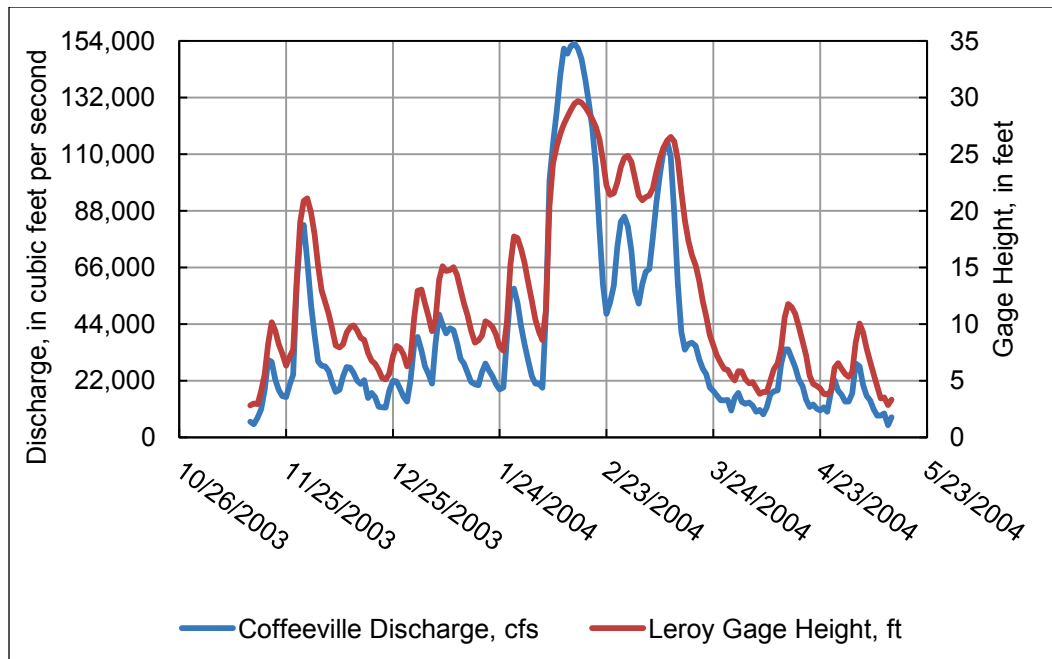


Figure 13. Coffeeville Gage flood frequency curve.

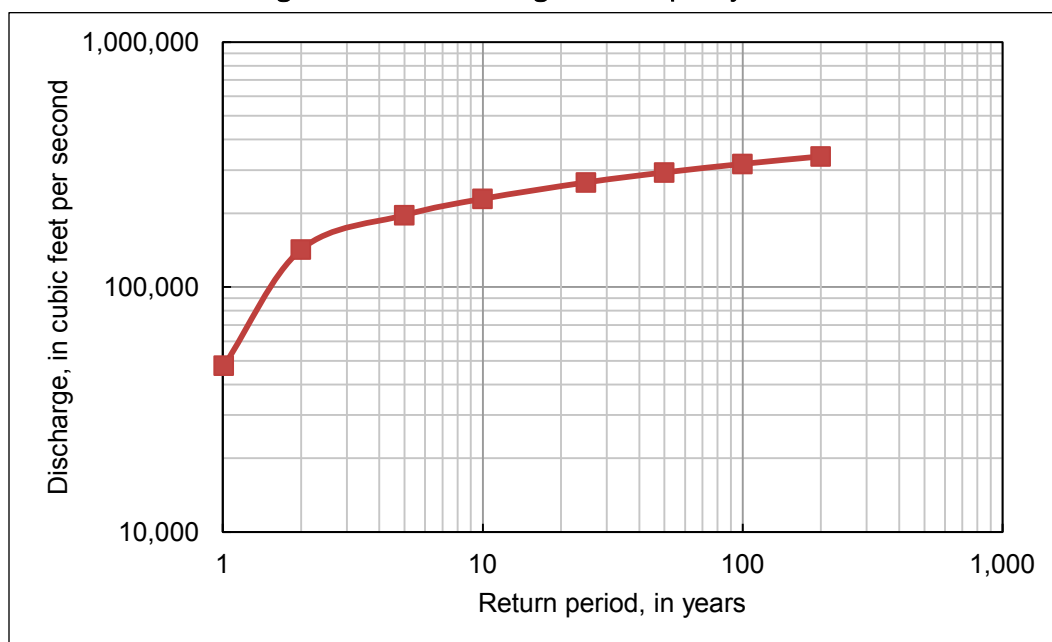


Figure 14. Estimated total sand concentration as a function of discharge at the Coffeeville Gage for 20 November 2003–11 May 2004.

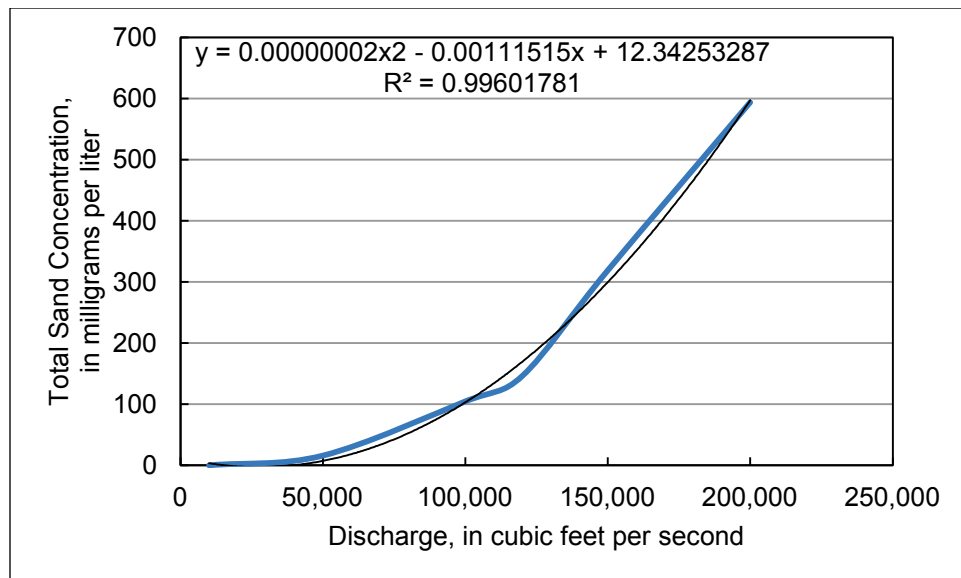


Figure 15. Estimated total silt concentration as a function of discharge at the Coffeeville Gage for 20 November 2003–11 May 2004.

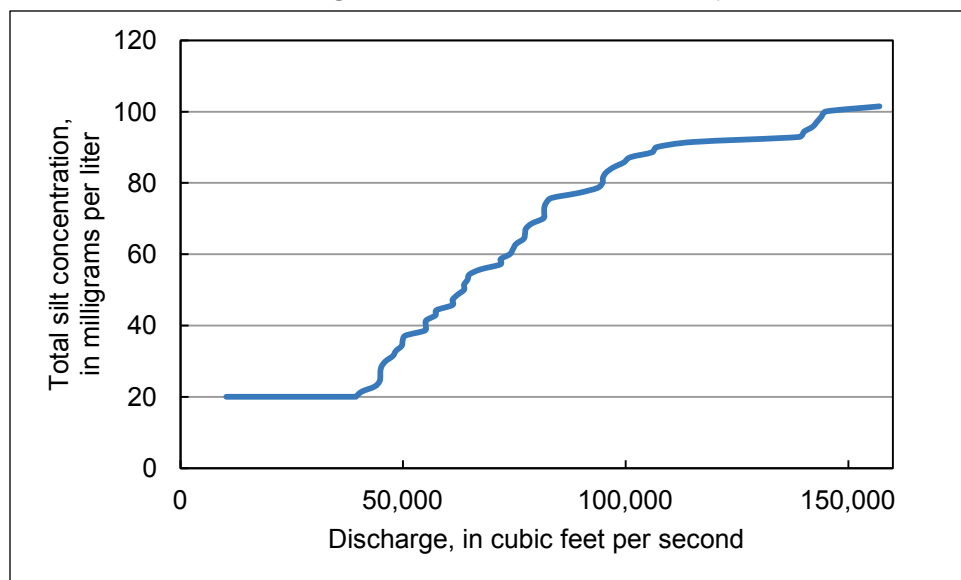


Table 2. Estimated sand fraction concentration as a function of grain size and flow at the Coffeeville Gage for 20 November 2003–11 May 2004.

Discharge, cubic feet per second	Concentration, milligrams per liter	Grain size, millimeters			
		0.085	0.177	0.354	0.707
Total		Concentration as a function grain size and flow, mg/L			
10,000	0.00	0.00	0.00	0.00	0.00
50,000	15.90	3.36	11.72	0.77	0.66
100,000	104.60	18.70	79.50	5.60	0.69
120,000	146.20	25.70	111.40	8.20	0.91
150,000	318.90	47.20	230.00	39.70	1.90
200,000	593.80	79.60	437.20	73.40	3.60

5.2 Mesh construction

5.2.1 Bathymetry data

Topography of overbank area was defined from a 2010 lidar survey. The 2004 bank-to-bank survey was used to define the in-channel bathymetry. Additionally, the Jackson Bar dredge cut was defined using a 20 November 2003 survey that was taken after the shoal material had been dredged (Figure 2). All survey data were truncated at an elevation greater than 30 ft, which corresponds to the 2 yr event at the upstream boundary.

5.2.2 Mesh materials

AdH classifies distinct features such as the channel, banks, and overbanks as *materials*. Thirteen materials were used to define the existing conditions domains (Figure 16) and fourteen for the alternatives domains. The materials are used to define key numerical parameterizations such as Manning's number. The Manning's number defines the bed roughness and is obtained through the validation process (Table 3). Eddy viscosity and diffusion were also defined by material as were sediment properties including sediment gradation, bed layers, molecular diffusion, and erosion rates.

Figure 16. Material number and location for the Jackson Bar 2004 existing-conditions model.

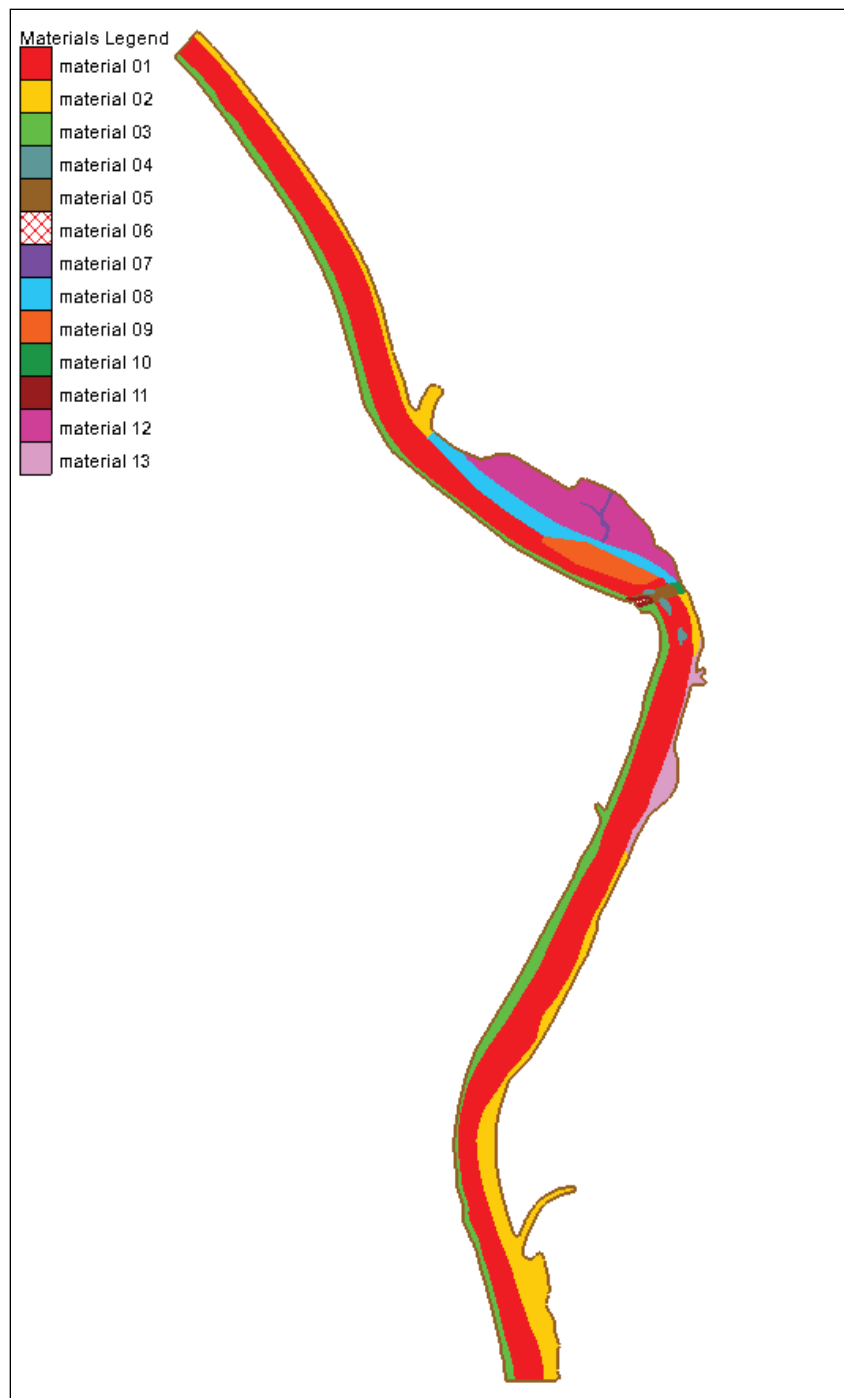


Table 3. Prescribed Manning's number for materials in the AdH models of the Jackson Bar vicinity.

Material number	Material name	Manning's number
1	Thalweg	0.031
2	Left Bank	0.038
3	Right Bank	0.038
4	Scour Holes	0.031
5	Bridge	0.031
6	Abutment	0.039
7	Creek	0.028
8	Jackson Bar	0.032
9	Jackson Bar Dredge Cut	0.032
10	Left Bridge	0.038
11	Right Bridge	0.038
12	Over Bank	0.04
13	Rip-Rap Bank	0.032
14	Training Structures	0.038

5.2.3 Upstream and downstream limits

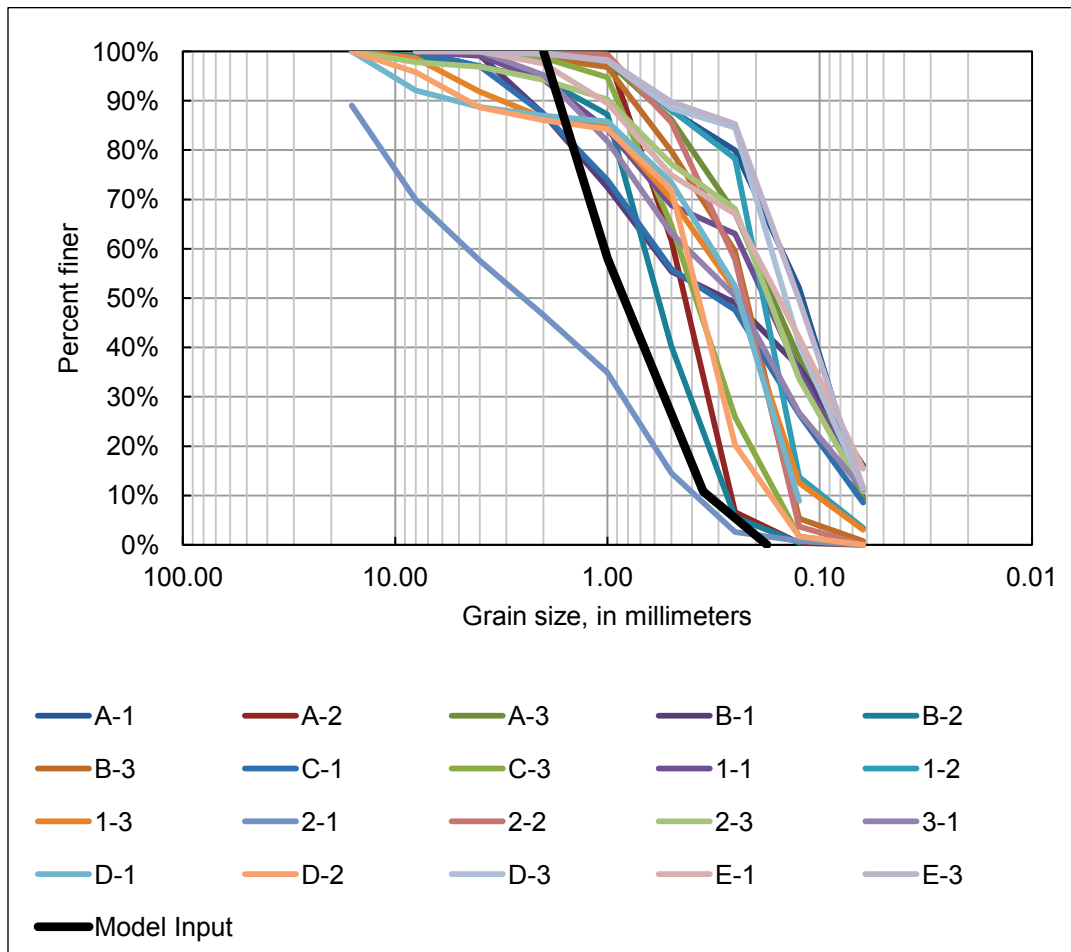
Upstream and downstream limits of a model are important because their selection can affect flow into and out of the model. The domain should extend sufficiently upstream so alternatives being evaluated do not produce changes to the streambed profile or the suspended sediment load at the upstream boundary (Thomas et al. 1981). Thus, the horizontal extents were chosen to extend from RM 92.5 to 87. These locations are also in relatively straight, alluvially stable sections (as recommended by Franco (1978)).

5.2.4 Bed gradation

Twenty bed grab samples were collected above the dredge cut to quantify grain size distribution. The bed samples showed a near uniform bed gradation throughout the domain (Figure 17). This gradation was applied in the model. Dredge cut data indicated that infill sediment was medium to coarse sand (0.25–1.00 mm). Preliminary simulations indicated that insufficient sediment was deposited in the dredge cut when compared to dredge volume data. In addition, dredge cut data indicated that the infill material was coarser than predicted in the preliminary simulations. To achieve the appropriate volume and grain size of infill material, the

sediment bed was coarsened by 50% for the D₁₀–D₇₀ sediment class sizes during model calibration. The D₉₀ class size remained the average for the grab sample data.

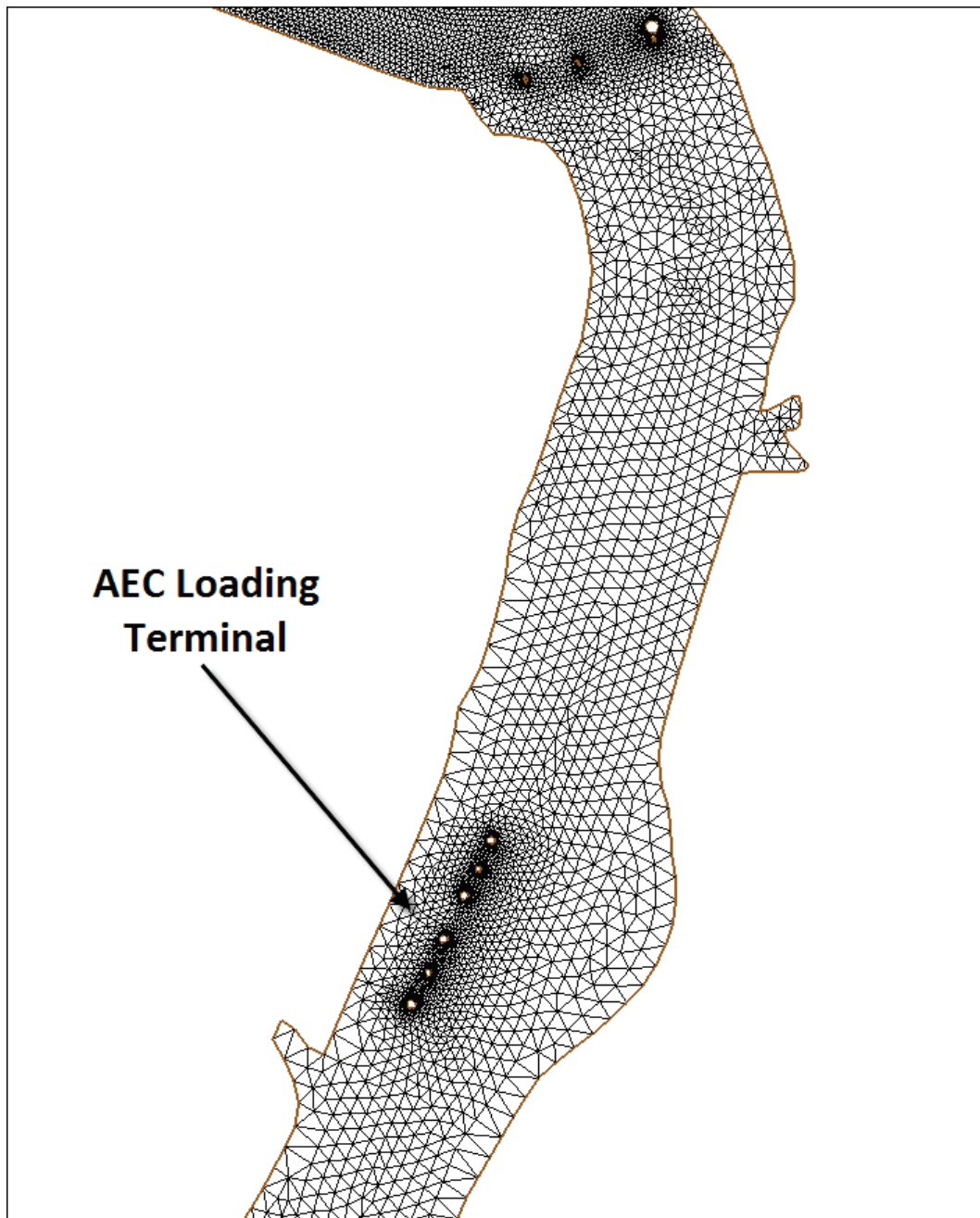
Figure 17. Collected sample bed gradations (11 November 2012) compared to model input gradation in the Jackson Bar vicinity.



5.3 Implementation of AEC Power Plant

For the AEC Power Plant existing conditions model, six mooring cells were added to the existing conditions model. The mooring cells form the basic structure of the receiving terminal at the AEC power plant (Figure 18). Location of the mooring cells came from aerial imagery. Along with the new mooring cells, a rectangular footprint was established in the mesh to measure the amount of shoaling that occurs at the facility. This new configuration was simulated in 3 of the 13 alternative runs.

Figure 18. AEC Power Plant existing conditions model with the six mooring cells for the AEC loading terminal near Jackson, AL.



6 Validation

Validation includes evaluating a model's capacity to reproduce the physics that are associated with a process to ensure that it properly represents the intended system (Wang et al. 2008). Here, two forms of validation for hydrodynamics and sediment were performed to ensure a reasonable solution. Validation of the hydrodynamics was conducted with gage data from the Leroy Gage, HEC-2 model, and WES physical model (PM). A sediment validation was implemented using dredging data. Then a check on the new existing conditions model was conducted.

6.1 Leroy Gage

The Leroy Gage was the only available gage within the model domain and was used as the initial check. It provided a time-series evaluation of water surface elevation (WSE). Comparisons between the field data and simulated data show close agreement (Figure 19). Using these data, the absolute value of the averaged daily difference between the field data and simulated data was 0.514 ft with a standard deviation of 0.194 ft. The correlation coefficient was estimated at 0.999 (Figure 20). A box plot shows close agreement when the data plots on a 45° angle. Additionally, the root mean squared error (RMSE) was 0.549 ft. Thus, at this location, a 6-inch (in.) variation between the field and the model exists. However, with a range of 30 ft in the hydrograph, the 6 in. deviation (1.6%) was deemed acceptable for a temporal hydrodynamic validation of WSE.

Unfortunately, the Leroy Gage is downstream of the study site and is only one point. The site only provides insight at one location and gives no indication of the spatial variation of WSE. It is possible for the water surface slope in the model to be tilted with the apex at the Leroy Gage providing a false sense of assurance. Further hydrodynamic validation could be used to ensure the spatial variation is represented.

Figure 19. Validation plot of Leroy field data vs. simulated data, 172-day hydrograph.

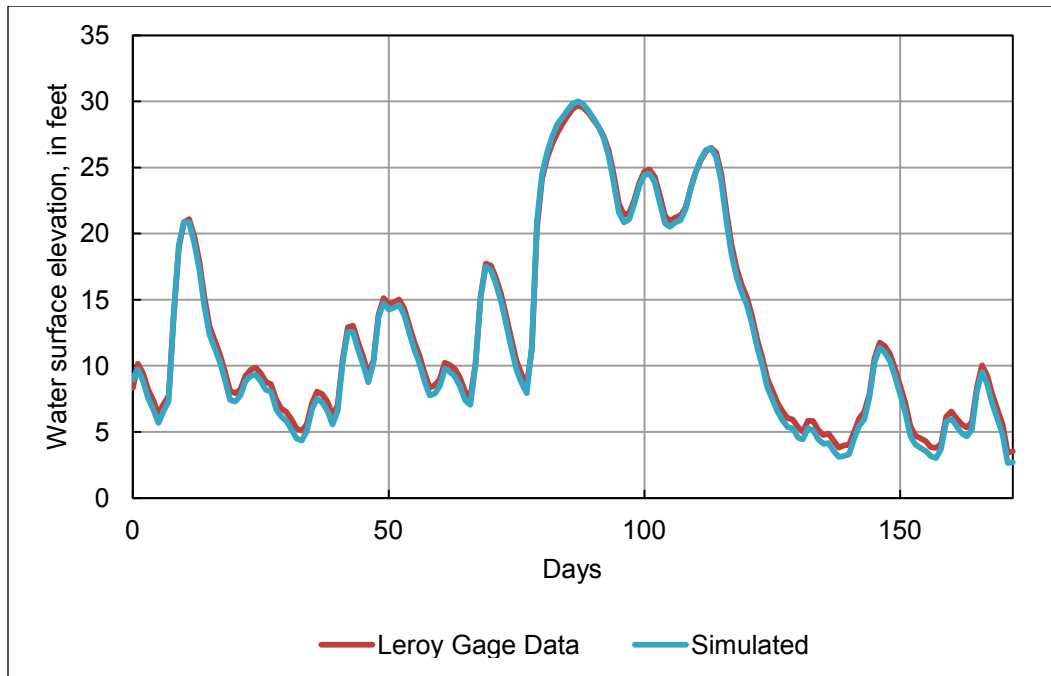
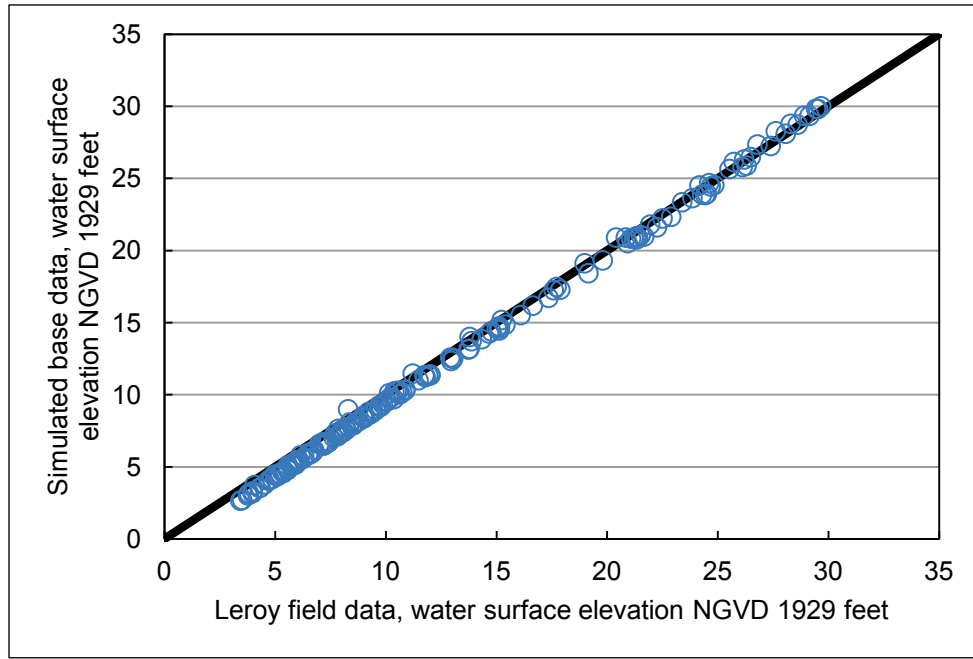


Figure 20. Simulated base data vs. Leroy Gage field data, 172-day hydrograph.



6.2 Model-to-model comparison

With limited field data, existing physical and numerical models were used to supplement the field data validation. The only available existing models were the HEC-2 model and 1987 WES PM. Both were carefully scrutinized to determine applicability. There were disadvantages and advantages with

using each model. The main disadvantage in the comparison was the difference in bathymetry. The HEC-2 and 1987 WES PM were simulated with 1984 bathymetry (USACE, SAM 1988). A comparison between the 1984 and 2004 bathymetry was made (Figures 21 and 22 showing cross sections 573 ft and 2,610 ft upstream of the bridge, respectively). The comparison showed the western meander in this reach for the 20 yr period. The channel has moved approximately 200 ft to the west while simultaneously deepening. This movement has enhanced the conditions for shoaling at Jackson Bar, increasing the difficulty for navigation. The main advantage of using the model-to-model comparison is that the HEC-2 model had results for water surface slope while the PM had velocity measurements.

Overall, the slope of the channel has not dramatically changed. It has slightly steepened through the bridge pass, but upstream it has stayed relatively consistent. The PM and AdH velocity comparison was done only along the center line of the thalweg in order to compensate for the bathymetric variation in both models.

Figure 21. Cross-section comparison between the AdH and 1987 WES PM bathymetry 573 ft upstream of the Norfolk Southern railroad bridge.

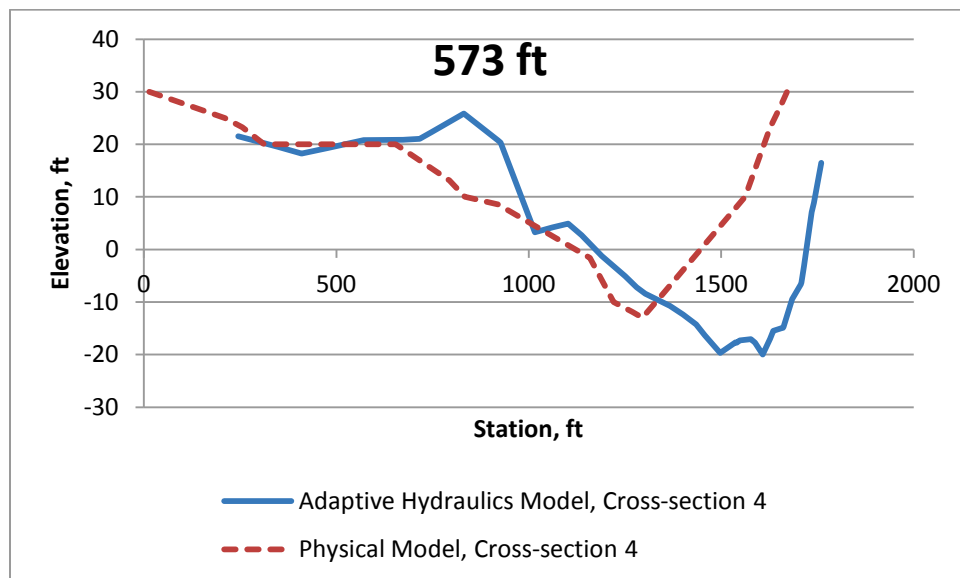
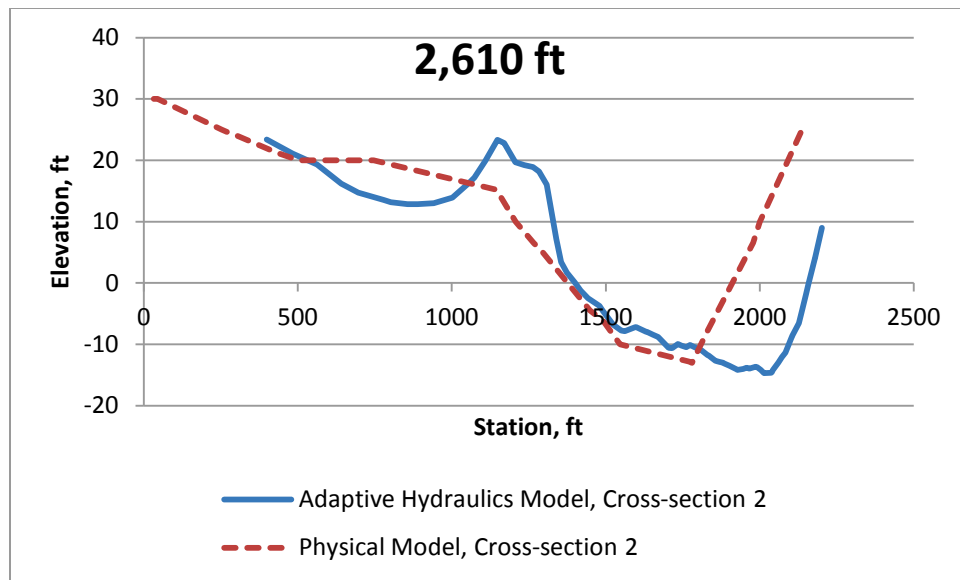


Figure 22. Cross-section comparison between the AdH model and 1987 WES PM bathymetry 2,610 feet upstream of the Norfolk Southern railroad bridge.



6.2.1 HEC-2 slope

Slope provides an indication of how well the velocities match and a spatial evaluation of the model WSE. The only available slope data were from an HEC 2 model done in the mid-1980s in conjunction with the PM. Although this is a model-to-model comparison, it still provides reasonable assurance as to the water surface slope accuracy in AdH. If the slopes did not correspond, then modifications would be necessary through the adjustment of the bed roughness and eddy viscosity.

A series of four steady-state simulations at different frequencies were conducted with the HEC-2 model. Those same flows were run in the AdH model. Four flows (20,000, 40,000, 60,000, and 140,000 ft³/sec) that occur in the selected hydrograph are compared here. Unfortunately, the 100,000 ft³/sec flow data were unavailable. The 140,000 and 100,000 ft³/sec flow correspond well with the 2 and 1 yr events, respectively.

The HEC-2 profile extends from -2,000 ft, downstream of the Norfolk Southern railroad bridge, to 8,000 ft upstream with the bridge at the zero mark. The profile includes the dredge cut area, which is 350–2,800 ft upstream of the Norfolk Southern railroad bridge. Table 4 shows the statistical analysis of the water surface slope comparison upstream of the Norfolk Southern railroad bridge. The lower flow events are in closer agreement than those of the higher flows. The correlation coefficient

increases with a decrease in discharge. The RSME decrease along with the average difference as flow decreases. The decrease in variation as a function of reduced flow is shown in Figures 23–26. The figures show the water surface slope compared to each other with the AdH results in red and the HEC-2 results in black.

Table 4. Statistical analysis comparison of HEC-2 and AdH model.

Event	140,000 ft ³ /sec	60,000 ft ³ /sec	40,000 ft ³ /sec	20,000 ft ³ /sec
Correlation	0.984	0.986	0.992	0.993
RMSE	0.064	0.032	0.012	0.008
Average Diff	0.028	0.011	0.004	0.004
Average Diff Stdev	0.016	0.012	0.004	0.002
Maximum HEC	29.100	21.700	17.700	10.950
Maximum AdH	28.998	21.618	17.699	10.942
Minimum HEC	28.500	21.350	17.490	10.810
Minimum AdH	28.438	21.366	17.515	10.817

Figure 23. HEC-2 and AdH frequency profile for 20,000 ft³/sec.

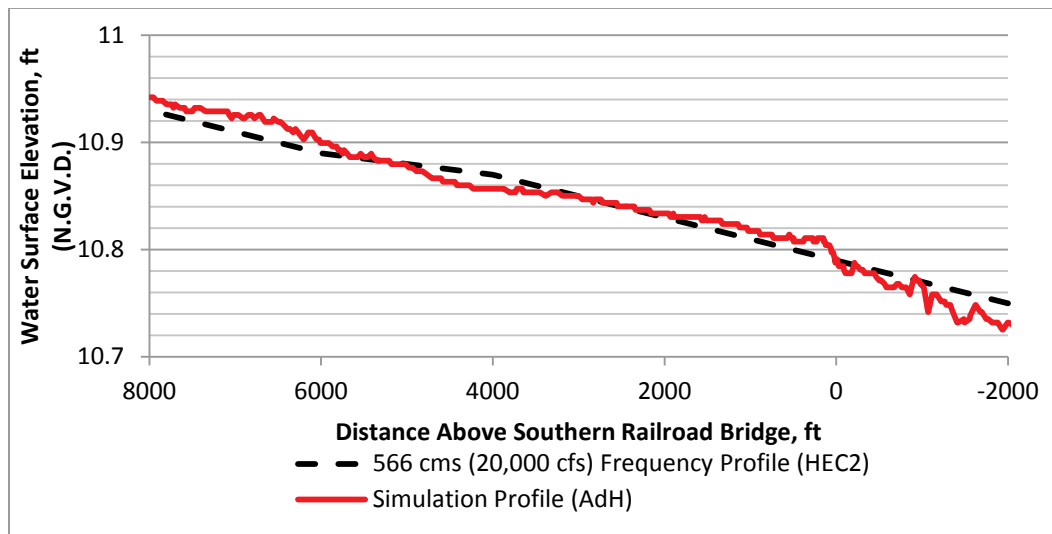


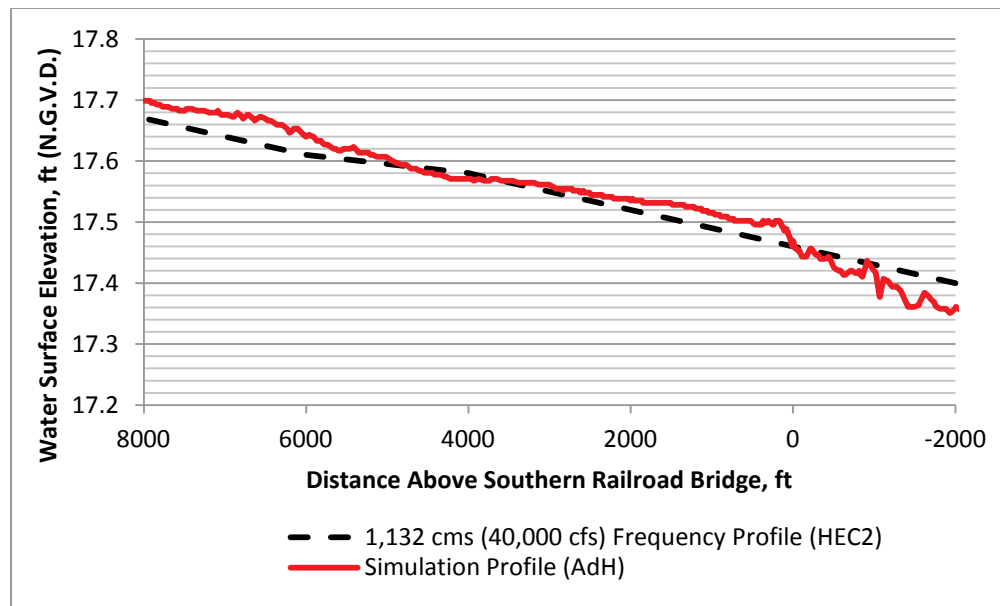
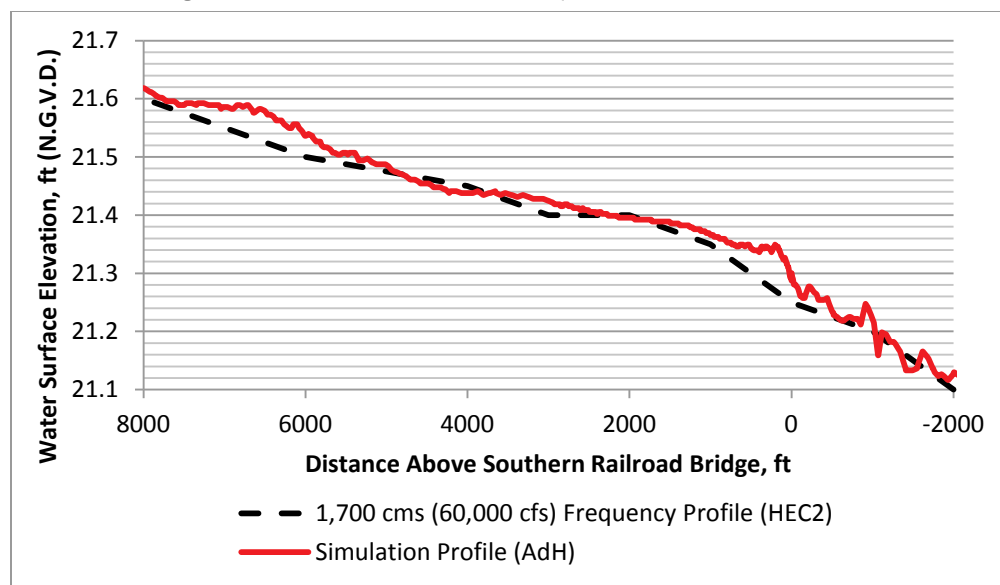
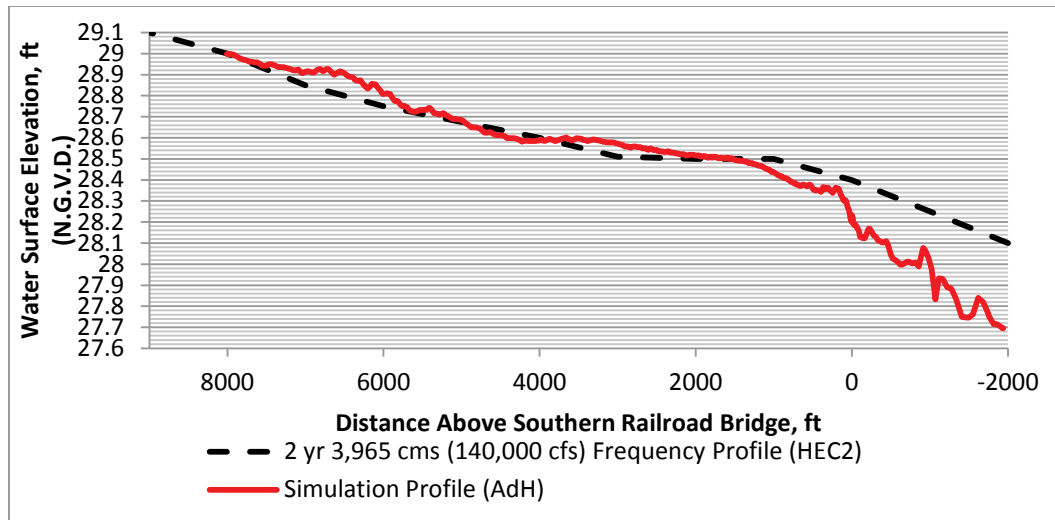
Figure 24. HEC-2 and AdH frequency profile for 40,000 ft³/sec.Figure 25. HEC-2 and AdH frequency profile for 60,000 ft³/sec.

Figure 26. HEC-2 and AdH frequency profile for 60,000 ft³/sec.

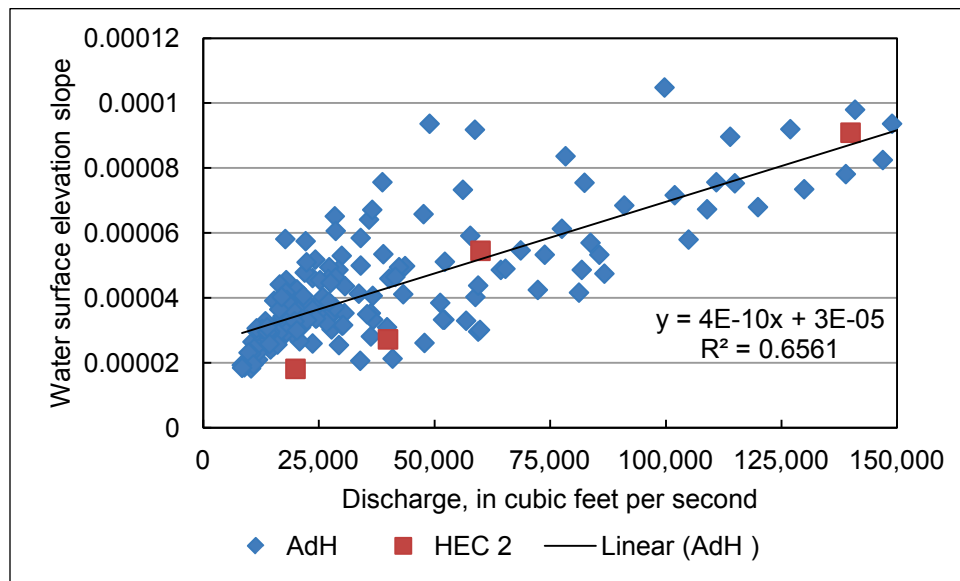
For the high flows, the primary concern was at and downstream of the Norfolk Southern railroad bridge. Figure 26 shows a significant deviation between the two models. This is not reflected in the statistical analysis because only data upstream of the bridge were analyzed. The differences at and downstream of the bridge were more than likely due to modeling difference between a 1D and 2D model, while both are attempting to simulate the 3D effects of flow through the bridge pass.

The HEC-2 model is not available, nor is it known how the model was set up. Typically, for normal flows, the HEC-2 model uses the normal bridge routine (USACE 1991). At a bridge in a 1D model, there are two head losses (entrance and exit losses) and structure losses for which to account (USACE 1995). First, HEC-2 accounts for the expansion and contraction losses upstream and downstream in terms of user-specified coefficients. Second, HEC-2 accounts for the loss of flow area for the bridge piers. It is unknown what expansion and contraction losses were used in the HEC-2 model and how or if the bridge piers were modeled. All these variations can have a significant near-field impact on the water surface elevation through the bridge pass while the far field might show negligible effect. Thus, only the data upstream of the bridge were analyzed in order to avoid the uncertainty at the bridge pass.

The slopes from the HEC-2 model were compared to the slopes from the AdH model hydrograph (Figure 26). For the lower flows, the AdH model predicted a slightly higher slope while for the higher flows the two models closely match. This is shown in the linear trend line fitted to the AdH data

with slopes of the various flows in the hydrograph (Figure 27). The analysis shows an opposite agreement from the first analysis, the steady state comparison (Figure 19), indicating that the dynamic behavior of the hydrograph affects the water surface slope for the lower flows. It is more important in the dynamic conditions that the higher flows concur because the higher flows transport the majority of the sediment.

Figure 27. HEC 2 slopes compared to AdH slopes.



6.2.2 1987 WES physical model (PM)

The third hydrodynamic validation dataset was the velocity information from the PM. The fundamental assumption for the validation between the PM and the AdH model is twofold. First, it is acknowledged that the channel has moved, but the overall cross-sectional area has remained similar, indicating that velocities have not cross-sectionally changed. Second, with a similar width and depth relative to the respective flow, the flow conveyance for normal depth is in close agreement between the two models (Figure 28). If both the cross-sectional area and conveyance have not changed, then it can be assumed that the velocities along the thalweg should be reasonably close.

The PM used the same flows simulated in the HEC-2 model. However, unlike the HEC-2 model, the 100,000 ft³/sec flow data were available for the PM.

Figure 28. Conveyance potential for normal depth in AdH and the 1987 WES PM.

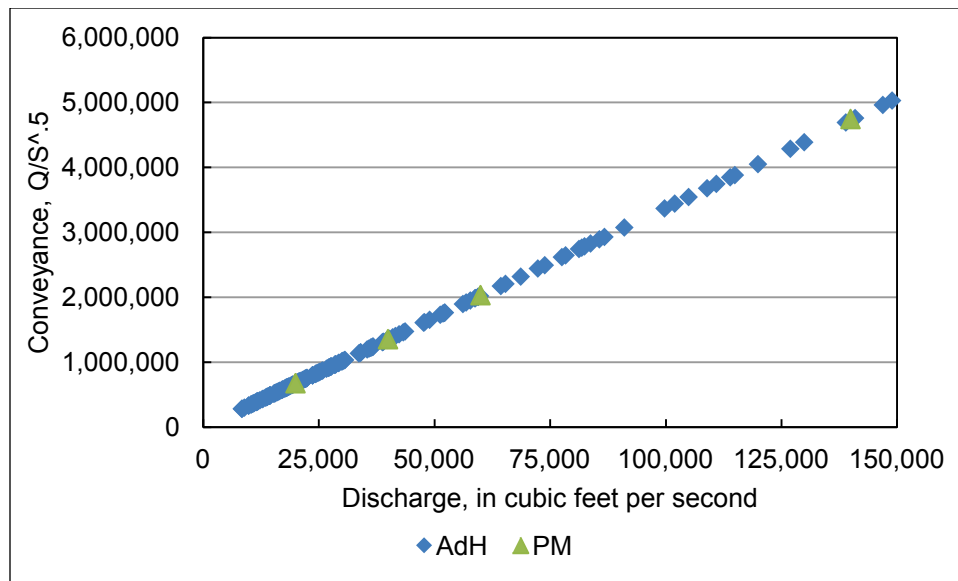


Table 5 shows the statistical analysis of the PM and the AdH model velocity data. Velocities along the thalweg were compared. The analysis showed reasonable correlation between the two models for the middle flows of 40,000, 60,000, and 100,000 ft³/sec. There was less agreement for the low event and even less for the high event, indicating impacts from the difference in geometry are greatest at the low and high flows. SAM has indicated that overbank filling for the right overbank area adjacent to the dredge cut would affect the high flows. The RMSE steadily increased with increased flow with the exception of the 100,000 ft³/sec event. As an overall match, the 100,000 ft³/sec showed the greatest agreement. The average differences in velocity indicated the best agreement for all flows with none greater than 4% deviation from the average maximum.

Table 5. Statistical analysis of the comparison of velocity along the thalweg between the 1987 WES PM and the AdH model.

Event	20,000 ft ³ /sec	40,000 ft ³ /sec	60,000 ft ³ /sec	100,000 ft ³ /sec	140,000 ft ³ /sec
Correlation	0.529	0.695	0.776	0.885	0.287
RSME	0.190	0.212	0.418	0.319	0.696
Average difference	0.088	0.055	0.290	0.083	0.279
Average difference in the standard deviation	0.173	0.211	0.311	0.318	0.658
Maximum 1987 WES PM	2.100	3.000	3.800	5.700	7.000
Maximum AdH	2.140	2.967	3.887	5.491	6.912
Minimum 1987 WES PM	1.400	2.100	2.500	3.700	4.800
Minimum AdH	1.643	2.375	3.069	4.159	5.264

The velocity profile comparisons along the respective thalwegs are shown in Figures 29–33. From statistical analysis and visual representation, there is reasonable agreement between the two models. The agreement indicates that the AdH model, while not matching perfectly, is behaving similarly to the WES PM. It is expected that the two models would have some disagreements because there are significant differences in bathymetry and modeling approaches. A directional comparison was not conducted because there is only unidirectional flow and no shown eddies exist on the PM data output. Additionally, the velocity vectors would be expected to shift due to the change in channel alignment.

Figure 29. 20,000 ft³/sec flow comparison for the AdH model and the 1987 WES PM.

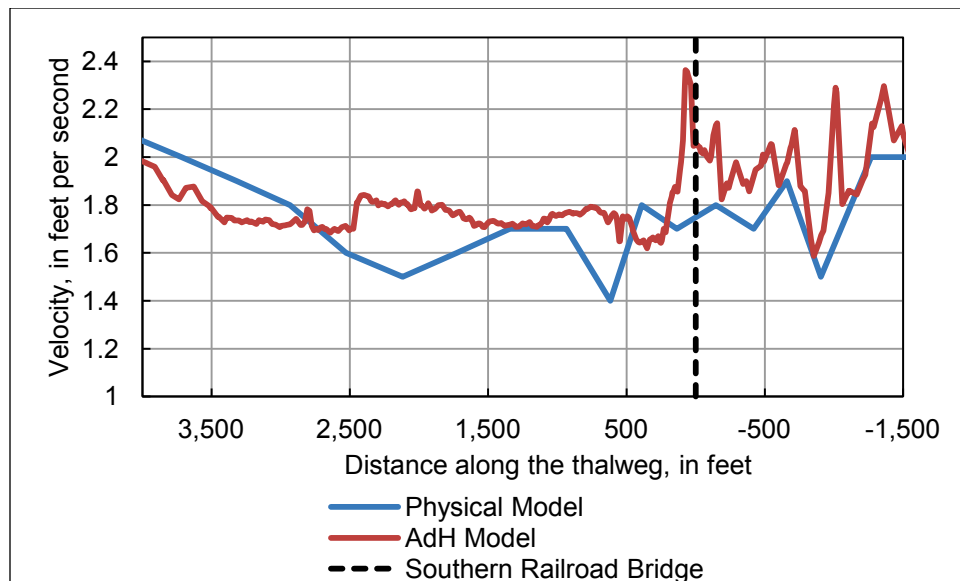


Figure 30. 40,000 ft³/sec flow comparison for the AdH model and the 1987 WES PM.

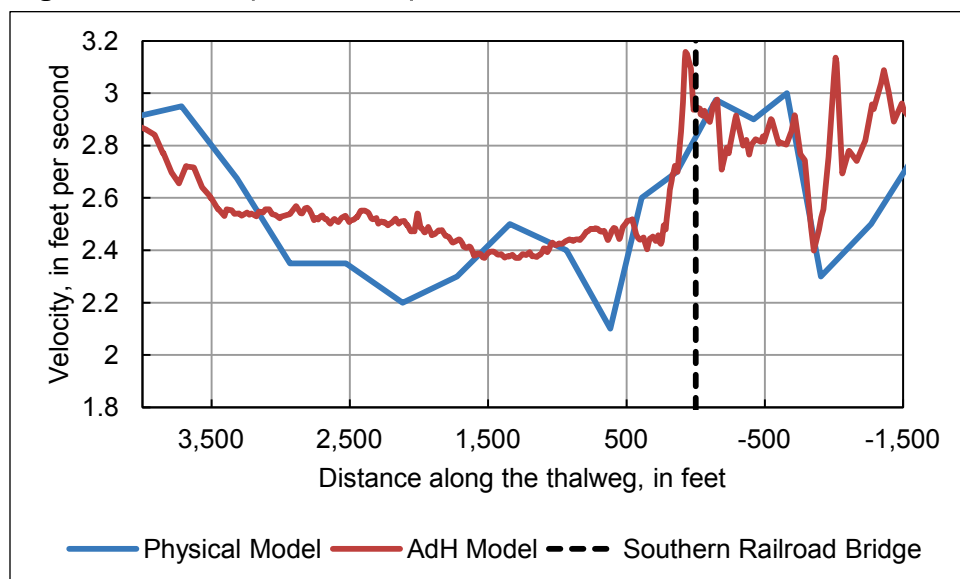


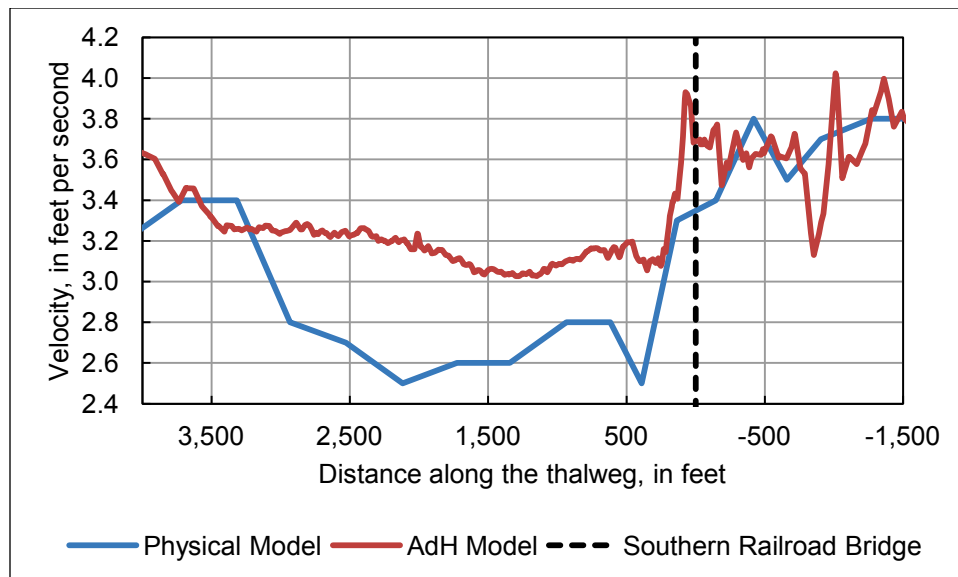
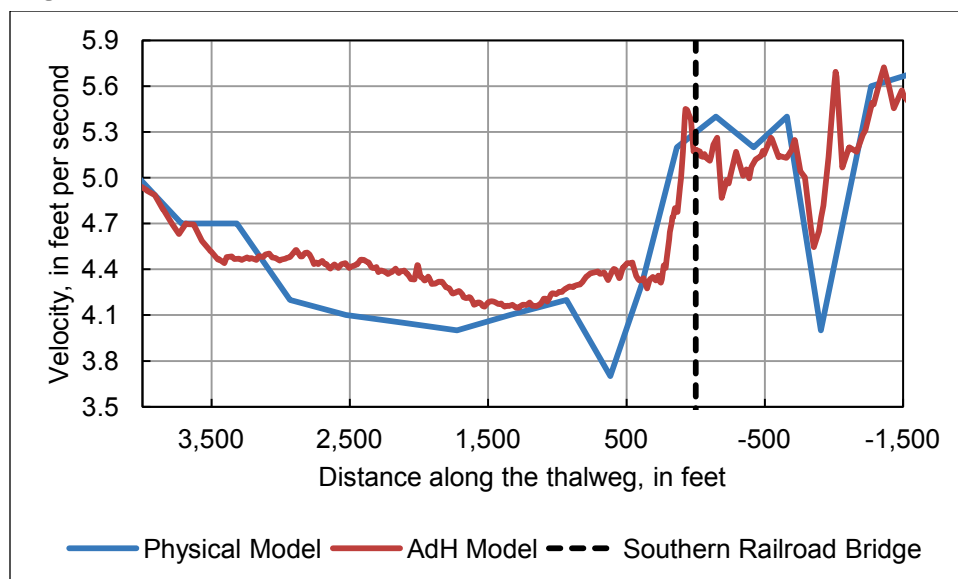
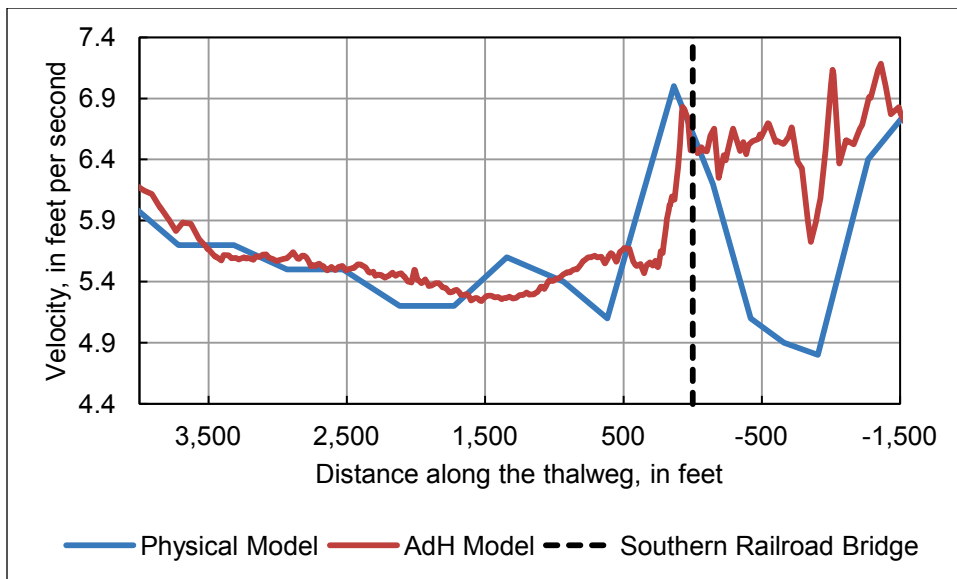
Figure 31. 60,000 ft³/sec flow comparison for the AdH model and the 1987 WES PM.Figure 32. 100,000 ft³/sec flow comparison for the AdH model and the 1987 WES PM.

Figure 33. 140,000 ft³/sec flow comparison for the AdH model and the 1987 WES PM.

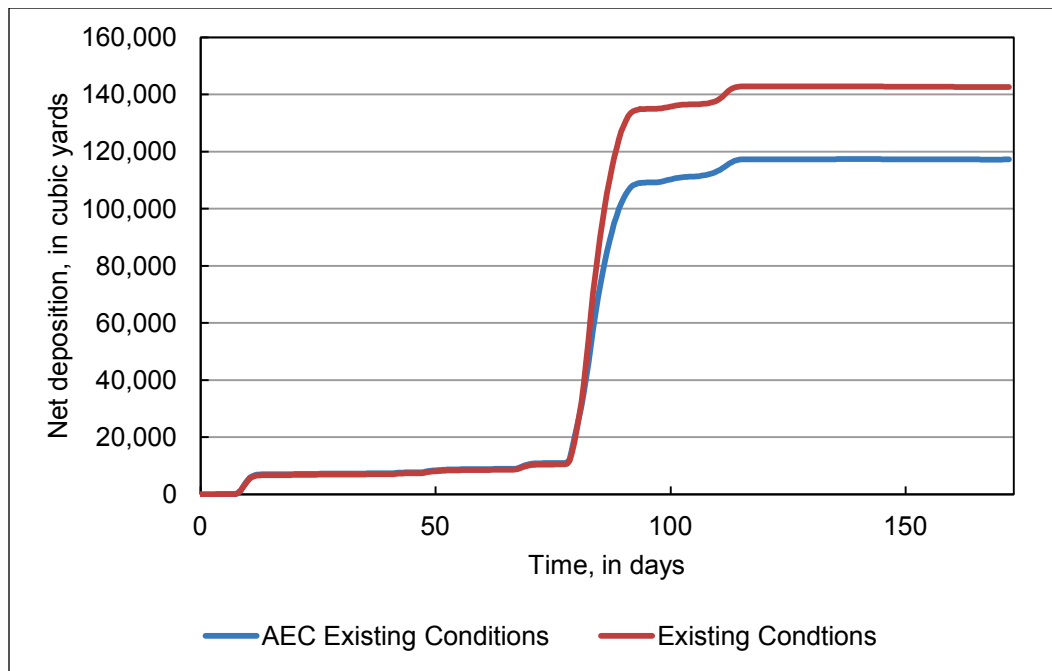
6.3 Sediment validation

A sediment validation was only conducted with the dredge data. The existing conditions model simulated a total volume of deposition in the 2004 dredge cut to be 143,000 yd³. This is compared to the reported volume of 145,084 yd³ (Figure 5), a 2% discrepancy.

6.4 Comparison of the AEC Power Plant existing conditions model

With the addition of the AEC mooring cells, a comparison was conducted between the two existing conditions models, existing conditions and AEC existing conditions. The comparison between the two models included dredging, water surface elevation, velocity, and bed shear stresses. For the AEC existing conditions, the total deposition was 117,000 yd³. The addition of the six cells reduced the total deposition in the dredge cut by 18%. The temporal accumulation of material in the 2004 dredge cut is shown in Figure 34. The peak of the hydrograph occurs at day 87. Figure 34 shows that the difference occurred around the peak of the hydrograph and was the only period where the slopes of the two lines diverge. At all other times, the accretion was relatively consistent. Isolation of this single peak event was required to understand the deviation between the two models.

Figure 34. Temporal accumulation of deposition in the 2004 dredge cut in the Jackson Bar, AL, vicinity.



It was unknown as to the cause of the differences in deposition between the two existing conditions models at the hydrograph peak, so water surface elevation, velocity, and bed shear stress were evaluated. The time series of water surface elevations at four flux lines were analyzed (Figure 35). The greatest impact for the peak flow occurred at the flux line downstream of the Norfolk Southern railroad bridge (Figure 36). The AEC existing conditions model was 3 in. higher than the existing conditions. This indicates an increased backwater condition for the AEC existing conditions model due to the installation of the cells in the model.

The velocity variation between the two existing conditions models was also analyzed (Figure 37). The difference in the AEC existing conditions model from the previous existing conditions was calculated for the peak flow event. A positive value indicates higher velocities in the existing conditions model while a negative value indicates higher velocities in the AEC existing conditions. It is shown that velocities have slowed in the AEC existing conditions model by 0.2–0.5 feet per second (ft/sec). This slowing condition or backwater extends to the upstream boundary.

Slight changes in velocity can have significant impacts on transport potential for a given flow because shear stress is a function of velocity squared. If the velocity is reduced by 50%, there is a 300% reduction in

shear stress. For Figure 38, the AEC existing conditions bed shear is subtracted from the existing conditions model. The figure shows a reduction in the bed shear upstream of the placed cells. The reduced bed shear spatially ranges from 0.0002 to 0.007 pounds per square foot (lb/ft^2) (0.01–0.35 pascals (Pa)) for the day-87 flow. A decrease in 0.13 Pa is the equivalent of mobilizing very fine sand and not mobilizing fine sand (Julien 2002).

Figure 35. Flux line locations in the model.

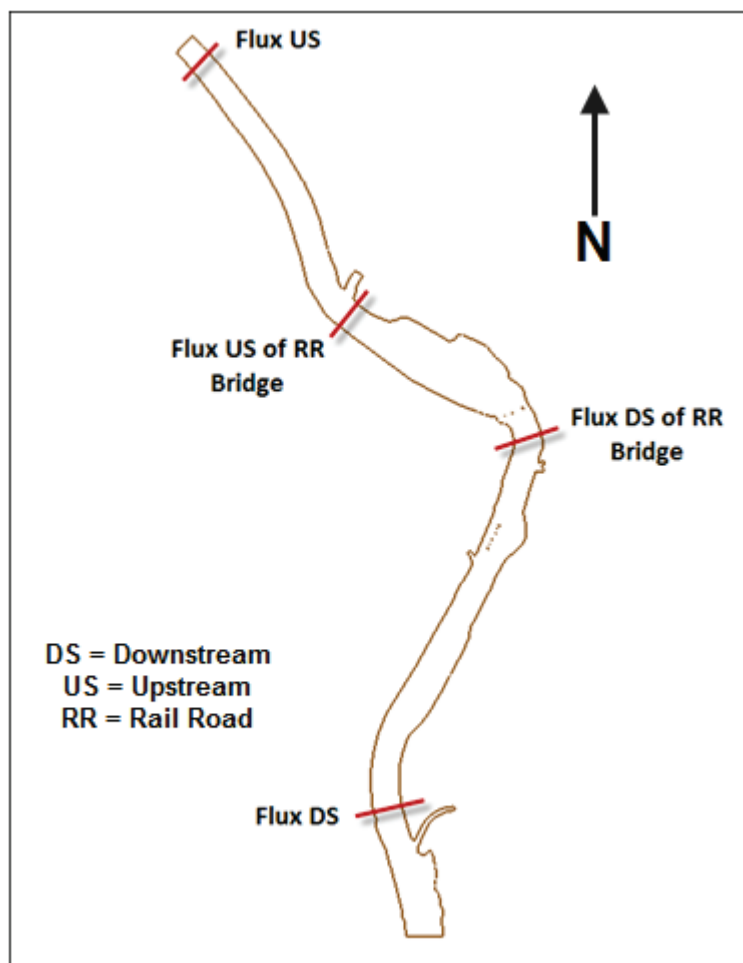
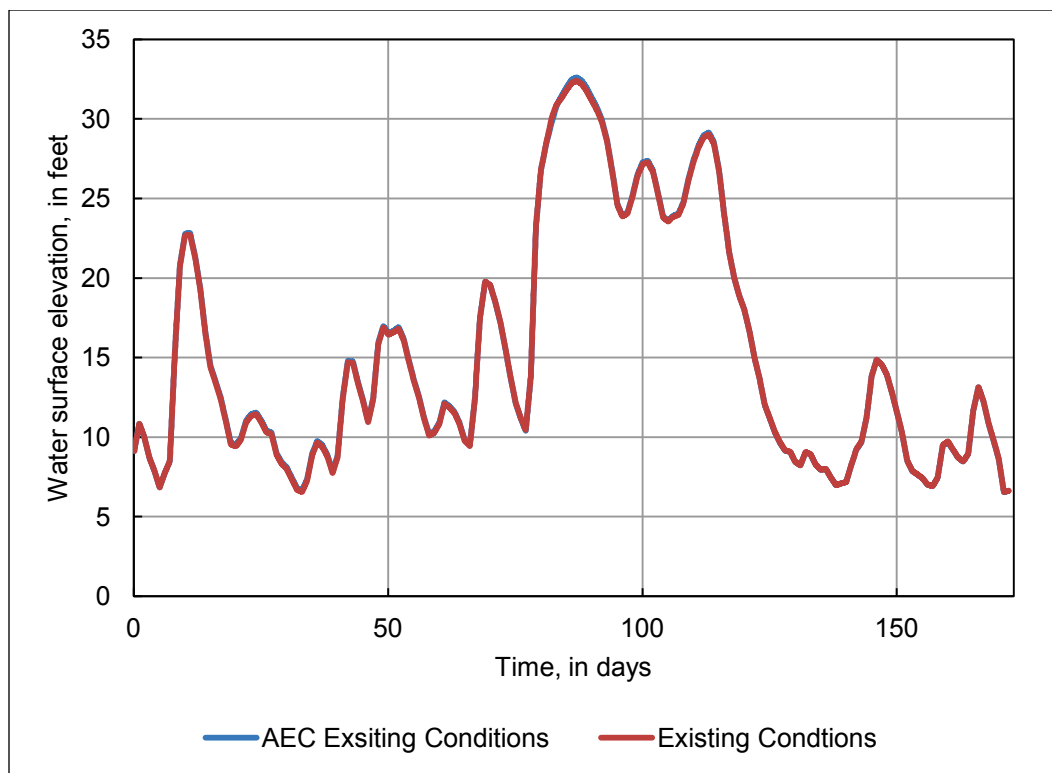


Figure 36. Flux downstream of Norfolk Southern railroad bridge.



The decrease in deposition at the dredge site is due to the backwater condition generated by the inserted mooring cells. Understanding that sediment supply for the model comes only from the bed, the backwater condition in the model generated an atypical result. With the reduction in bed shear from the backwater condition, the model was not able to entrain and move enough sediment out of the bed to generate the same amount of deposition in Jackson Bar. Therefore, the supply of sediment was altered between the two existing conditions models.

While the mooring cells do exist in the river, the system functionality is not limited like the model. Since the model's sediment supply comes only from the bed, a reduction in transport potential will affect the amount of material deposited throughout the domain. In the actual river, the supply comes from the banks and beyond the upstream boundary of the model. Furthermore, the vertical spatial limits of the model were trimmed and may not provide the same amount of cross-sectional area that exists in the field. The model merely represents the wet river bottom and only captures a portion of the physics.

Figure 37. Existing conditions minus AEC existing conditions velocity during the peak hydrograph flow at day 87 (red: AEC less; blue: AEC more).

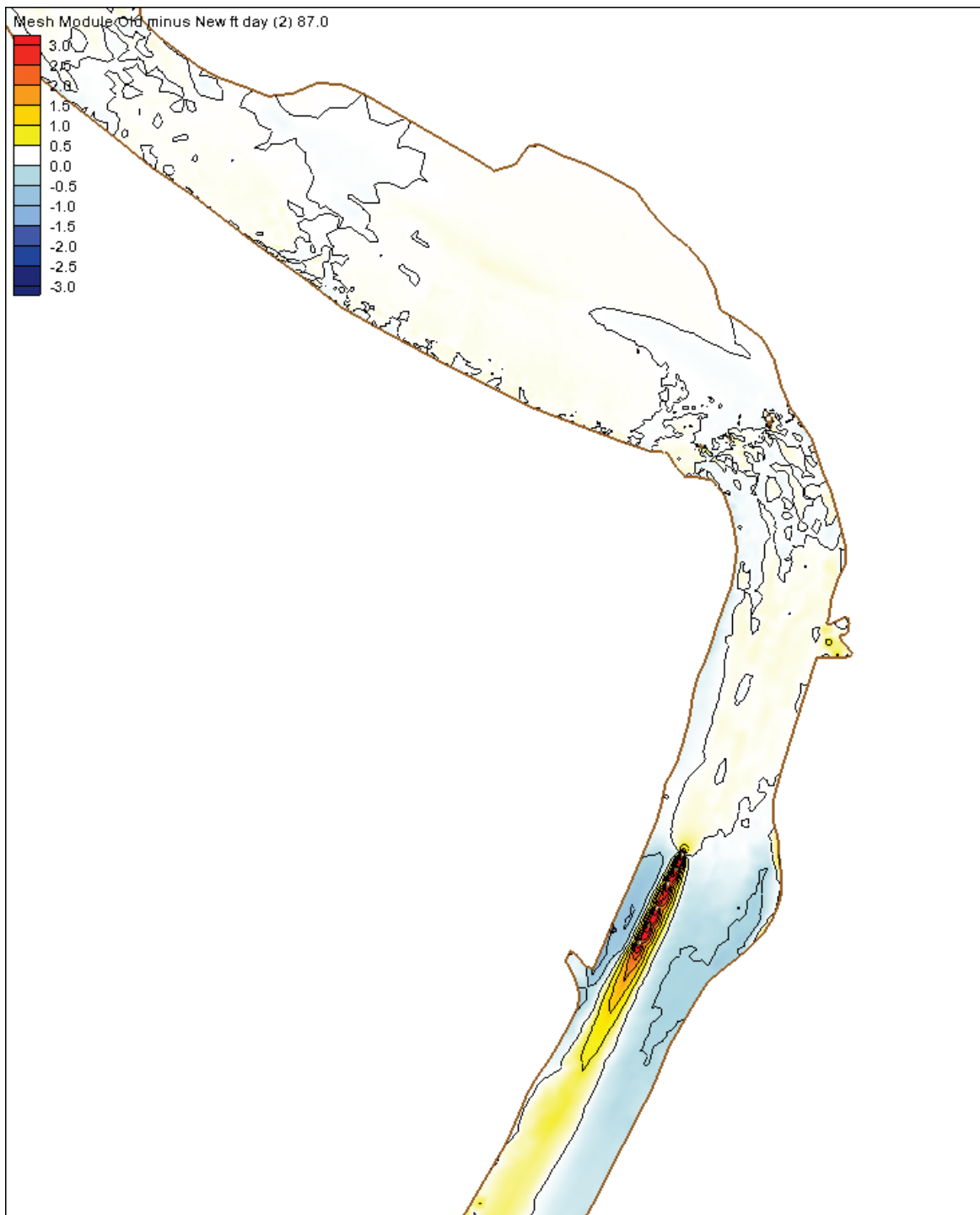
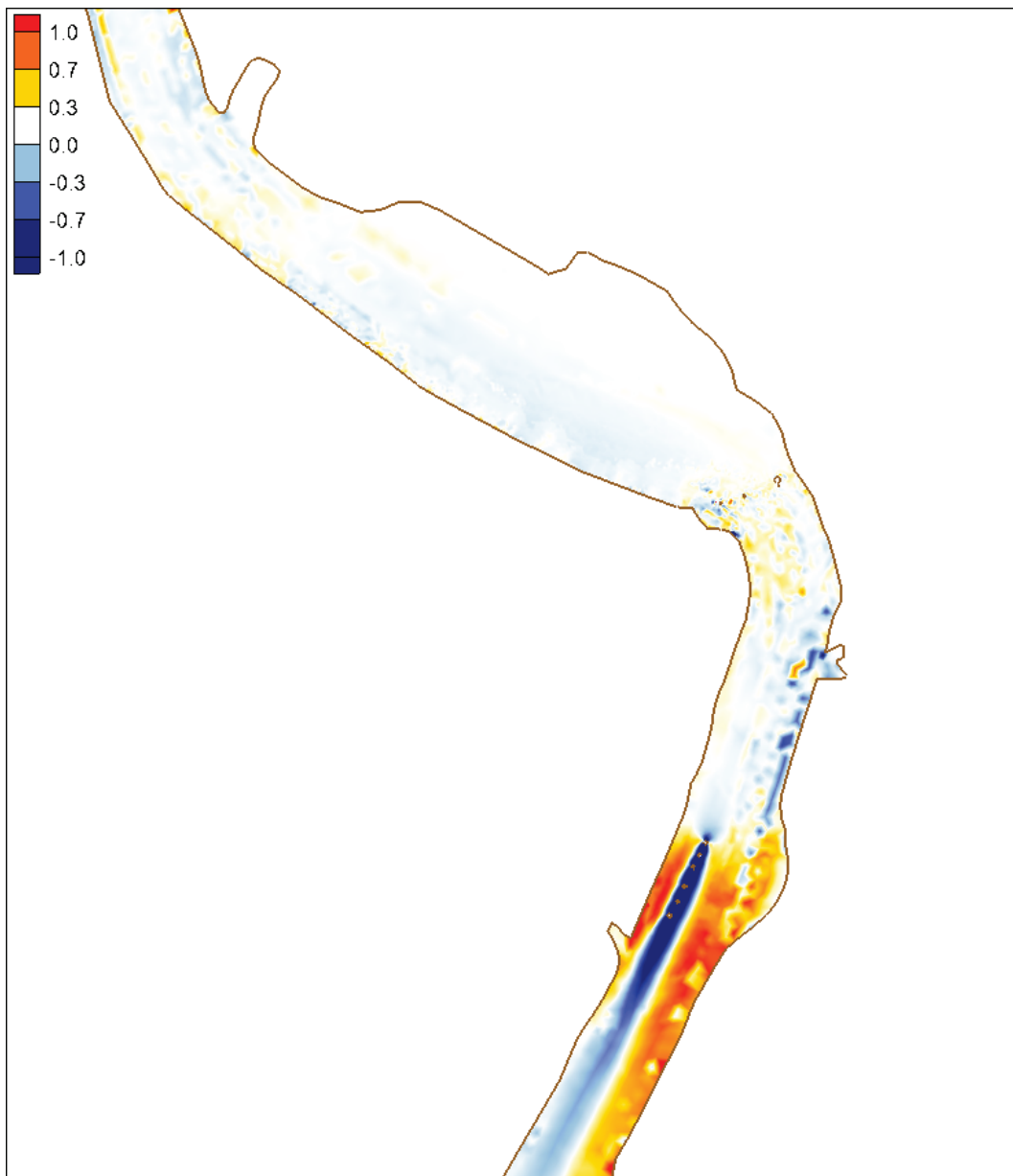


Figure 38. Bed shear AEC existing conditions minus existing conditions (red: AEC more; blue: AEC less).



7 Alternatives

Three potential shoaling reduction alternatives for the Jackson Bar were selected. The three alternatives implement one or a combination of multiple river training structures. All alternatives attempt to push currents to the left bank to minimize shoaling in the Jackson Bar. The plans described in detail in the first three sections are the 100% alternatives. These are the complete alternatives that have the maximum-sized training structures (i.e., 100%-build plans that will fit in the river given the required navigation clearances). Ten variations of the alternatives are simulated and are briefly described in section 7.4. Five alternatives, plans A–E, were initially presented to SAM, and from these, three of the alternatives were selected for further investigation, Plans B–D.

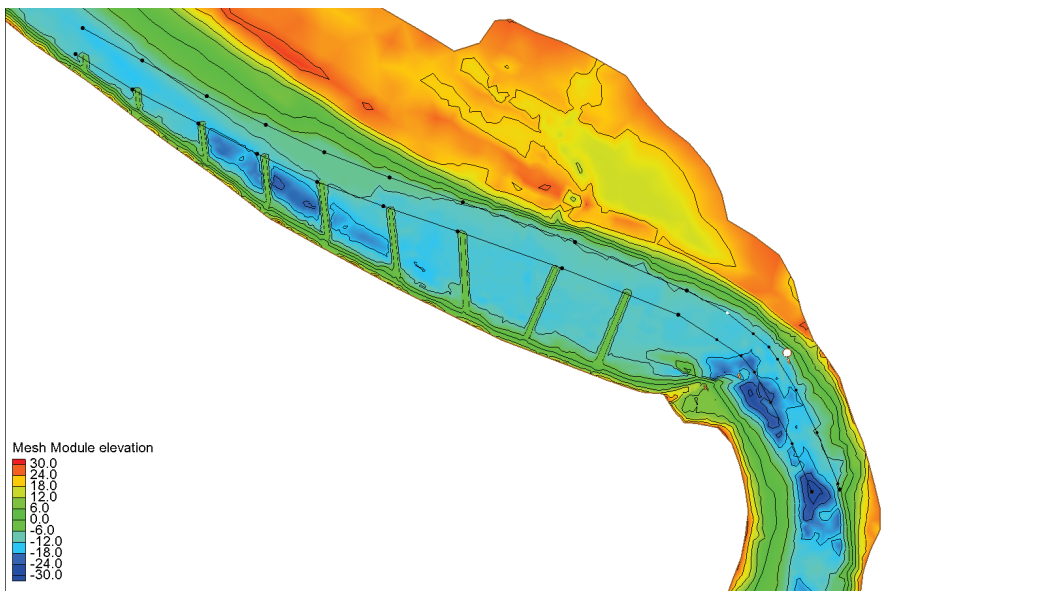
7.1 Plan B

Bendway weirs, first conceived in 1988 by Thomas J. Pokerefke, Jr. (Derrick et al. 1994), are defined as transverse rock structure in the navigation channel of a bend and are angled 30° upstream (Parchure 2005). Primary features include a crest elevation low enough to allow normal traffic to pass unimpeded, a significant length and height that captures an appropriate portion of the river conveyance at the cross section to produce hydraulic improvements (Parchure 2005), and a bulk head that ties the weir into the bank to prevent bank erosion.

Hydraulically, bendway weirs disrupt the secondary helical flow pattern. The disruption in the helical flow shifts the flow over and stabilizes the erosional side of the bend and encroaches on the depositional side, shifting the channel.

A modified bendway weir configuration, which also can be considered low-head dikes, was implemented for Plan B (Figure 39). The main goal of the weir field for Jackson Bar was to force the river crossing farther upstream for better channel alignment. This is not considered a typical application of the bendway weir concept. The bendway weir field was located primarily in the crossing upstream of the bridge, and only a portion was located in the bend.

Figure 39. Plan B bathymetry with training structure alignment and channel layout.



The bendway weir field consists of nine weirs that start approximately one mile upstream of the bridge (1800 ft upstream of the 2004 dredge cut) and allows for a 500 ft spacing (400–1,400 ft spacing typical (Parchure (2005)). As consistent with bendway weir design, the first seven are angled upstream while the last two, on the downstream end, are perpendicular to the bank. The first seven attempt to force the flow to the left bank. Then the final two weirs realign the flow with the bridge to form a smooth transition through the navigation pass.

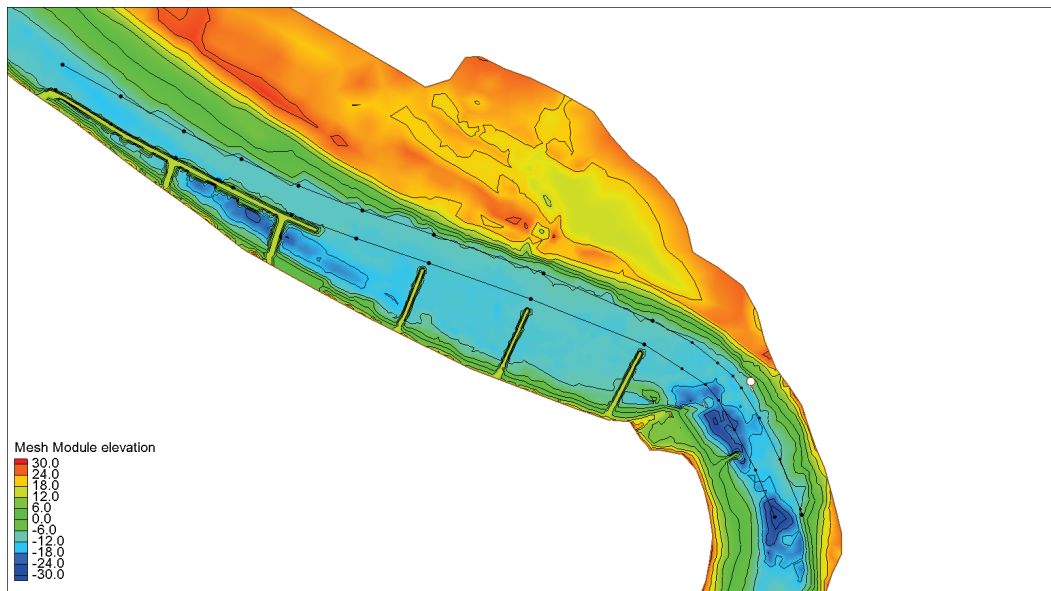
By definition, bendway weirs are in the defined navigation channel. However, for this application, the weir field skirts the right toe of the authorized channel allowing for a 200 ft channel free of any rip-rap. The weirs were kept out of the navigation channel to minimize interference with any future dredging needs. From weirs 3 through 6, counting from the upstream end down, a channel was cut in the model to allow for appropriate clearances. The cut removes a portion of the in-channel disposal. All weirs were flat top weirs and only sloped up at the bank to form an appropriate tie back. For additional protection, a 60 ft bulkhead was constructed. The bulkhead is a rock revetment that protects the bendway weir-keyed tie back. The length of the bulkhead was selected based on three times the bank height of 20 ft. One-third was extended upstream with the remaining portion downstream of the structure.

Four bendway weir crest elevations were simulated (−12, −9, −6, and 3 ft). From the four simulations, a design curve was constructed to aid in the selection of an appropriate height.

7.2 Plan C

For Plan C, a kicker and a series of transverse dikes were combined (Figure 40). Along with the structures, a pilot channel was cut through a portion of the in-channel disposal bar upstream of the dredge cut. The kicker, which is a longitudinal dike or retard, is a rock-filled structure that runs nearly parallel and close to the toe of the channel. It functions by reducing shear forces induced from secondary currents behind the structure, gradually forcing the thalweg over (Julien 2002), thereby improving channel alignment through thalweg redirection. The kicker starts approximately 1 mile upstream of the bridge and ends 0.50 mile downstream from its start.

Figure 40. Plan C bathymetry with training structure alignment and channel layout.



The top width of the kicker is 10 ft. The kicker is tied into the bank with two tie backs 1,000 ft apart. The tie backs maintain stability of the structure, protecting against scour and structural failure. Furthermore, they help induce deposition behind the structure, allowing the structure to ultimately backfill. Transverse dikes project perpendicularly from the bank into the channel and force the thalweg away from the bank. The dikes prevent the thalweg from moving back to the right bank. Typically with a dike field, the channel will deepen, forming a narrower cross section. Here

the primary goal is to more forcefully induce the thalweg crossing sooner, allowing for a smoother navigation pass alignment.

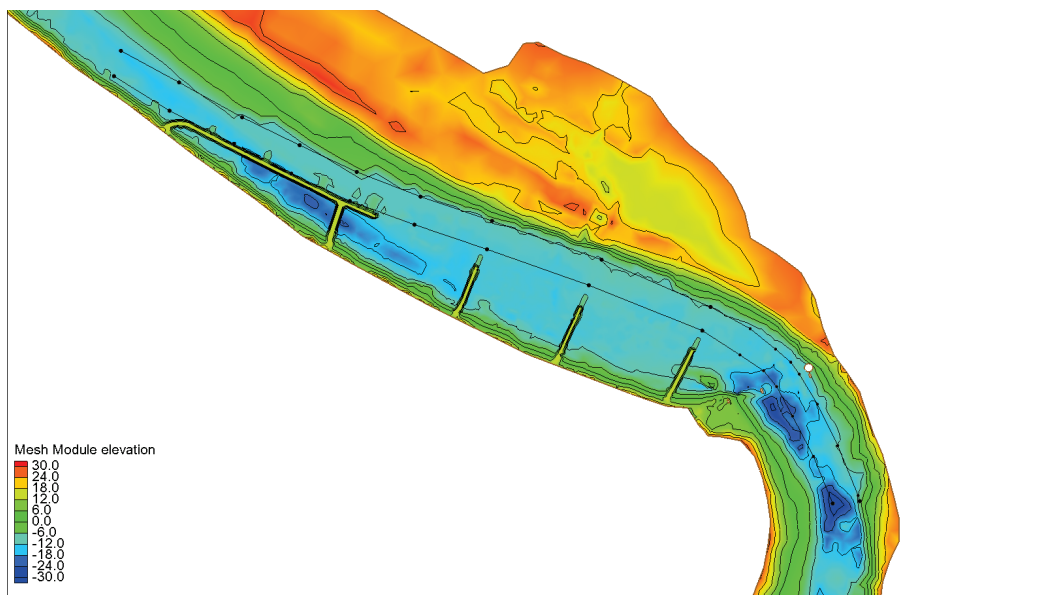
For Plan C, four transverse dikes were implemented. The first three were located upstream of the bridge. The fourth dike was downstream. All four training structures were set at approximately 800 ft spacing. The downstream-most dike was approximately 500 ft downstream of the Norfolk Southern railroad bridge. All four were rock filled and have a top width of 10 ft. A higher probability of success is assumed for Plan C structures than the other plans due to the increase in flow blockage provided by these types of training structure. To fully understand the potential of Plan C, the structures were simulated at various elevations. Three crest elevations were simulated (3, 11, and 21 ft). From the three simulations, a design curve was constructed to aide in the selection of an appropriate height.

7.3 Plan D

Plan D includes a series of bendway weirs, transverse dikes, and a kicker to redirect and retain the thalweg on the left side of the channel (Figure 41). The kicker starts 500 ft farther downstream than the Plan C kicker. The Plan D kicker only used one tie back and had a top width of 10 ft. In this configuration the shorter kicker requires significantly less rock for construction. Bendway weirs were placed upstream of the kicker and along the in-channel side of the kicker. Two bendway weirs were upstream of the kicker while four bendway weirs were tied directly into the kicker. The two bendway weirs upstream were angled 30° upstream, and the four along the kicker were perpendicular and were approximately 100 ft long. These six bendway weirs were approximately 400 ft apart. The bendway weirs were intended to aid the shorter kicker in moving the crossing upstream, while using less rock than the larger Plan C kicker.

Three transverse dikes transition downstream from the kicker. The dikes, just as in Plan C, were spaced 800 ft apart. Top width was 10 ft. The difference in this plan was that the tips of the transverse dikes transition into bendway weirs. These bendway weirs are approximately 80 ft long and end at the right edge of the defined channel. Based on information learned from the previous alternatives, the elevations of the kicker and transverse dike were set at 11 ft while the bendway weirs were 9 ft NGVD 1929.

Figure 41. Plan D bathymetry with training structure alignment and channel layout.



7.4 Additional plans

Beyond the 100% alternatives (Plan B–D), variations of each were simulated. These variations attempted to address two issues. First, as previously stated, the required crest elevation of the structures was unclear, so seven of the alternatives for Plans B and C evaluated the effect of various top elevations. Second, as with all river training structure behavior, it is difficult to numerically model and capture their exact behavior with a 2D model. Understanding the behavior of a partial 100% alternative was important, so four simulations were devoted to this aspect. The partial 100% alternatives simulate only a portion of the training structures shown previously and represent an in-between stage of construction. All alternative simulations are listed and described in Table 6.

Table 6. Alternative plan descriptions.

Alternative	Description
Plan B	Bendway weirs set at a top elevation of -12 ft NGVD
Plan B_2	Bendway weirs set at a top elevation of 3 ft NGVD
Plan B_3	Bendway weirs set at a top elevation of -6 ft NGVD
Plan B_4	Bendway weirs set at a top elevation of -9 ft NGVD
Plan C	Kicker and transverse dikes set at a top elevation of 3 ft NGVD
Plan C_3	Kicker and transverse dikes set at a top elevation of 21 ft NGVD
Plan C_4	Kicker and transverse dikes set at a top elevation of 11 ft NGVD
Plan C Kicker	Kicker only set at a top elevation of 11 ft NGVD
Plan D	Kicker and transverse dikes set at a top elevation of 11 ft NGVD with bendway weirs at -9 ft NGVD
Plan D Kicker	Kicker only (without dikes or bendway weirs) and set at a top elevation of 11 ft NGVD
Plan D Power Plant	Kicker and transverse dikes set at a top elevation of 11 ft NGVD with bendway weirs at -9 ft NGVD
Plan D Kicker DS Dike Power Plant	Kicker from Plan D along with the Plan C downstream of bridge dike, The kicker set at a top elevation of 11 ft NGVD and dike at 3 ft NGVD
Plan D 50% Dike Power Plant	Kicker and 50% length on transverse dikes set at a top elevation of 11 ft NGVD no with bendway weirs

8 Results

The results of the alternative model simulations provide insight into the dredging reduction potential and possible navigation impacts. For the existing conditions models and Plan D alternative models, the results shown are deposition at the end of the hydrograph, velocity, and bed shear stress. For Plan B and Plan C alternatives, which are shown to be less desirable, only the deposition and velocity difference results are shown. The outputs provide the basic insight into the potential in each alternative as related to dredging reduction. Results are shown with the 2004 dredge cut outlined in black.

8.1 Existing conditions models

Two existing conditions models were created for the purpose of comparison to the alternatives. Results from both are shown to provide an understanding of the character of the system and its current behavior. The first model, existing conditions, was used for the validation. The second model, AEC existing conditions model, was created to evaluate the potential of shoaling at the AEC power plant.

8.1.1 Existing conditions model

The existing conditions model showed the shoaling patterns as expected at Jackson Bar. It adequately calculates the volume of shoaling that was dredged in the 2004 dredge cut for Jackson Bar. The model also illustrates the manner in which the right bank is undermined (Figure 42). Peak velocities occur at day 87 when the maximum flood occurs (Figure 43). Maximum bed shear along Jackson Bar is 3.31 Pa with an average of 0.38 Pa (Figure 44).

8.1.2 AEC existing conditions model

The AEC existing conditions model also showed the shoaling patterns as expected at Jackson Bar. However, it calculated 18% less dredging than was conducted in 2004 for Jackson Bar. Just as in the existing conditions, it also illustrated the manner in which the right bank is undermined (Figure 45). Peak velocities occur at day 87 when the maximum flood occurs (Figure 46). Maximum bed shear along Jackson Bar is 3.21 Pa with an average of 0.42 Pa (Figure 47).

Figure 42. Existing conditions deposition (feet) at the end of the simulation, Jackson Bar.

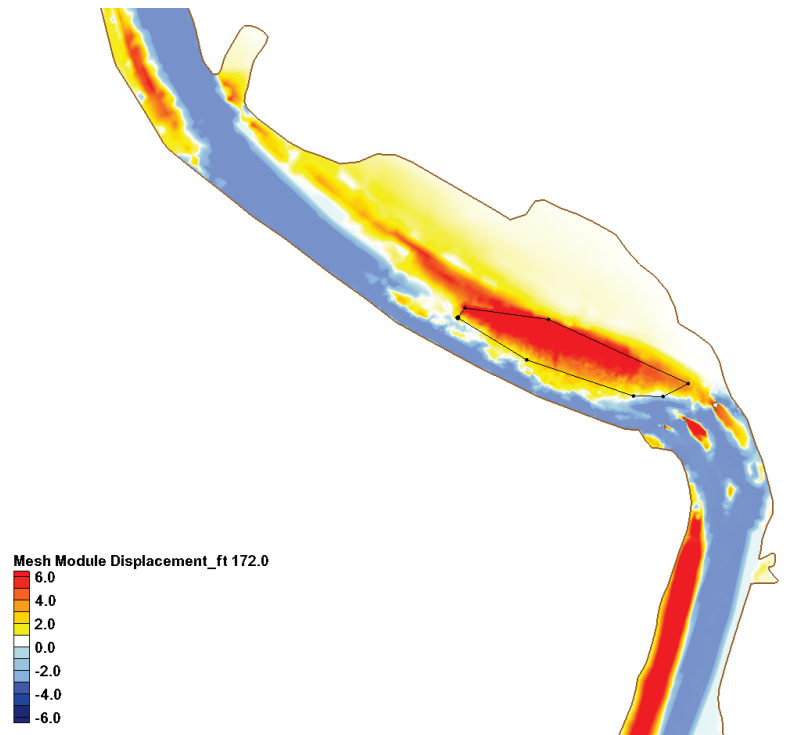


Figure 43. Existing conditions velocities (feet/second) at peak flow, day 87.

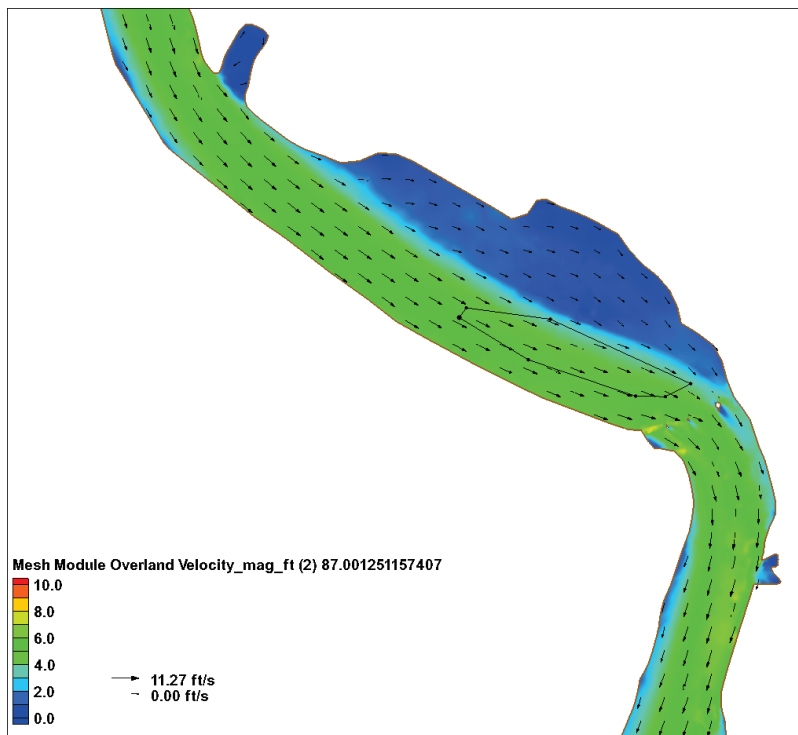


Figure 44. Existing conditions maximum bed shear stress, in pascals.

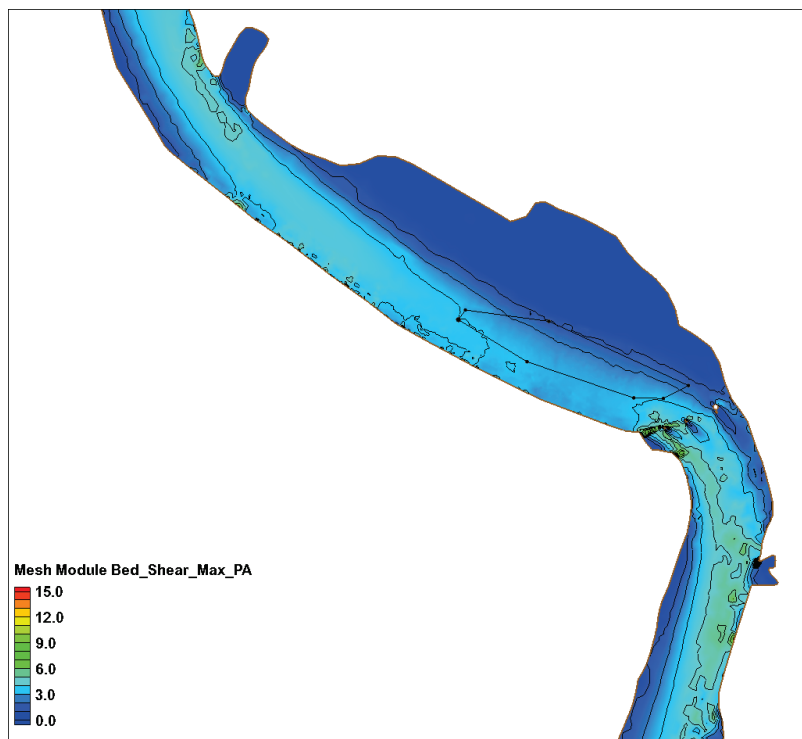


Figure 45. AEC existing conditions deposition (feet) at the end of the hydrograph, Jackson Bar.

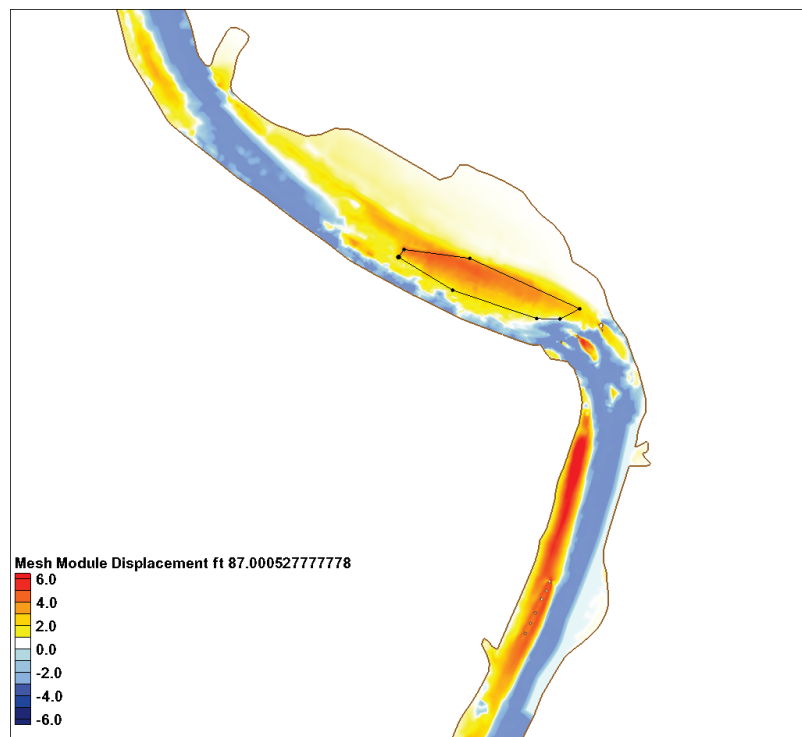


Figure 46. AEC existing conditions velocities (feet/second) at peak flow, day 87.

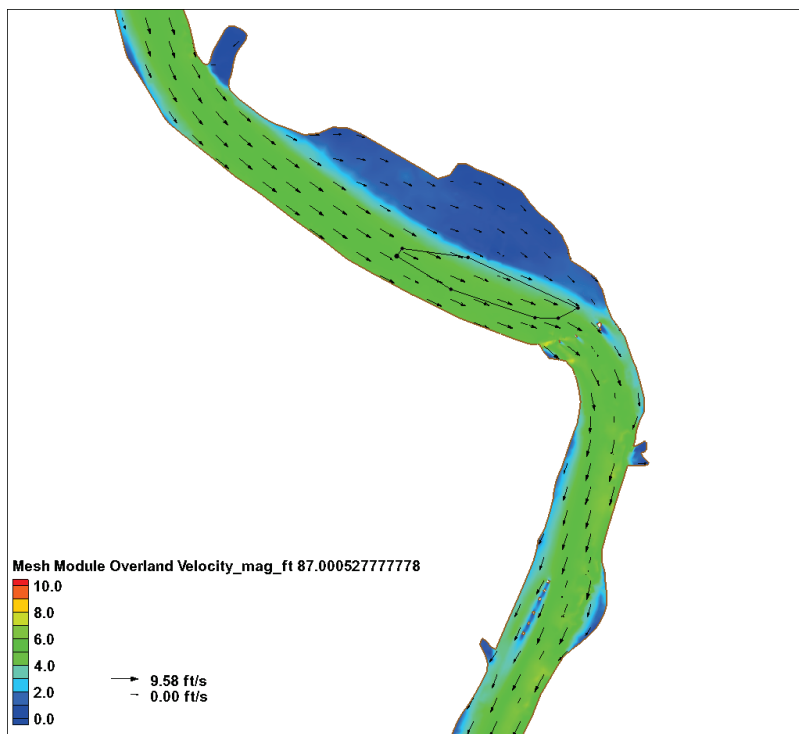
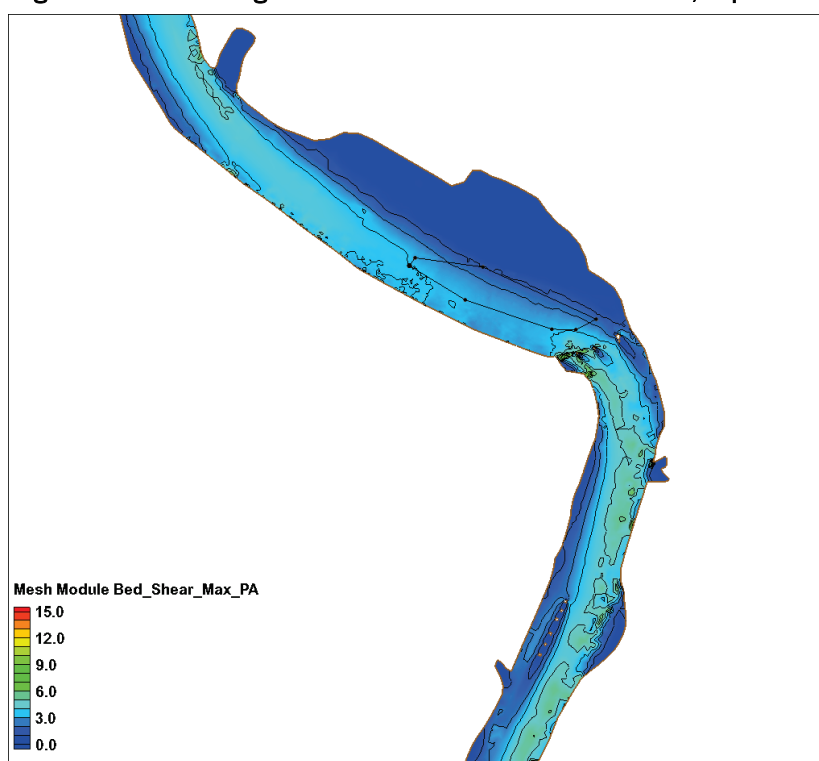


Figure 47. AEC existing conditions maximum bed shear stress, in pascals.



8.2 Plan B

The addition of bendway weirs changed the currents and adjusted the deposition at Jackson Bar. However, with the exception of Plan B_2, none of the alternatives could maintain the channel (Figures 48–51). The varied depositional impacts of the four alternatives are shown in Figure 52. The curve in Figure 52 provides a design guideline for structure top elevation.

The temporal velocity variations comparing all Plan B alternatives and the existing conditions model are shown in Figures 53 and 54. For all the alternatives, velocities peak 2,000 ft upstream of the Norfolk Southern railroad bridge along the thalweg (Figures 55–58). For Plan B, Plan_2, Plan B_3, and Plan B_4, the most significant increase for the velocities was approximately 0.5 ft/sec above the existing conditions (Table 7). The Plan B_2 increase was more considerable with a maximum increase of 3.6 ft/sec.

Figure 48. Plan B_2 deposition (feet) at the end of the simulation.

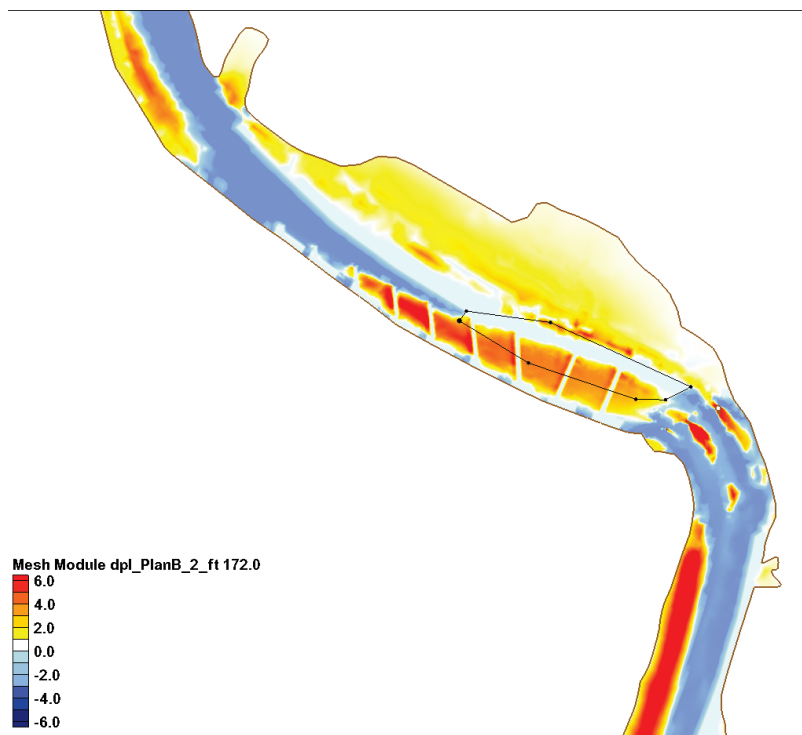


Figure 49. Plan B_3 deposition (feet) at the end of the simulation.

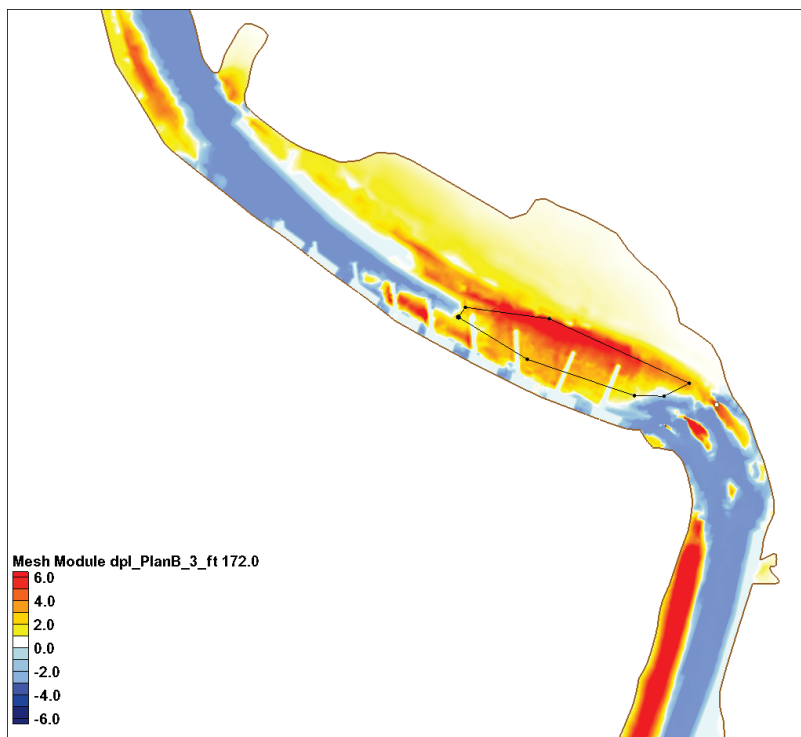


Figure 50. Plan B_4 deposition (feet) at the end of the simulation.

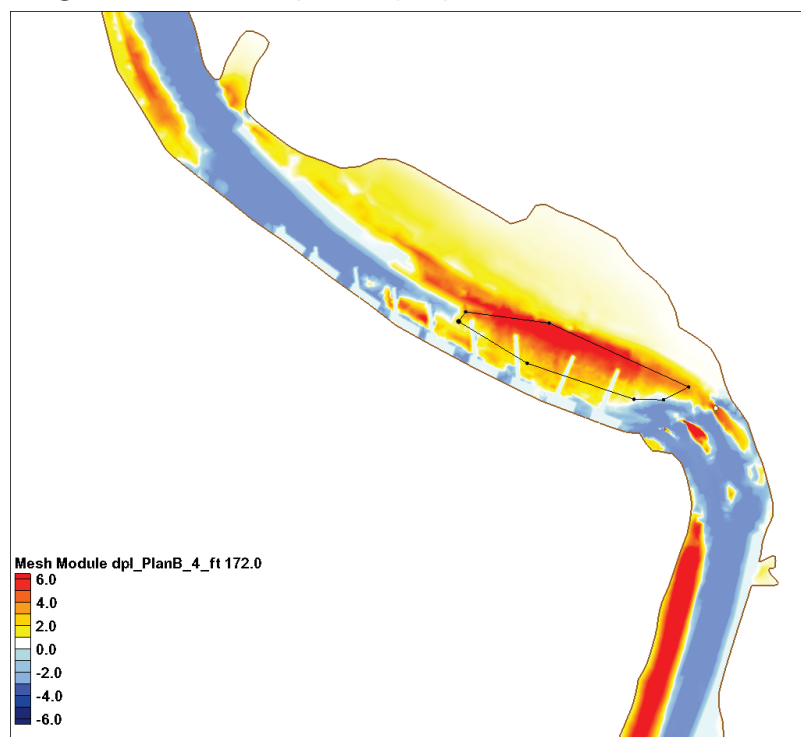


Figure 51. Plan B deposition (feet) at the end of the simulation.

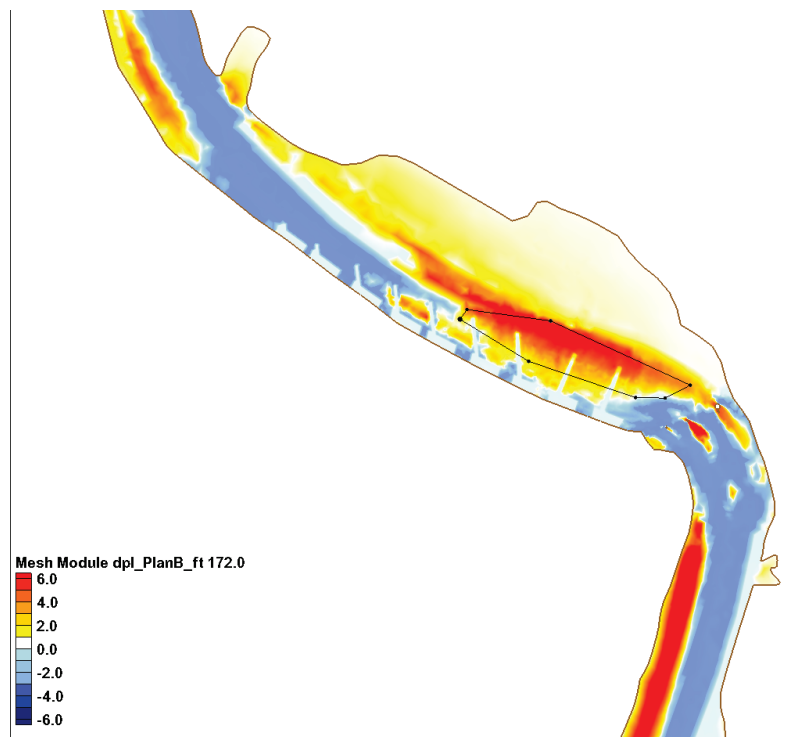


Figure 52. Deposition in dredge cut vs. structure elevation for Plan B alternatives.

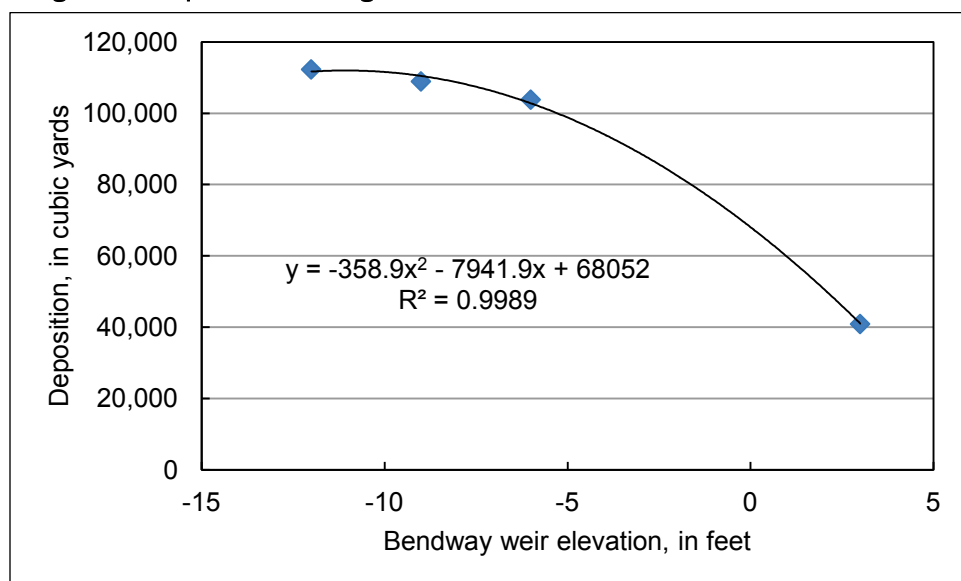


Figure 53. Velocity comparisons for Plan B at the Norfolk Southern railroad bridge.

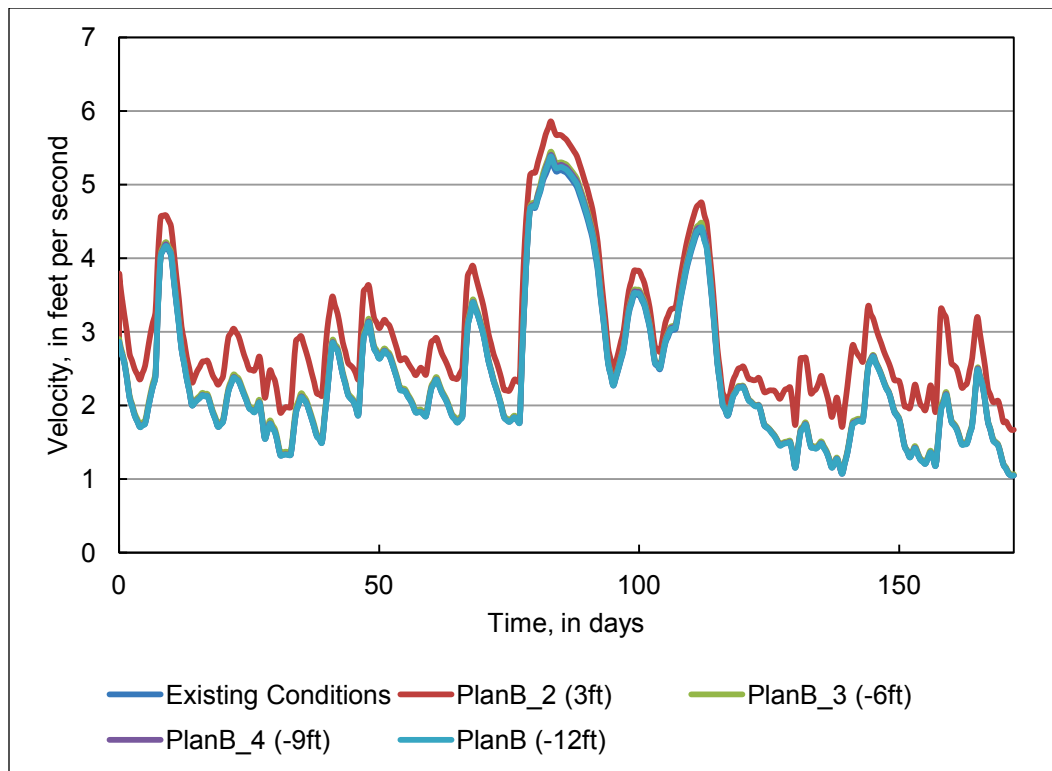


Figure 54. Velocity comparisons for Plan B, 2,000 ft upstream of the Norfolk Southern railroad bridge.

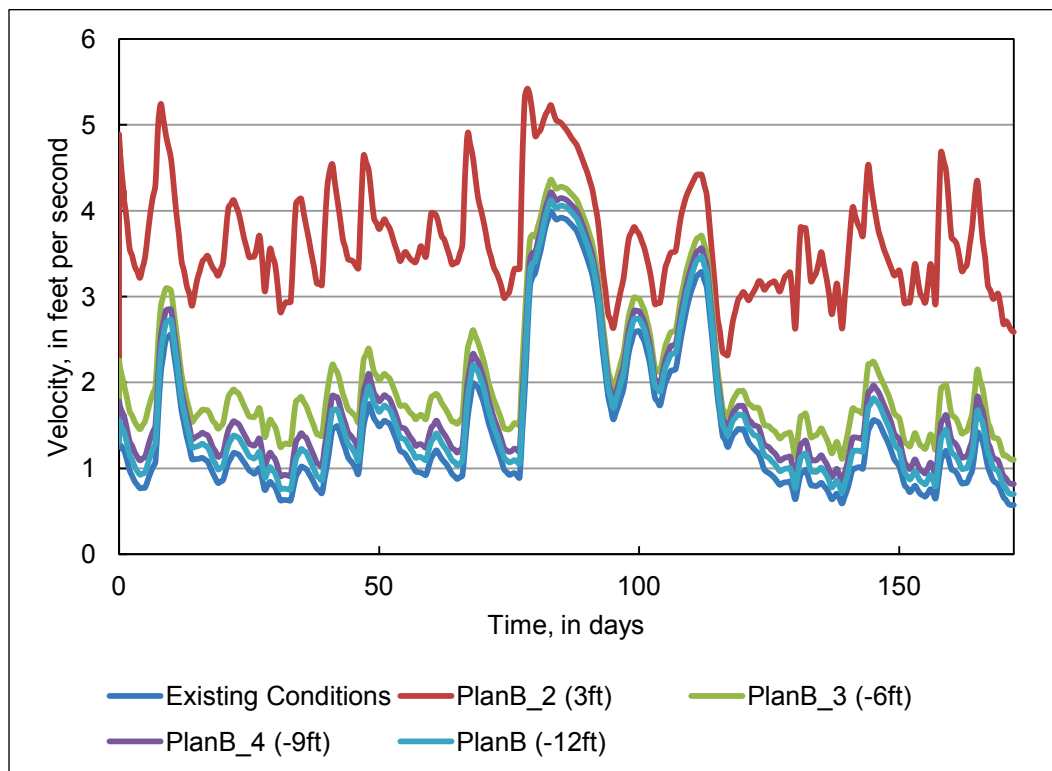


Figure 55. Plan B_2 minus existing conditions, velocity difference, feet/second (red: Plan B_2 higher; blue: Plan B_2 lower).

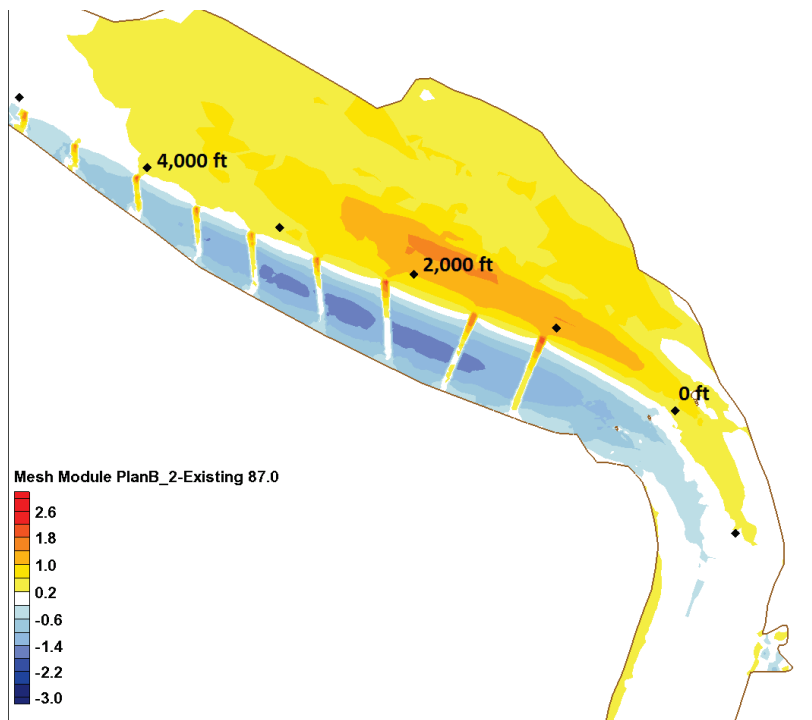


Figure 56. Plan B_3 minus existing conditions, velocity difference, feet/second (red: Plan B_3 higher; blue: Plan B_3 lower).

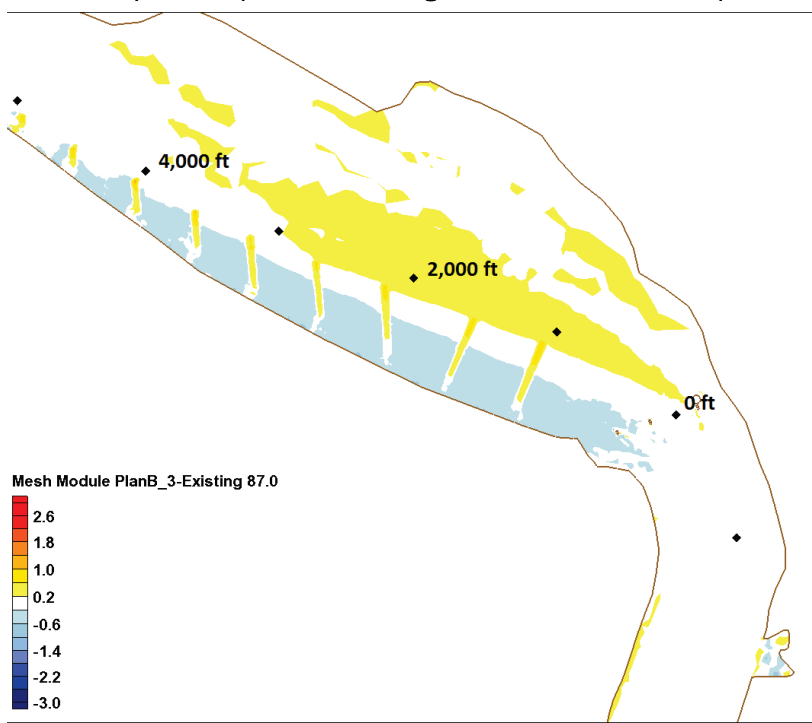


Figure 57. Plan B_4 minus existing conditions, velocity difference, feet/second (red: Plan B_4 higher; blue: Plan B_4 lower).

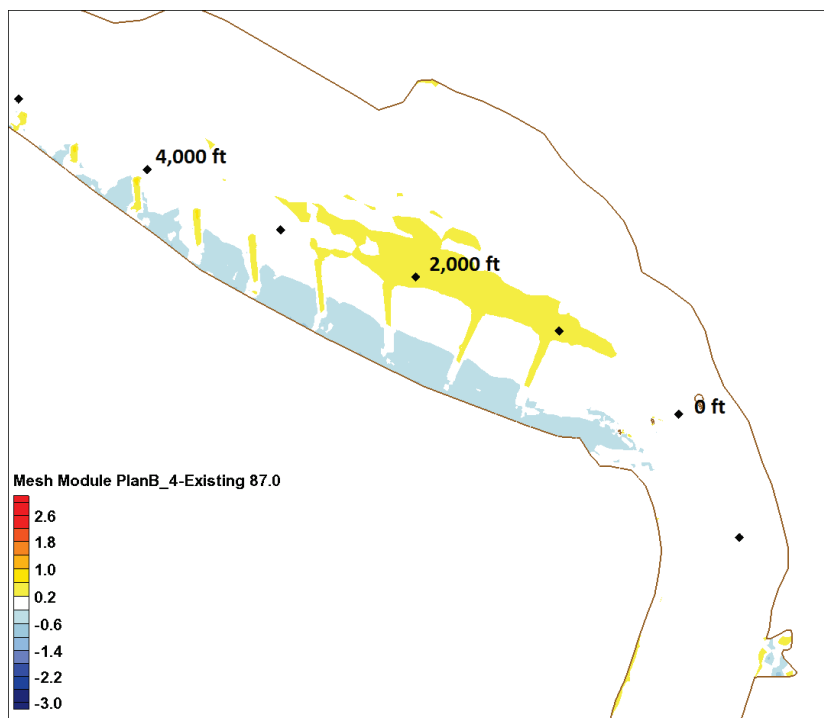


Figure 58. Plan B minus existing conditions, velocity difference, feet/second (red: Plan B higher; blue: Plan B lower).

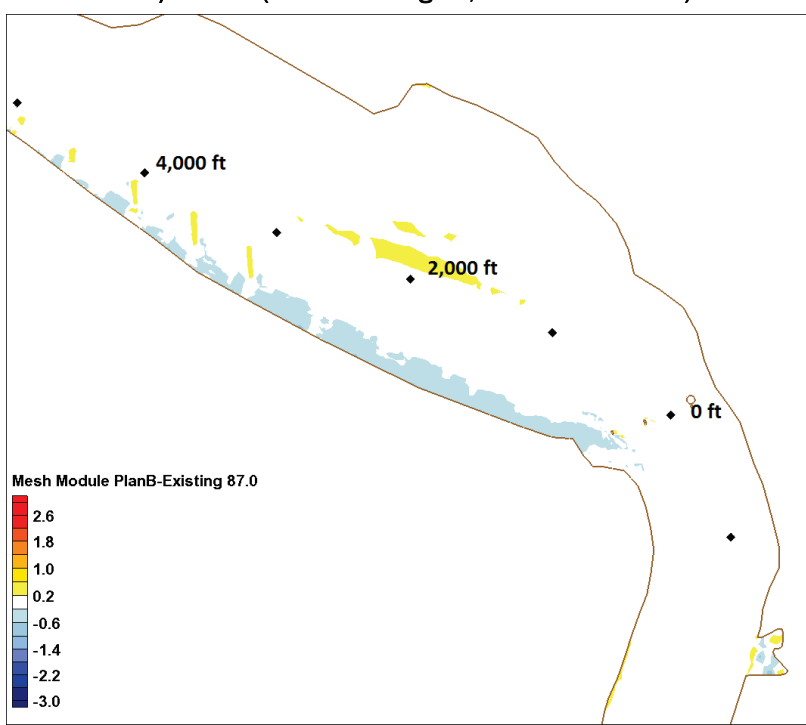


Table 7. Statistical analysis of velocity, in feet per second, for Plan B alternatives minus existing conditions.

Station, feet	Statistical measure	Plan B_2	Plan B_3	Plan B_4	Plan B
0	average	0.608	0.035	0.007	-0.002
	standard deviation	0.208	0.025	0.02	0.015
	variance	0.0432	0.0006	0.0004	0.0002
	maximum	1.37	0.13	0.08	0.06
	minimum	0.17	-0.09	-0.06	-0.05
1,000	average	2.373	0.502	0.239	0.116
	standard deviation	0.628	0.115	0.053	0.031
	variance	0.3949	0.0132	0.0028	0.0009
	maximum	3.71	0.73	0.35	0.18
	minimum	0.97	0.27	0.12	0.04
2,000	average	2.466	0.643	0.334	0.186
	standard deviation	0.734	0.176	0.076	0.038
	variance	0.5383	0.031	0.0058	0.0015
	maximum	3.59	0.98	0.5	0.28
	minimum	0.92	0.31	0.19	0.11
3,000	average	1.842	0.474	0.234	0.101
	standard deviation	0.603	0.172	0.095	0.067
	variance	0.3634	0.0295	0.0091	0.0045
	maximum	2.938	1.017	0.596	0.341
	minimum	0.578	0.149	0.065	-0.009
4,000	average	0.764	0.237	0.154	0.104
	standard deviation	0.249	0.07	0.035	0.02
	variance	0.0619	0.0048	0.0012	0.0004
	maximum	1.35	0.5	0.29	0.18
	minimum	0.31	0.11	0.08	0.06
5,000	average	-0.074	-0.02	-0.012	-0.007
	standard deviation	0.041	0.017	0.016	0.015
	variance	0.0017	0.0003	0.0002	0.0002
	maximum	-0.01	0.02	0.03	0.04
	minimum	-0.47	-0.11	-0.07	-0.08

8.3 Plan C

The additions of a kicker and transverse dikes created a significant redirection of the thalweg. The redirection dramatically adjusted the deposition at Jackson Bar. All plans could wholly or partially maintain the channel (Figures 59–62). The varied depositional impacts of the four alternatives are shown in Figure 63. The curve in Figure 63 provides a design guideline for structure top elevation.

The temporal velocity variations comparing all Plan C alternatives and the existing conditions model are shown in Figures 64 and 65. For all the alternatives, velocities peak at approximately 2,000 ft upstream of the bridge (Figures 66–69). Plan C_3 had the most significant increase for velocities with a peak of approximately 6.2 ft/sec above the existing conditions and a temporal average over the hydrograph of 3.2 ft/sec (Table 8). For Plan C_4, the temporal average increase was 2.8 ft/sec with a maximum of 4.8 ft/sec. However, both Plan C_4 and Plan C_3 maintained the channel.

Figure 59. Plan C deposition (feet) at the end of the simulation.

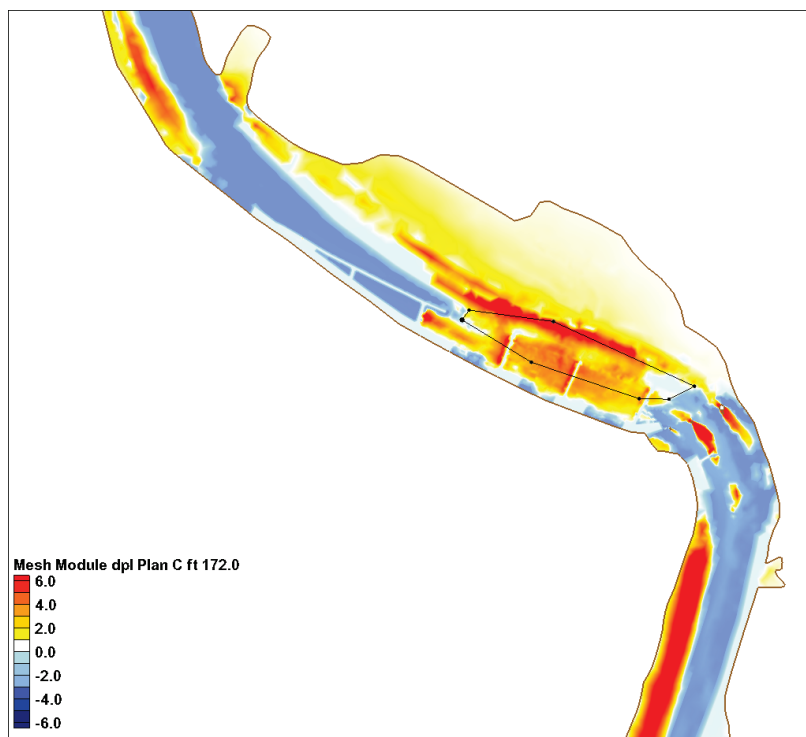


Figure 60. Plan C_4 deposition (feet) at the end of the simulation.

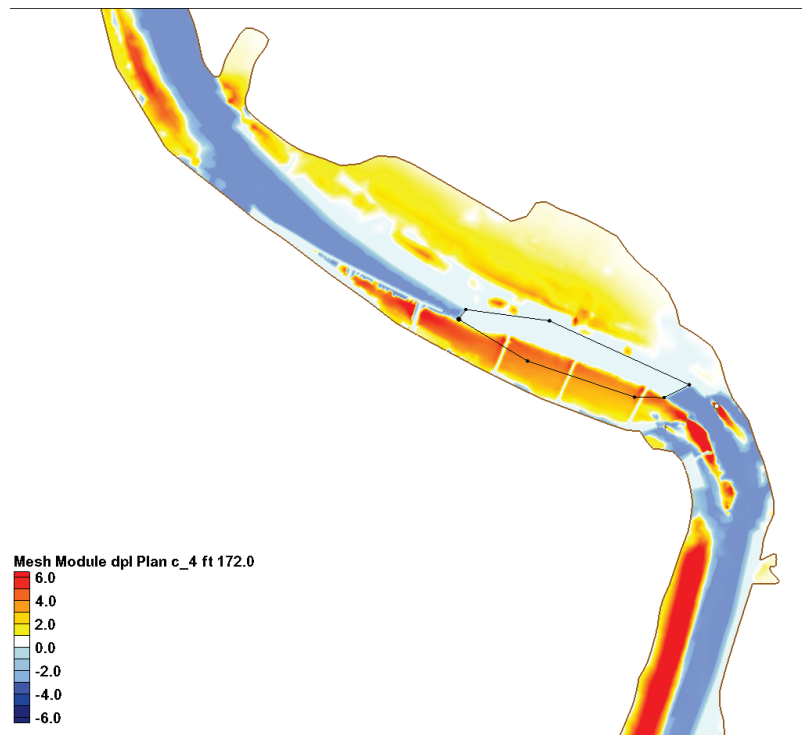


Figure 61. Plan C_3 deposition (feet) at the end of the simulation.

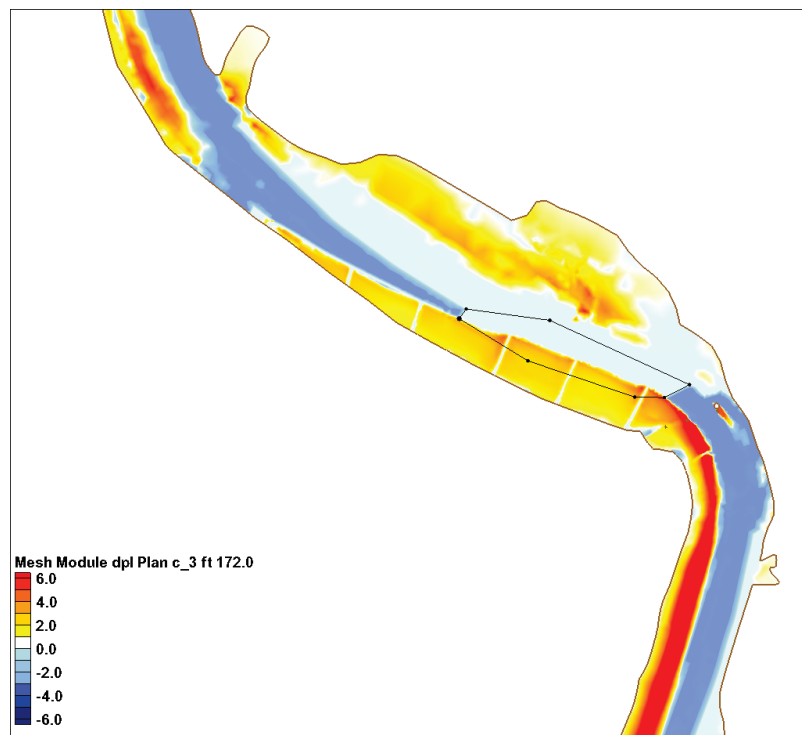


Figure 62. Plan C Kicker deposition (feet) at the end of the simulation.

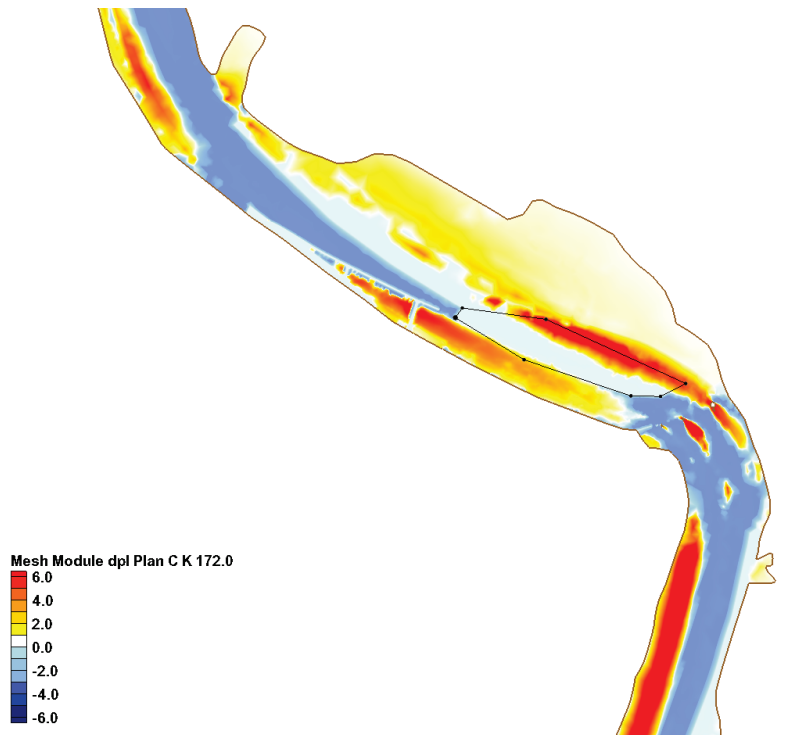


Figure 63. Deposition in dredge cut vs. structure elevation for Plan C alternatives.

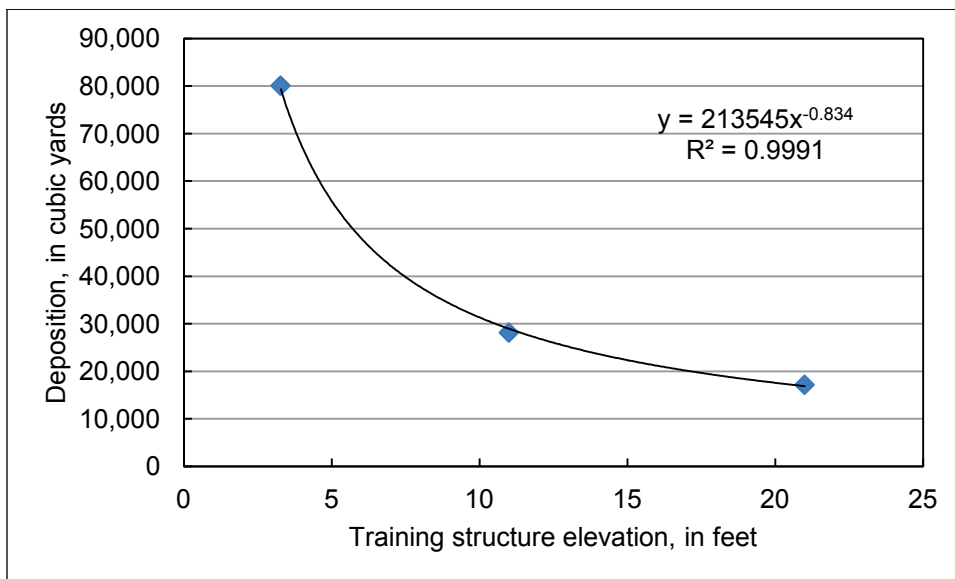


Figure 64. Velocity comparisons for Plan C at the Norfolk Southern railroad bridge.

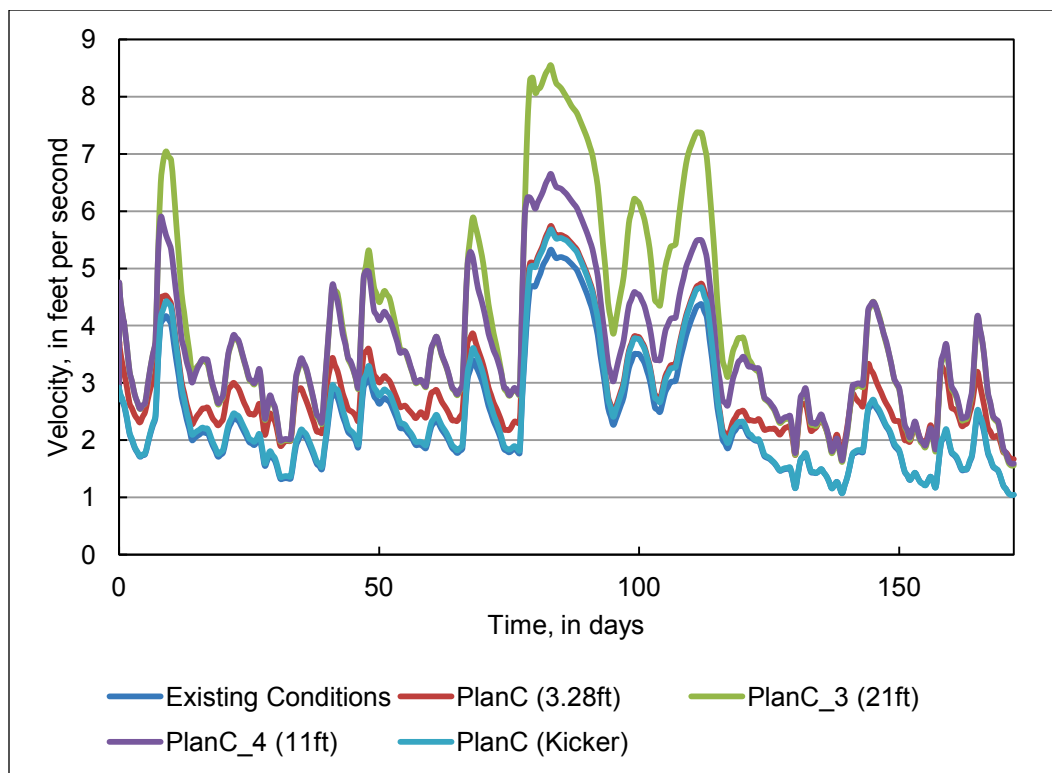


Figure 65. Velocity comparisons for Plan C, 2,000 ft upstream of the Norfolk Southern railroad bridge.

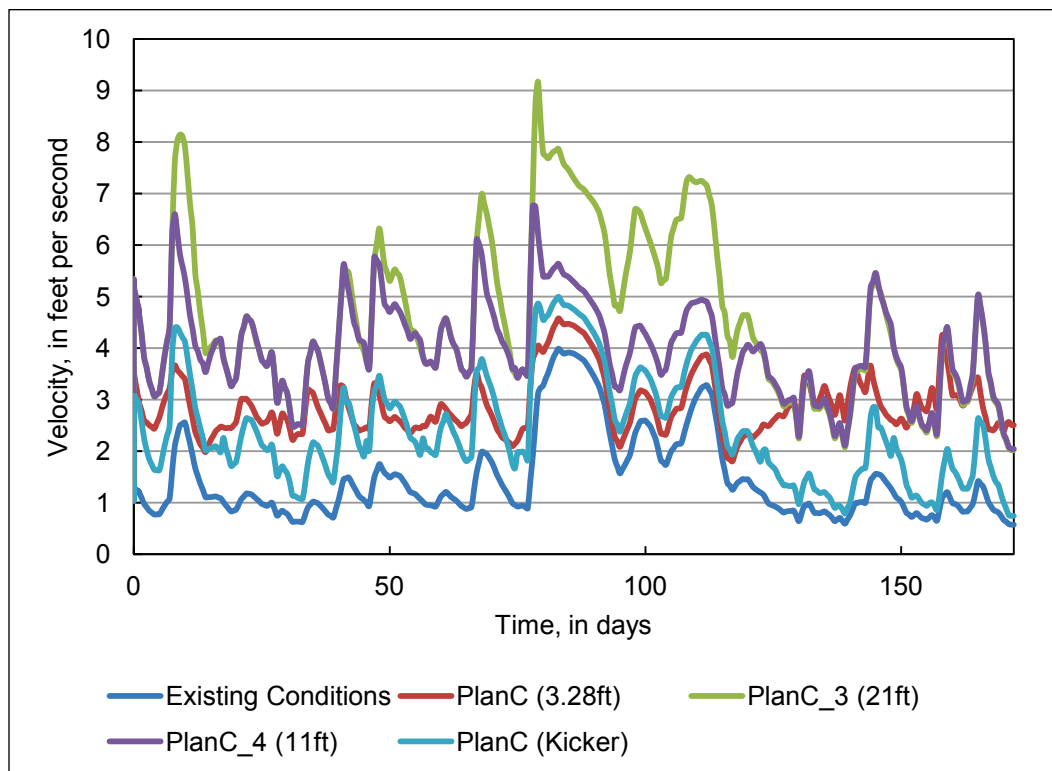


Figure 66. Plan C minus existing conditions, velocity difference, feet/second (red: Plan C higher; blue: Plan C lower).

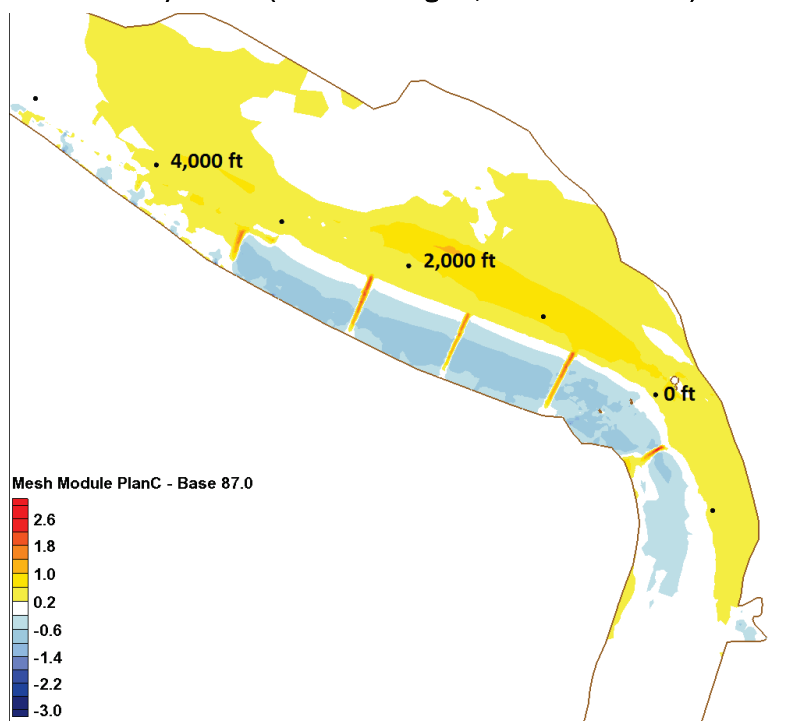


Figure 67. Plan C_3 minus existing conditions, velocity difference, feet/second (red: Plan C_3 higher; blue: Plan C_3 lower).

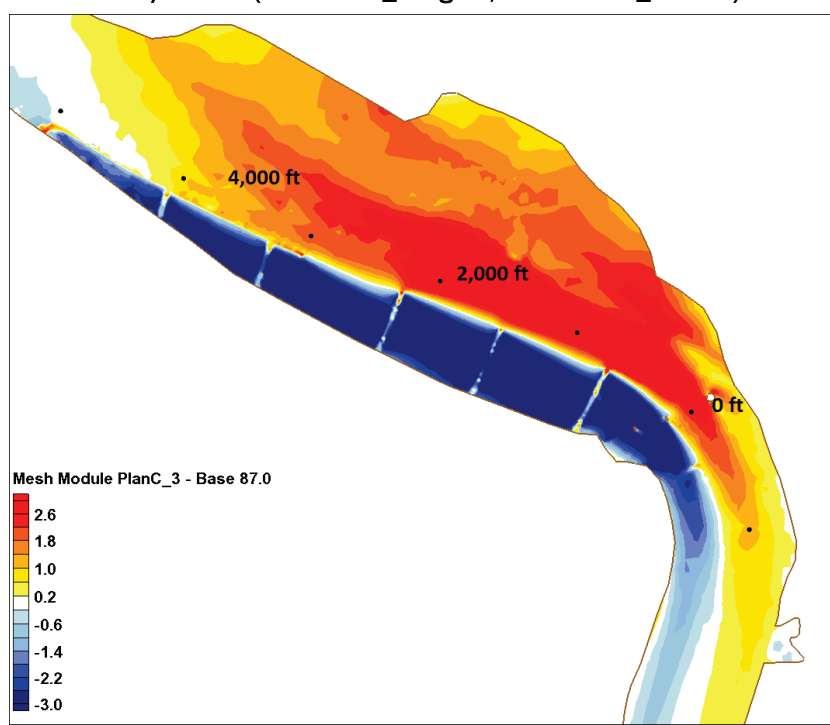


Figure 68. Plan C_4 minus existing conditions, velocity difference, feet/second (red: Plan C_4 higher; blue: Plan C_4 lower).

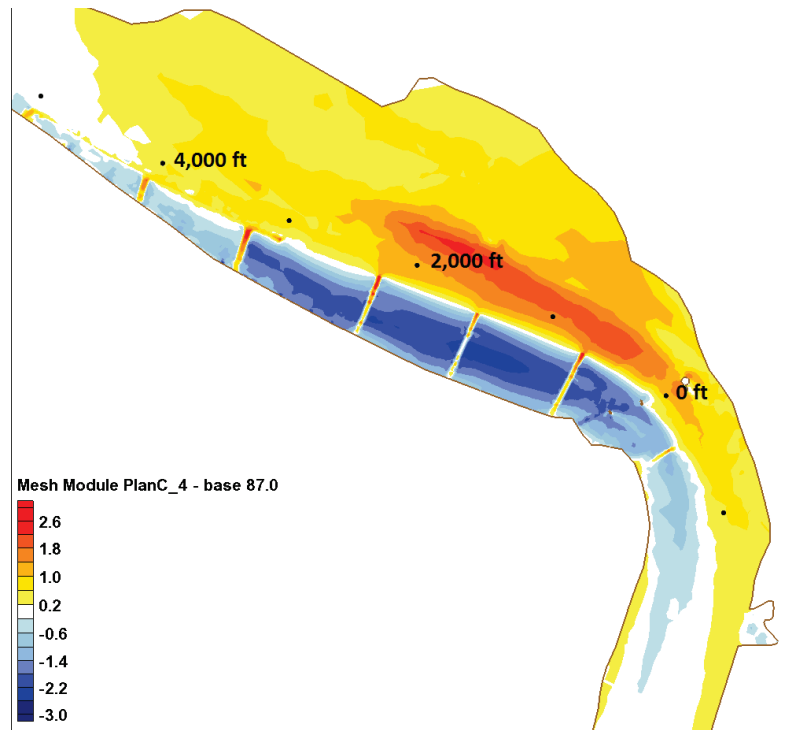


Figure 69. Plan C Kicker minus existing conditions, velocity difference, feet/second (red: Plan C higher; blue: Plan C lower).

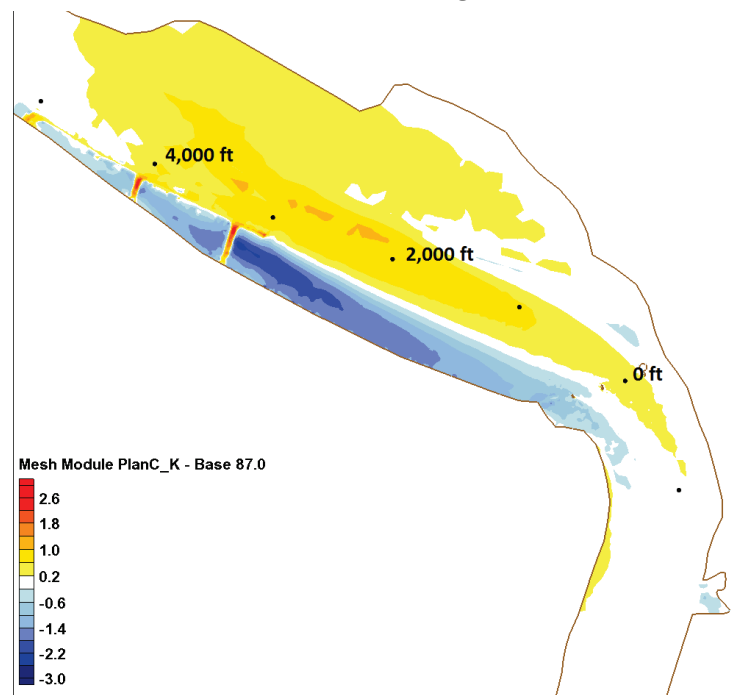


Table 8. Statistical analysis of velocity, in feet per second, for Plan C alternatives minus existing conditions.

Station, feet	Statistical measure	Plan C	Plan C_3	Plan C_4	Plan C K
0	average	0.565	1.553	1.271	0.083
	standard deviation	0.197	0.625	0.335	0.094
	variance	0.0390	0.3902	0.1120	0.0088
	maximum	1.35	3.64	2.42	0.36
	minimum	0.17	0.51	0.54	-0.17
1,000	average	1.439	2.791	2.440	0.217
	standard deviation	0.433	0.784	0.612	0.256
	variance	0.1872	0.6154	0.3747	0.0656
	maximum	2.57	5.65	4.13	1.04
	minimum	0.54	1.12	1.13	-0.64
2,000	average	1.580	3.256	2.844	1.174
	standard deviation	0.586	0.805	0.822	0.500
	variance	0.3439	0.6481	0.6756	0.2500
	maximum	3.15	6.18	4.83	2.31
	minimum	0.43	1.45	1.34	-0.27
3,000	average	0.975	2.291	1.981	2.093
	standard deviation	0.367	0.438	0.613	0.597
	variance	0.1347	0.1921	0.3754	0.3565
	maximum	1.99	3.70	2.96	3.06
	minimum	0.30	1.38	0.74	0.96
4,000	average	0.548	1.019	0.906	0.972
	standard deviation	0.136	0.206	0.267	0.288
	variance	0.0184	0.0423	0.0715	0.0831
	maximum	0.87	1.42	1.42	1.51
	minimum	0.27	0.59	0.44	0.47
5,000	average	0.037	0.086	0.070	0.113
	standard deviation	0.022	0.046	0.045	0.040
	variance	0.0005	0.0021	0.0020	0.0016
	maximum	0.07	0.15	0.13	0.17
	minimum	-0.21	-0.31	-0.32	-0.03

8.4 Plan D

The additions of a kicker, bendway weirs, and transverse dikes created a significant redirection of the thalweg. The redirection dramatically adjusted the deposition at Jackson Bar. Both alternatives maintain the channel (Figures 70–71). The temporal velocity variations comparing both Plan D alternatives and the existing conditions model are shown in Figures 72 and 73. For both alternatives, velocities peak farther upstream than those of the previous plans at approximately 3,000 ft upstream of the bridge (Figures 74 and 75). Plan D had the most significant velocity increase with a peak approximately 3.6 ft/sec above the existing conditions and a temporal average over the hydrograph of 2.3 ft/sec (Table 9). For Plan D Kicker, the temporal average increase was 2.3 ft/sec with a maximum of 3.2 ft/sec. However, both Plan D and Plan D Kicker maintained the channel.

The temporal maximum bed shear stress for Plan D minus existing conditions ranged in the Jackson Bar vicinity from 5.3–0 Pa with an average of 2.32 Pa. The temporal maximum shear for Plan D in the same area was 8.01 Pa with the average 1.19 Pa. The temporal maximum bed shear stress for Plan D Kicker minus existing conditions ranged in the Jackson Bar vicinity from 4.5–0 Pa with an average of 1.58 Pa. The temporal maximum shear for Plan D in the same area was 6.02 Pa with an average of 0.94 Pa. Figures 76 and 77 show bed shear differences.

Figure 70. Plan D deposition (feet) at the end of the simulation.

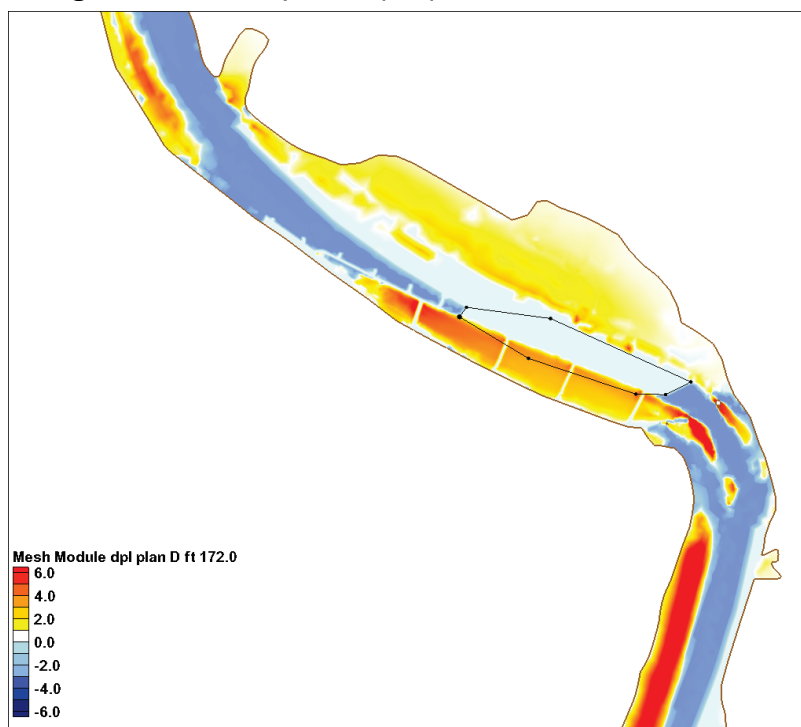


Figure 71. Plan D Kicker deposition (feet) at the end of the simulation.

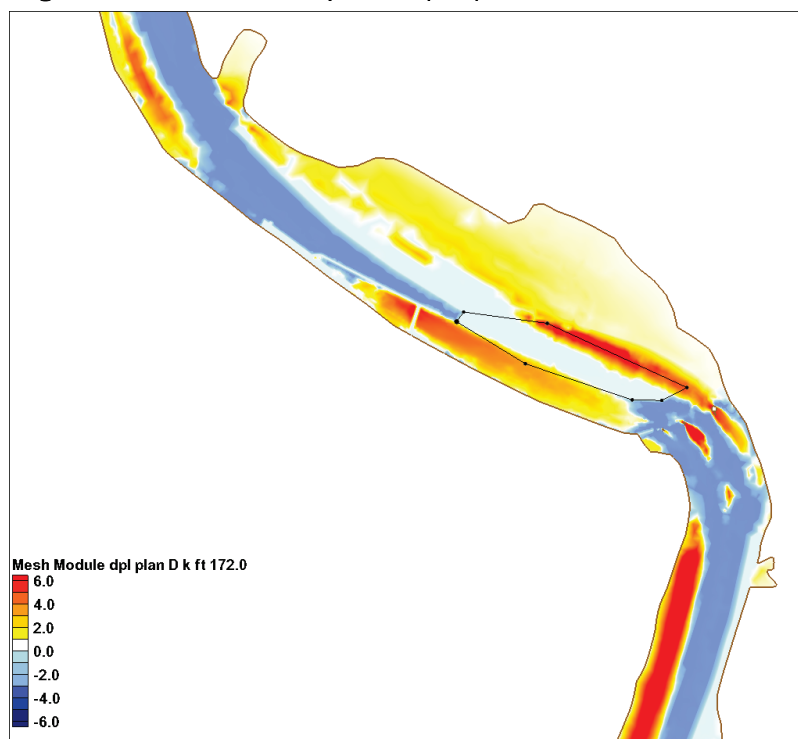


Figure 72. Velocity comparisons for Plan D at the Norfolk Southern railroad bridge.

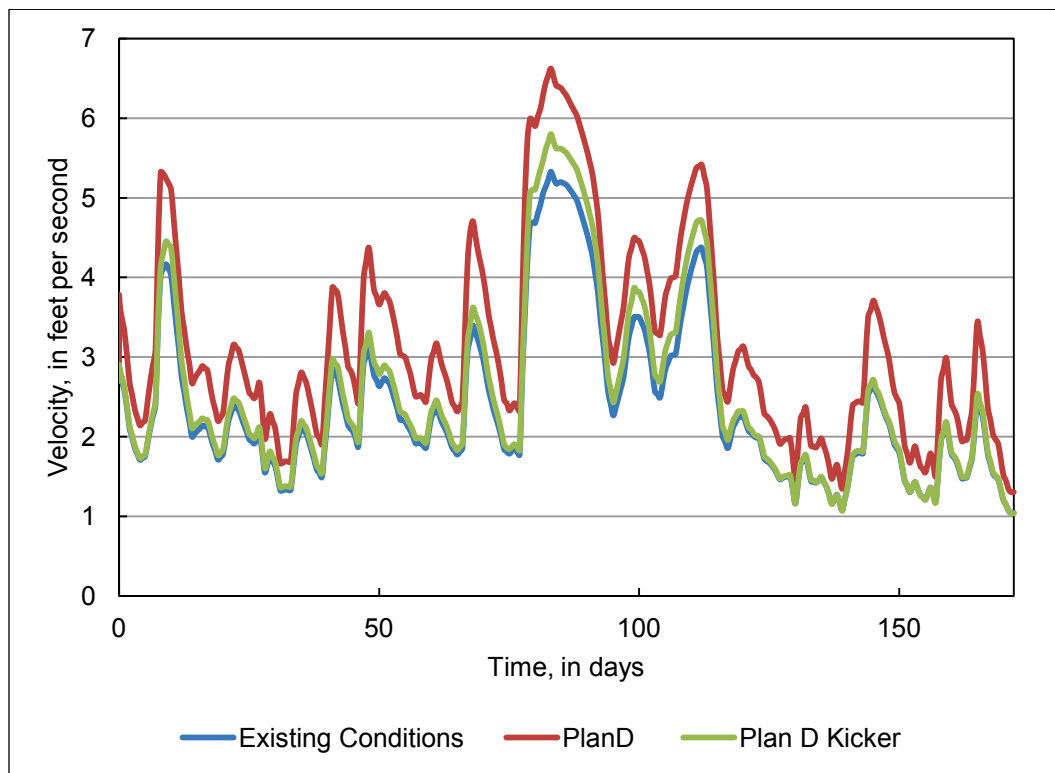


Figure 73. Plan D, 3,000 ft upstream of the Norfolk Southern railroad bridge.

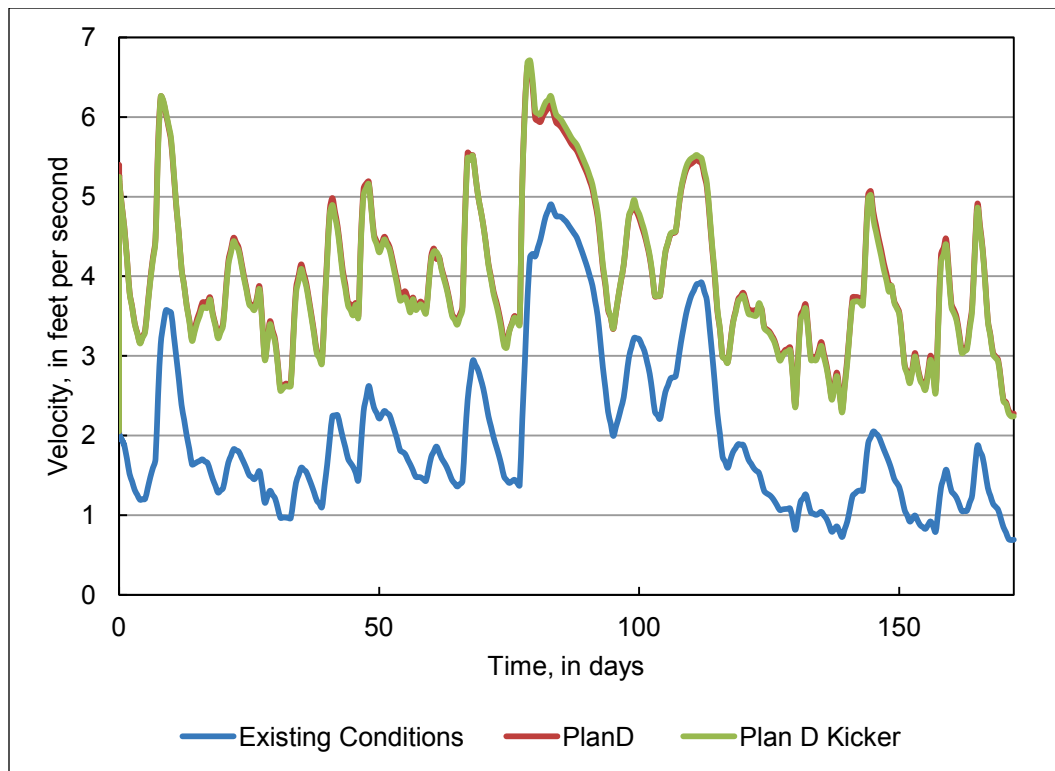


Figure 74. Plan D minus existing conditions, velocity difference, feet/second (red: Plan D higher; blue: Plan D lower).

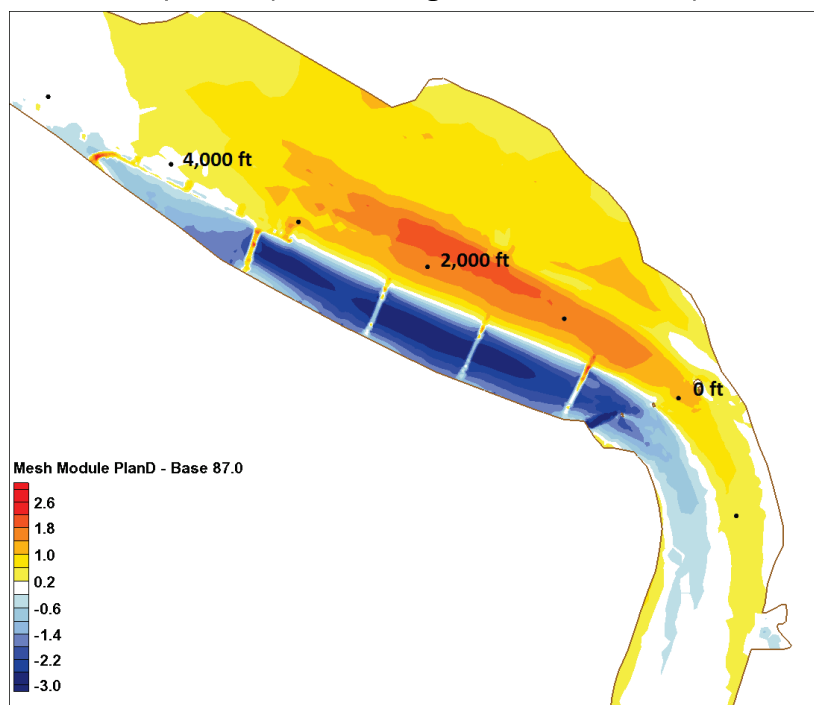


Figure 75. Plan D Kicker minus existing conditions, velocity difference, feet/second (red: Plan D Kicker higher; blue: Plan D Kicker lower).

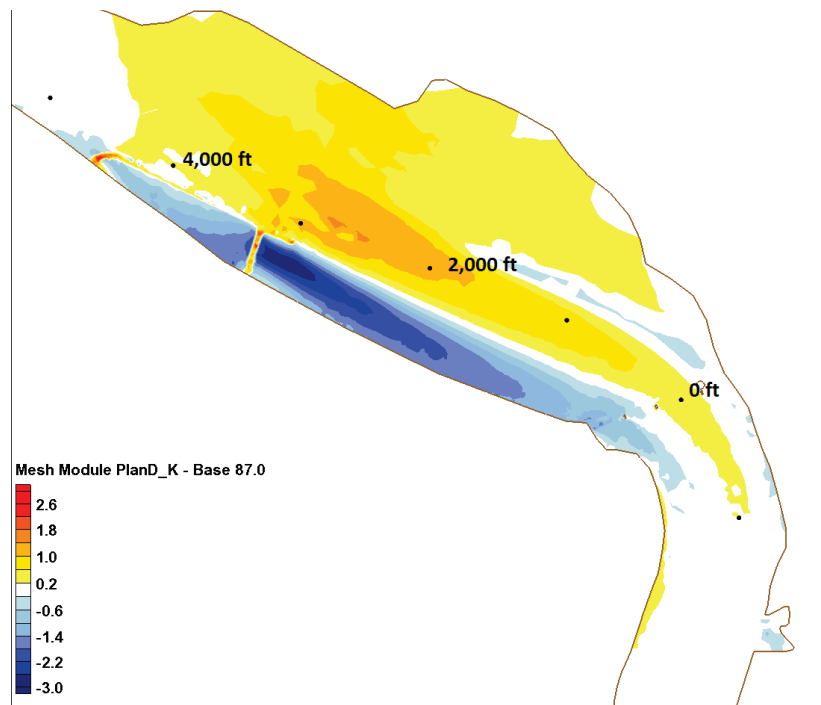


Table 9. Statistical analysis of velocity, in feet per second, for Plan D alternatives minus existing conditions.

Station, feet	Statistical measure	Plan D	Plan D_K
0	average	0.757	0.098
	standard deviation	0.225	0.113
	variance	0.0505	0.0127
	maximum	1.52	0.47
	minimum	0.26	-0.18
1,000	average	1.739	0.386
	standard deviation	0.420	0.273
	variance	0.1760	0.0747
	maximum	2.93	1.29
	minimum	0.74	-0.79
2,000	average	2.003	1.509
	standard deviation	0.507	0.541
	variance	0.2572	0.2923
	maximum	3.57	2.52
	minimum	0.83	-0.38

Station, feet	Statistical measure	Plan D	Plan D_K
3,000	average	2.278	2.263
	standard deviation	0.588	0.575
	variance	0.3458	0.3306
	maximum	3.35	3.20
	minimum	1.07	1.15
4,000	average	0.808	0.833
	standard deviation	0.320	0.314
	variance	0.1021	0.0987
	maximum	1.39	1.33
	minimum	0.11	0.18
5,000	average	-0.065	-0.061
	standard deviation	0.040	0.035
	variance	0.0016	0.0013
	maximum	0.01	0.01
	minimum	-0.37	-0.28

Figure 76. Maximum bed shear for Plan D minus existing conditions, pascals (red: Plan D higher; blue: Plan D lower).

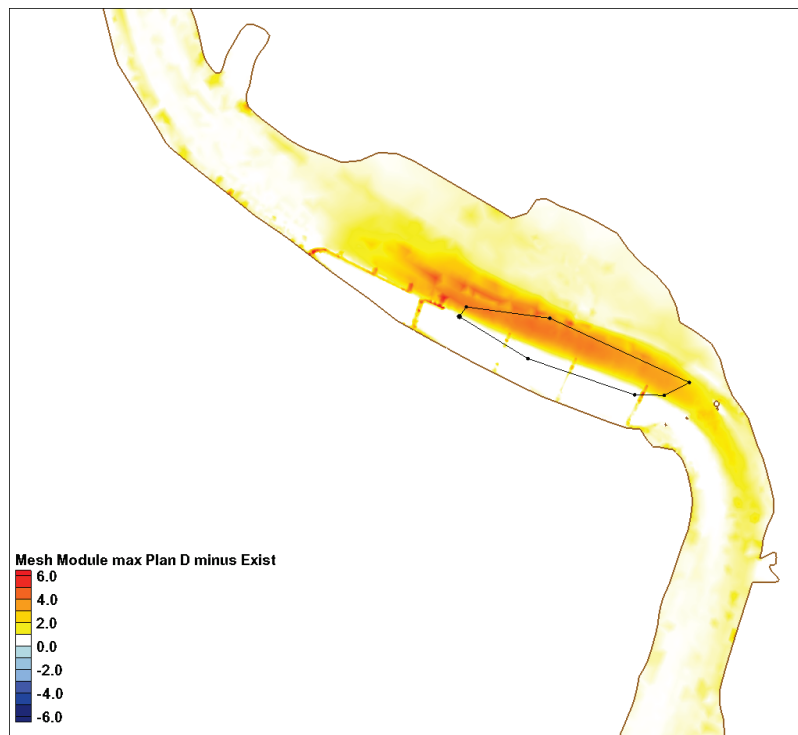
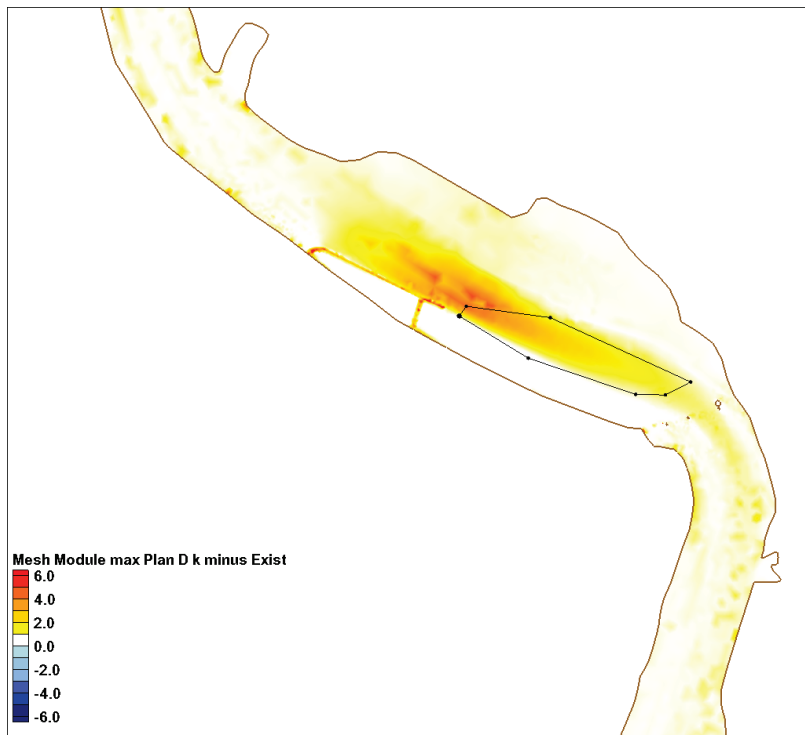


Figure 77. Maximum bed shear for Plan D Kicker minus existing conditions, pascals (red: Plan D Kicker higher; blue: Plan D Kicker lower).



8.5 Plan D AEC Power Plant

The addition of the AEC cells to Plan D required additional simulations of the Plan D Kicker and bendway weirs with transverse dikes. Again, these training structures created a significant redirection of the thalweg. The redirection dramatically adjusted the deposition at Jackson Bar. The plans, kicker only and kicker with 50%-length dikes, maintain the channel (Figures 78–80). The temporal velocity variations comparing Plan D Power Plant, Plan D 50% Dike DS Dike Power Plant, Plan D Kicker DS Dike Power Plant alternatives, and the AEC existing conditions model are shown in Figures 81 and 82. Here, for both alternatives, velocities peak approximately 3,000 ft upstream of the bridge (Figures 83–85). Plan D Power Plant had the most significant increase for velocities with a peak of approximately 3.19 ft/sec above the existing conditions and a temporal average increase over the hydrograph of 1.96 ft/sec (Table 10). For Plan D 50% Dike DS Dike Power Plant, the temporal average increase was 1.92 ft/sec with a maximum of 3.12 ft/sec. For Plan D Kicker DS Dike Power Plant, the temporal average increase was 1.98 ft/sec with a maximum increase of 2.4 ft/sec. However, all three plans maintained the channel.

The temporal maximum bed shear stress for Plan D Power Plant minus AEC existing conditions ranged in the Jackson Bar vicinity from 5.35 to 0 Pa with an average increase of 1.97 Pa. The temporal maximum shear for Plan D Power Plant in the same area is 7.71 Pa with the average 1.26 Pa. The temporal maximum bed shear stress for Plan D 50% Dike DS Dike Power Plant minus AEC existing conditions ranged in the Jackson Bar vicinity from 3.9 to 0 Pa with an average increase of 1.86 Pa. The temporal maximum shear for Plan D 50% Dike DS Dike Power Plant in the same area is 5.75 Pa with the average 1.08 Pa. The temporal maximum bed shear stress for Plan D Kicker DS Dike Power Plant minus AEC existing conditions ranged in the Jackson Bar vicinity from 4.41 to 0 Pa with an average increase of 1.54 Pa. The temporal maximum shear for Plan D Kicker DS Dike Power Plant in the same area was 6.05 Pa with the average 1.05 Pa. Figures 86–88 show bed shear differences.

Figure 78. Plan D Power Plant deposition (feet) at the end of the simulation.

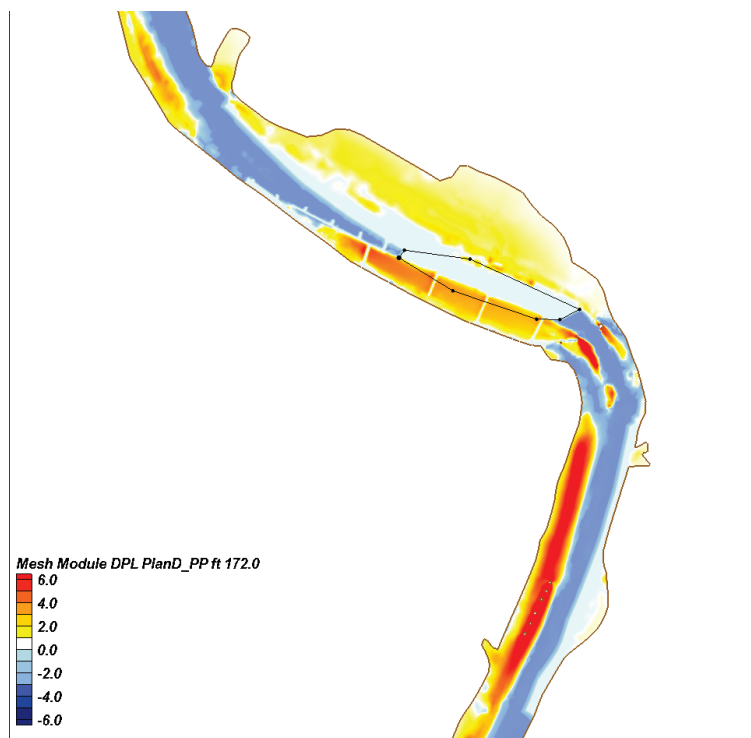


Figure 79. Plan D 50% Dike Downstream Dike Power Plant deposition (feet) at the end of the simulation.

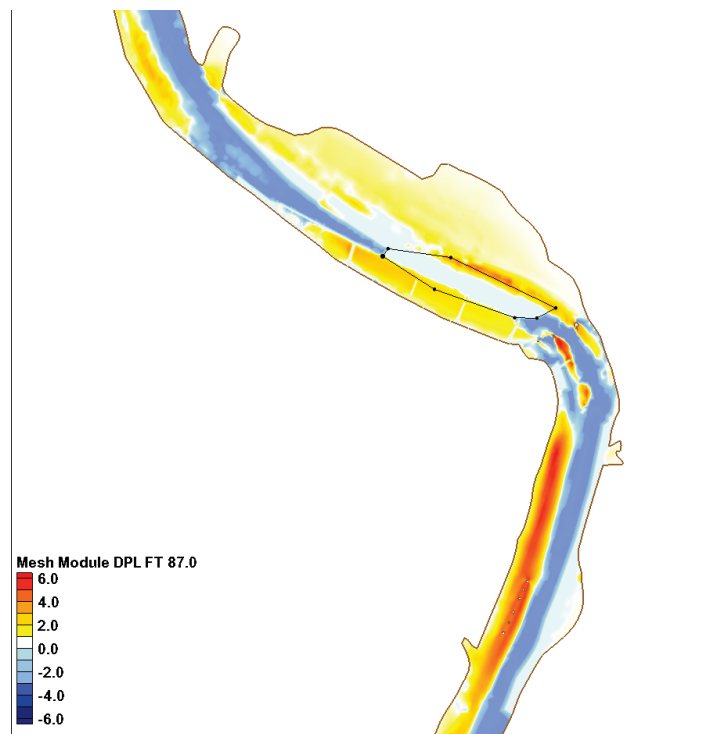


Figure 80. Plan D Kicker Downstream Dike Power Plant deposition (feet) at the end of the simulation.

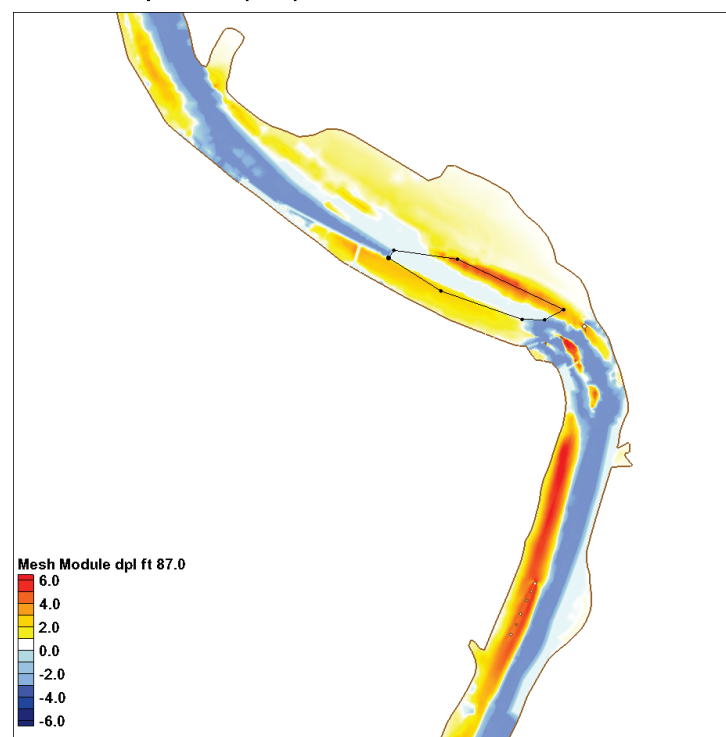


Figure 81. Velocity comparisons for Plan D Power Plant at the Norfolk Southern railroad bridge.

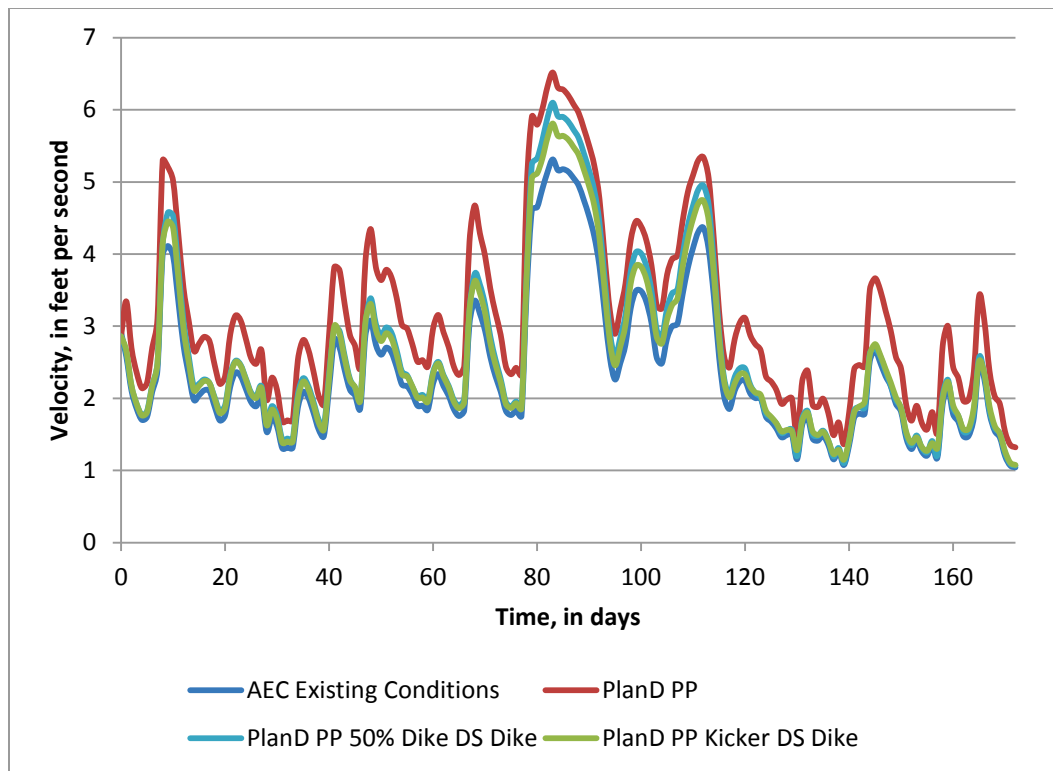


Figure 82. Velocity comparison for Plan D Power Plant, 3,000 ft upstream of the Norfolk Southern railroad bridge.

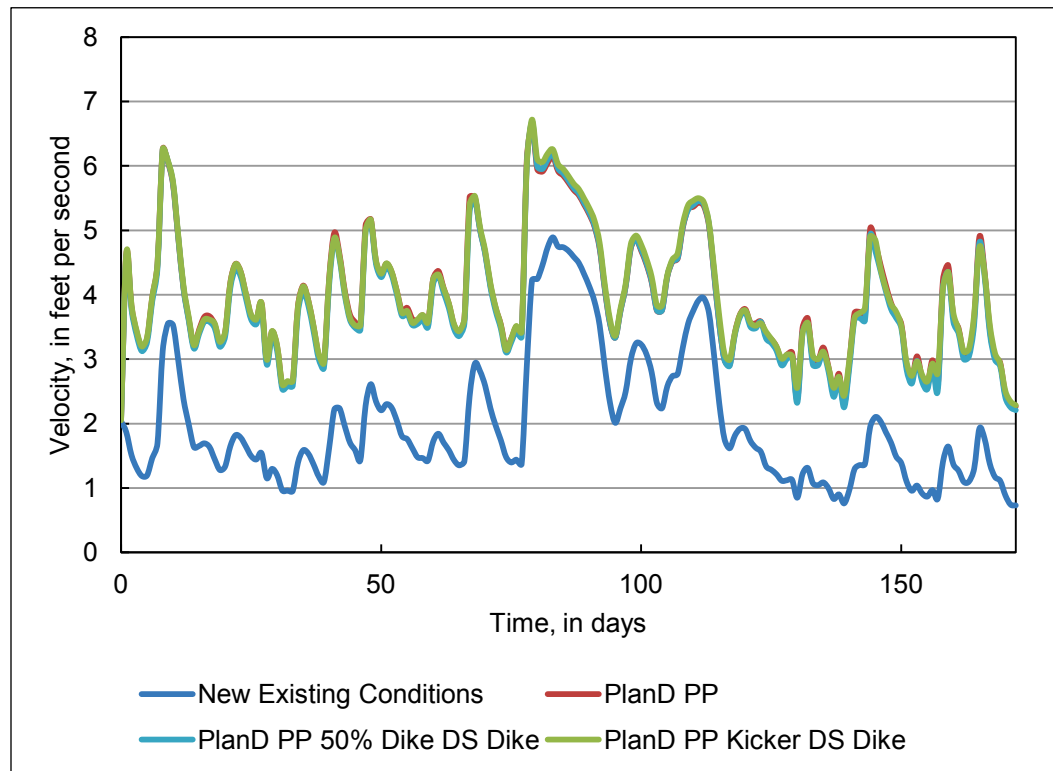


Figure 83. Plan D Power Plant minus AEC existing conditions, feet/second (red: Plan D higher; blue: Plan D lower).

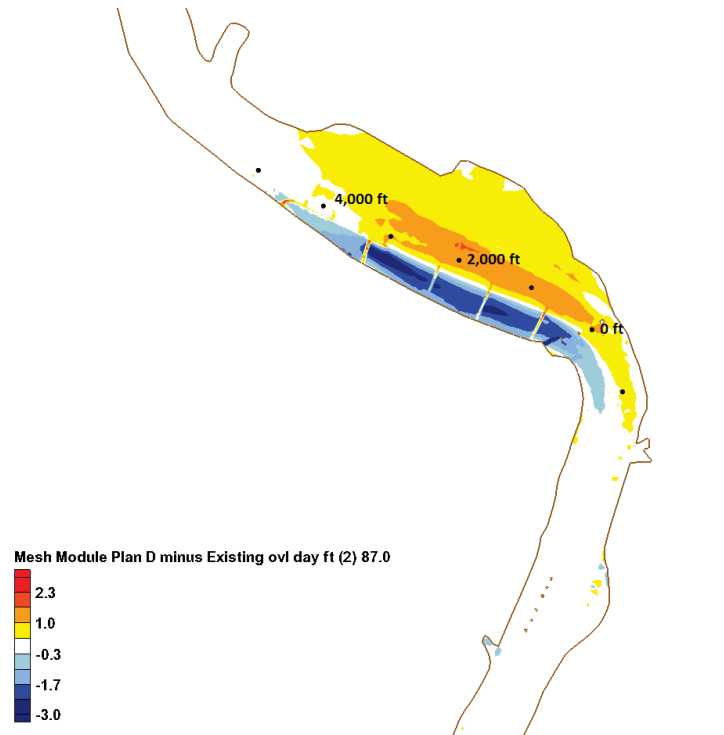


Figure 84. Plan D 50% Dike Downstream Dike Power Plant minus AEC existing conditions, feet/second (red: Plan D higher; blue: Plan D lower).

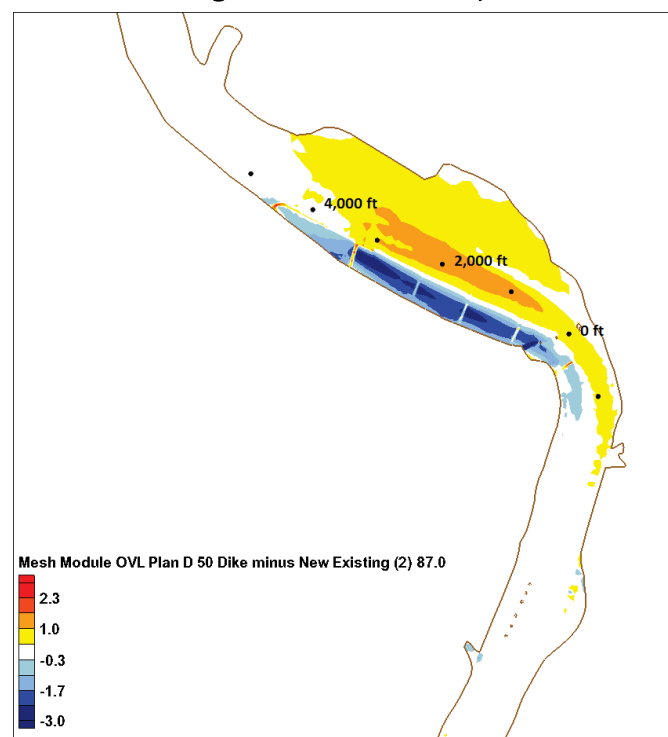


Figure 85. Plan D Kicker Downstream Dike Power Plant minus AEC existing conditions, feet/second (red: Plan D higher, blue: Plan D lower).

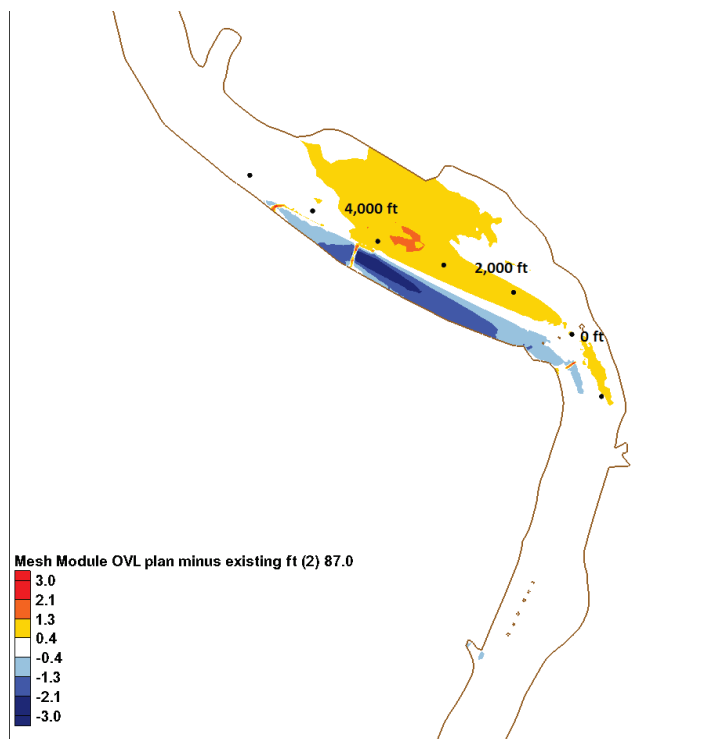


Table 10. Statistical analysis of velocity, in feet per second, for Plan D Power Plant alternatives minus AEC existing conditions.

Station, feet	Statistical measure	Plan D Power Plant	Plan D 50% Dike DS Dike Power Plant	Plan D Kicker DS Dike Power Plant
0	average	0.731	0.224	0.168
	standard deviation	0.252	0.200	0.122
	variance	0.0635	0.0400	0.0149
	maximum	1.44	0.79	0.50
	minimum	0.28	0.01	0.02
1,000	average	1.559	0.785	0.347
	standard deviation	0.414	0.337	0.306
	variance	0.1713	0.1135	0.0937
	maximum	2.92	1.84	1.28
	minimum	0.74	0.28	-0.06
2,000	average	1.657	1.303	1.132
	standard deviation	0.381	0.412	0.373
	variance	0.1452	0.1699	0.1389
	maximum	2.95	2.66	2.41
	minimum	1.01	0.45	0.36

Station, feet	Statistical measure	Plan D Power Plant	Plan D 50% Dike DS Dike Power Plant	Plan D Kicker DS Dike Power Plant
3,000	average	1.963	1.919	1.982
	standard deviation	0.480	0.452	0.445
	variance	0.2302	0.2039	0.1981
	maximum	3.20	3.12	3.13
	minimum	1.04	1.07	1.13
4,000	average	0.675	0.692	0.685
	standard deviation	0.262	0.260	0.266
	variance	0.0685	0.0678	0.0706
	maximum	1.27	1.30	1.24
	minimum	0.14	0.17	0.14
5,000	average	-0.049	-0.053	-0.038
	standard deviation	0.029	0.025	0.032
	variance	0.0008	0.0006	0.0011
	maximum	0.001	-0.008	0.085
	minimum	-0.154	-0.138	-0.122

Figure 86. Maximum bed shear for Plan D Power Plant minus AEC existing conditions, pascals (red: Plan D higher; blue: Plan D lower).

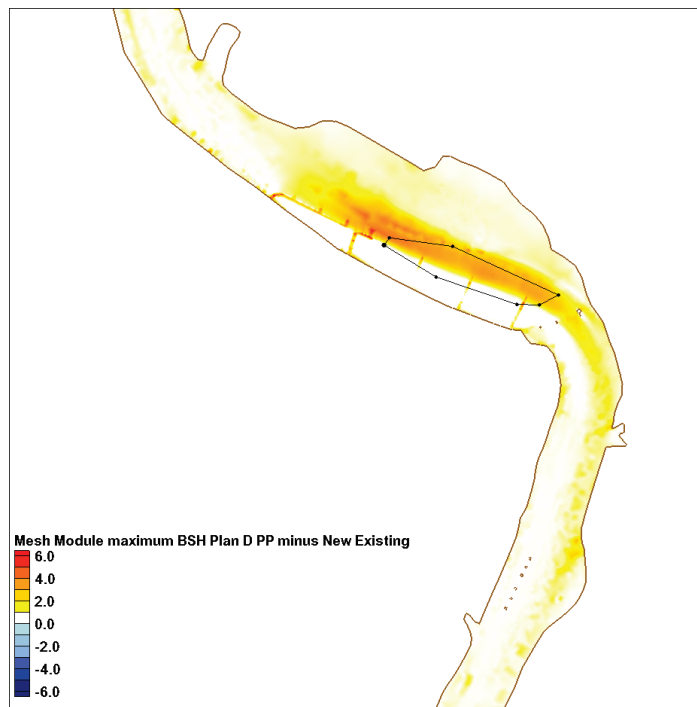


Figure 87. Maximum bed shear for Plan D 50% Dike DS Dike Power Plant minus AEC existing conditions, pascals (red: Plan D higher; blue: Plan D lower).

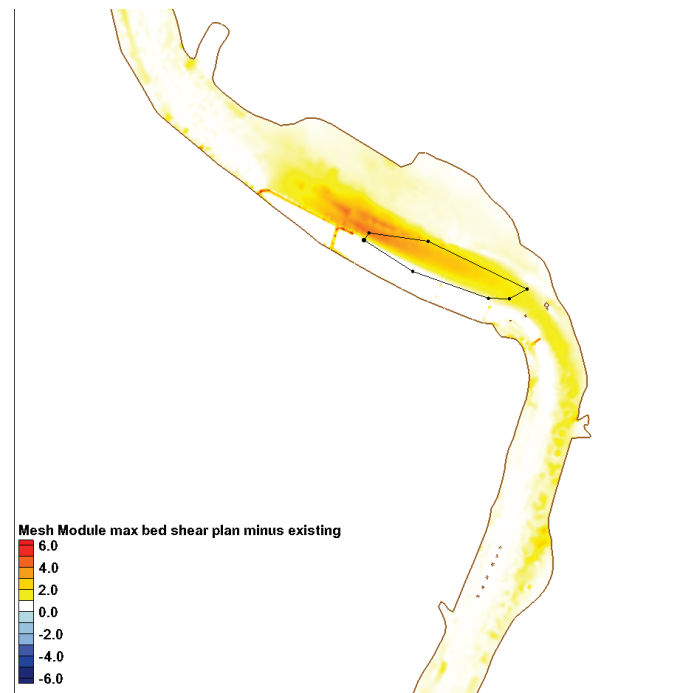
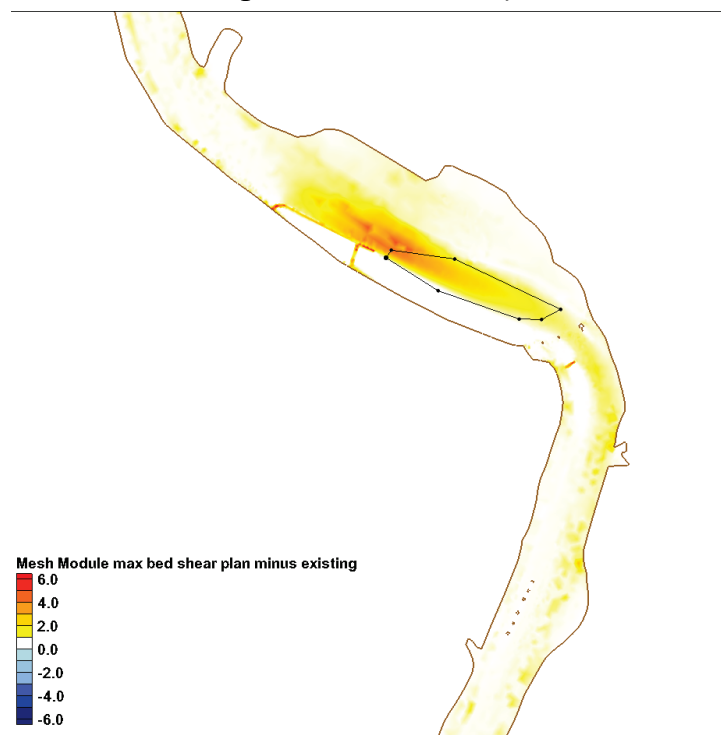


Figure 88. Maximum bed shear for Plan D Kicker DS Dike Power Plant minus AEC existing conditions, pascals (red: Plan D higher; blue: Plan D lower).



8.6 Deposition at AEC Power Plant

There was concern that deposition at Jackson Bar would be shifted downstream when the selected alternative was constructed. To evaluate this, analysis around the AEC receiving terminal was conducted. Figure 89 shows the deposition footprint used to compare impacts from the various alternatives. The depositional footprint identified in Figure 89 is the spatial location that is evaluated to calculate the amount of shoaling or erosion that may occur around the terminal. In Figure 90, a typical deposition in the footprint is shown. Table 11 presents the deposition and percent increase as related to each alternative.

Figure 89. AEC Power Plant deposition footprint (dark-blue rectangle).

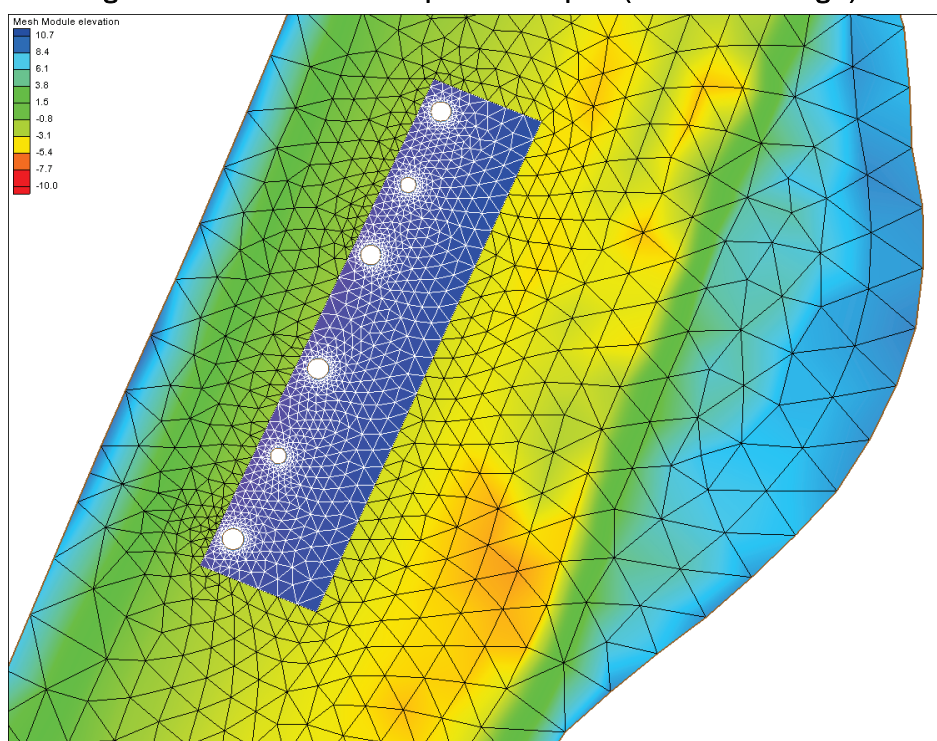


Figure 90. Typical deposition (feet) pattern around AEC terminal, Plan D Kicker DS Dike (red is deposition; blue is erosion).

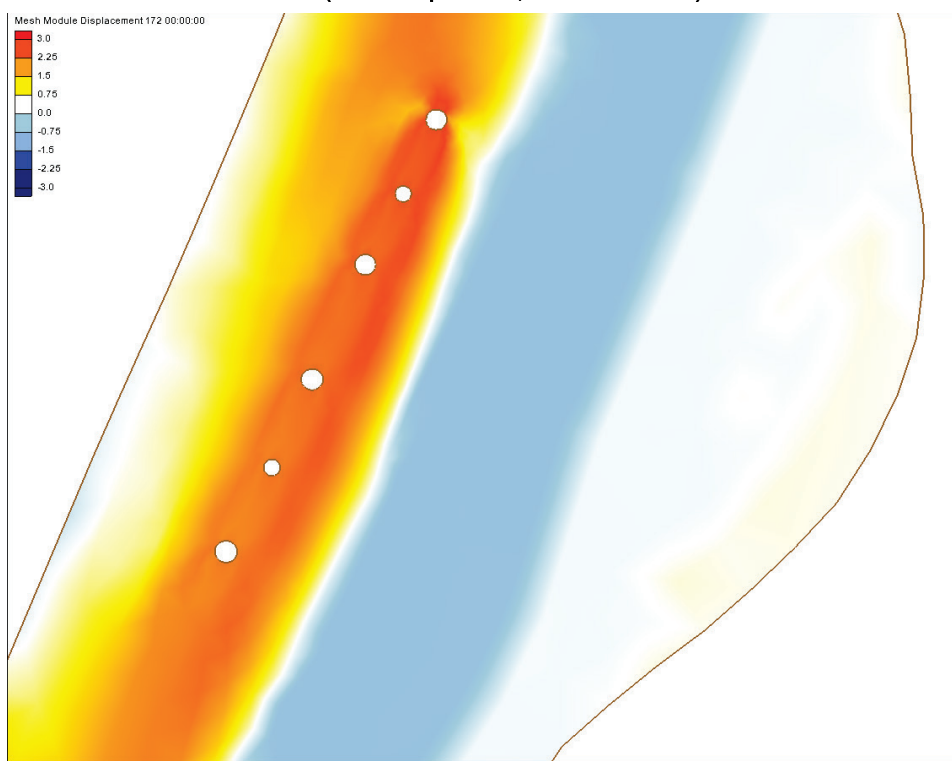


Table 11. Deposition volumes and percent increases for the deposition footprint at the AEC power plant.

Alternative	Cubic yards	Percent increase
AEC existing conditions	24,400	--
Plan D Kicker DS Dike Power Plant	26,700	9.5%
Plan D 50 % Dike DS Dike Power Plant	27,600	12.8%
Plan D Power Plant	27,700	13.4%

9 Discussion

The main criterion for evaluating the alternatives is the volume of deposition occurring in the 2004 dredge cut. The deposition in the cut is representative of the amount of dredging required to meet current navigation requirements. All alternatives were evaluated and deposition volumes are compared in Table 12. The percent reduction in dredging is shown plotted in Figure 91.

Any alternative that did not achieve an 80% reduction was not considered a plausible alternative (Figure 91). At this reduced rate, it would take multiple years for the accumulation to require dredging. However, if the alternative induces velocities too high to safely navigate, then the alternative should not be implemented. The average velocity increase should not exceed 1.5 ft/sec upstream of the Norfolk Southern railroad bridge and through the bridge pass for safe navigation. The average increase in velocities above the existing conditions models is shown in Figure 92.

Table 12. Alternative deposition in dredge cut comparison.

Alternative ('= feet)	Structure elevation, feet	Deposition, cubic yards
PlanB (-12')	-12	112,000
PlanB_4 (-9')	-9	109,000
PlanB_3 (-6')	-6	104,000
PlanB_2 (3')	3	40,900
Plan_C (3.28')	3.28	80,100
PlanC_3 (21')	21	17,200
PlanC_4 (11')	11	28,200
Plan D (11' & -9')	11	6,540
Plan D Kicker (11')	11	25,100
Plan C Kicker (11')	11	41,100
PlanD PP (11')	11	7,230
PlanD PP Kicker DS Dike (11')	11	23,200
PlanD PP 50% Dikes DS Dike (11')	11	5,410

Figure 91. Percent reduction in dredging for all alternatives.

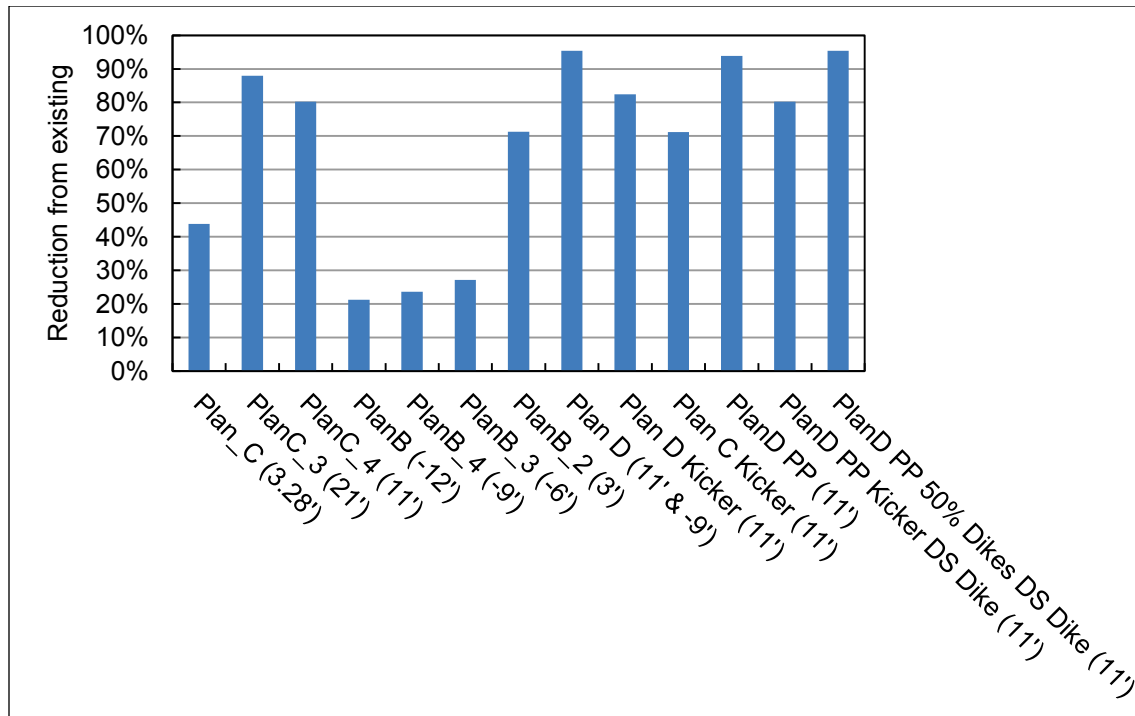
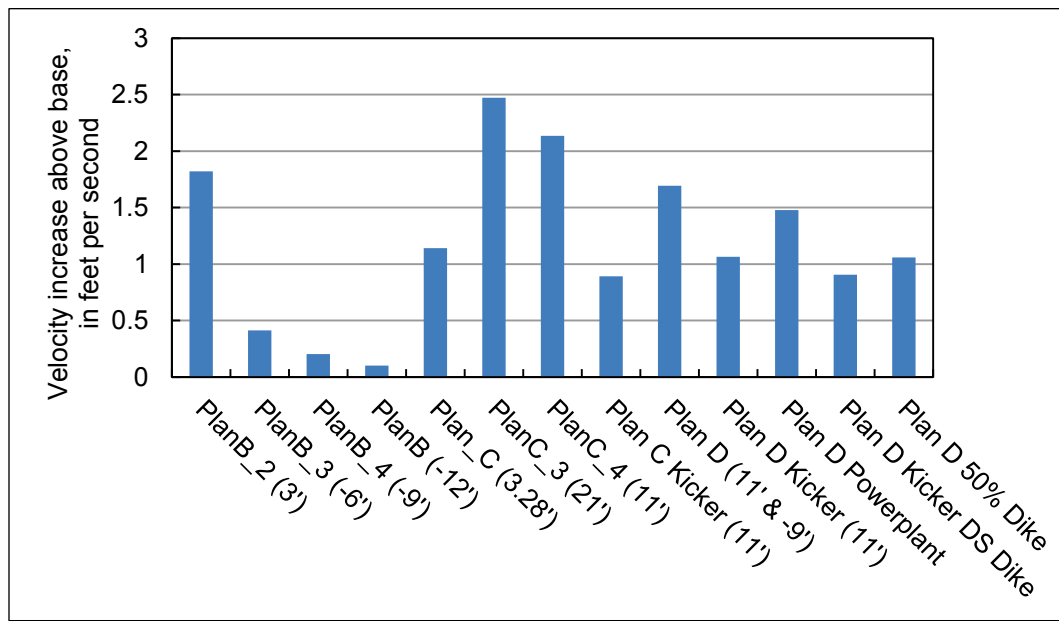


Figure 92. Average velocity increase above the existing conditions models.



9.1 Plan B

The Plan B alternatives proved to be the least successful of the alternatives (Table 12). The only Plan B alternative that significantly improved deposition conditions was the highest top elevation alternative at +3 ft. At this height, the structures are emergent and behave similar to dikes.

Navigation over the structures at a dike elevation would be unadvised, since the low-water flow is approximately 3 ft NGVD and the authorized channel depth is 9 ft.

The majority of the sediment transport occurs at the higher flows. For the Plan B alternatives, the lower flows produced the greatest amount of velocity change. This indicates that when the flow is in the channel or below bank, the structures have the greatest impact. However, the lower flow velocities are not sufficient for transport and are unable to remove accumulated sediment. Plan B alternatives did not achieve 80% removal or reduction of the accumulated sediment from the dredge cut; however, the simulations did generate a design curve for bendway weir heights. This curve provided insight for designing Plan D.

9.2 Plan C

The Plan C alternatives, unlike the Plan B alternatives, significantly reduced deposition in dredge cut. This reduction is apparent in the shoaling patterns shown in the data presented in Section 8.3 and Table 12. The main reason for this improvement was structure elevation. The training structures for Plan C are blocking more flow, forcing currents to the left bank. This mobilizes the sediment to keep it moving through the reach and also resuspend deposited bed material.

Two of the alternatives (PlanC_3 and Plan C_4) achieved similar shoaling reduction results. This provided insight into the advantages for increasing structure heights. Plan C_4 had a top elevation of 11 ft while Plan C_3 used a top elevation of 21 ft. From the analysis of these two alternatives, it is evident that the 21 ft top elevation structure provides minimum returns given the increased amount of rock required for construction. Furthermore, when the kicker alone was simulated (Plan C Kicker), a significant amount of shoaling reduction was still achieved.

Velocities were consistently greater than the existing conditions for the full range of flow. This indicates that the structures are able to shift currents to the left bank throughout the simulated hydrograph. Velocity values for Plan C_4 were significantly higher than the existing conditions model as shown in Table 8, while those of Plan C Kicker were acceptable. For both, the velocity increase was throughout the entire 5,000 ft of reach analyzed upstream of the bridge. Plan C_4 meets the 80% dredging reduction requirement but does not meet the maximum velocity requirement.

Conversely, Plan C Kicker meets the velocity requirement but not the dredging requirement.

9.3 Plan D

Plan D alternatives proved to be the most successful of the base alternatives. The main reason was the optimized structure heights and alignment. Plan D alternatives were optimized through the simulations of the previous two base alternatives. The shorter kicker in Plan D is a more efficient design for shoaling reduction than that of the Plan C kicker. The shorter kicker has less drag but blocks the same amount of flow area. It more quickly accelerates the flow, conserving the system's energy. This allows the concentration of the forcing on the left bank to be greater, mobilizing more sediment. Among the three 100% alternatives (Plan B, Plan C, Plan D) the most efficient structure is the Plan D Kicker.

Both the Plan C and D alternative were able to maintain the channel. However, the Plan D alternative performed the best. It maintained the channel and prevented significant deposition on the left bank. The transverse dikes backfilled, and the remaining material was forced downstream. Though not as efficient as Plan D, the Plan D Kicker alternative was able to remove a large amount of shoaling. The Plan D Kicker alternative did have deposition along the left bank, which was inside the dredge-cut footprint. Both alternatives achieved 80% or greater shoaling reduction.

The velocities for the Plan D alternatives peak at approximately 2,000–3,000 ft upstream of the bridge. Through the navigation pass, the increase above the existing conditions was typically less than 1 ft/sec. While from 2,000–3,000 ft upstream, maximum velocities peaked at approximately 2 ft/sec. However, the average remained within the expected maximum velocity increase for the reach. Though not as high as the Plan C velocities, the manner in which they were focused on the problem area aided in the success of the Plan D training structures. Once the thalweg was on the left side via the kicker, the transverse dikes kept it on the left bank. The increased velocities on the left side naturally remove deposited sediment in the dredge cut.

As with the velocities, the training structures focused and increased the bed shear stress along the left bank. The maximum increase in bed shear along the left bank for both alternatives is sufficient enough to move

medium gravel-size material. The average shear stresses for both alternatives can move very fine gravel. This provides shear stress much greater than that required to move medium to very fine sand that is annually dredged. If the bed shear stresses remain in this magnitude range and are consistently applied to Jackson Bar, then deposition in the reach should dramatically decrease as indicated by the simulations. The three Plan D alternatives (those without the AEC power plant) are viable options for dredge volume reduction while not overly increasing channel velocities.

9.4 Plan D AEC Power Plant variation

The Plan D AEC Power Plant alternatives performed equally as well as the Plan D alternatives. Due to the previous backwater condition generated by the mooring cells, the velocities and bed shear stresses were slightly less than those in Plan D. However, the behavior of the model did not change with the addition of the mooring cells. The alternative simulated in the power plant variation that was not in the original Plan D alternative was the dikes at 50% length. This alternative proved to be extremely successful.

The velocities for the Plan D Power Plant alternatives peak at approximately 2,000–3,000 ft upstream of the bridge. Through the bridge pass, the increase above the AEC existing conditions was typically less than 0.75 ft/sec. While from 2,000–3,000 ft upstream, maximum velocities peaked at an approximately a 2 ft/sec increase. However, the average remained 0.5 ft/sec below the maximum velocity increase threshold for the reach.

The maximum increase in bed shear along the left bank for all three alternatives is sufficient enough to move medium gravel-size material. Likewise the average shear stress for all three alternatives can move very fine gravel. This provides shear stress much greater than that required to move medium to very fine sand that is dredged annually. If the bed shear stresses remain in this magnitude range and are consistently applied to Jackson Bar, then deposition in the reach should dramatically decrease as indicated by the simulations. All three Plan D Power Plant alternatives are viable options for dredge reduction while not overly increasing channel velocities.

The Plan D AEC Power Plant alternatives showed that the basic configuration of the model was not ideal for the analysis of deposition at

the AEC power plant terminal. Fundamentally, the deposition that was shown in the AEC existing conditions model was not occurring in the field. Rather, the terminal was experiencing scour. This study suggests that scour will not be worsened by the construction of the training structures. All three models showed an increase in deposition above the AEC existing conditions model. It is expected that the scour will either be partially eliminated through increased sediment load or no appreciable change will be noticed. This is because the bed shear is great enough to move material coming from Jackson Bar.

9.5 Alternative selection

A three-fold screening approach was applied to determine the feasibility of dredge mitigation for each alternative. First, deposition in the dredge footprint was compared to the alternatives' respective existing conditions plan to obtain the dredge volume reduction. Second, from a navigation standpoint, the increases in velocity due to the alternatives were compared. Third, the structure volume required to construct the training structures was compared as a proxy for a cost analysis. From these three points of comparison, a final determination for the recommended alternative was made.

9.5.1 Dredging

All material deposited in the dredge template was assumed to be the same material removed during dredging. Ultimately the dredge material reported is that volume above the original start depth/volume from the start of the run. The start depth was based on the November 2003 survey conducted after the prior dredging event. From this invert elevation, the same calculated volume from the respective existing conditions was measured, and a percent reduction in shoaling/dredging from existing was estimated. This provided a base of comparison for all alternatives (Figure 91). All Plan D and Plan D Power Plant alternatives meet the requirement for dredge volume reduction.

9.5.2 Velocity

The average velocity above the existing conditions upstream of the Norfolk Southern railroad bridge was calculated for all alternatives (Figure 92). The Plan D and Plan D Power Plant were not below the 1.5 ft/sec velocity increase threshold requirement. Thus, the remaining alternatives were then

evaluated with both velocity increase and the dredge reduction. From this filtering, Plan D 50% Dikes is the most beneficial. The Plan D 50% Dikes average impact is only 1 ft/sec above the AEC existing conditions. The velocities for this alternative are only slightly faster than the Plan D Kicker velocities but have a significant increase on dredge volume reduction.

9.5.3 Volume of rock for each plan

As a final comparison check, and one that would provide insight into construction cost, the structure volumes were estimated from their respective meshes. While not an exact measurement, the information provides a base of comparison (Table 13). From this comparison the Plan D 50% dike provided the best impact while requiring a limited structure volume.

Table 13. Training structure volumes of rock.

Plan & structure elevation	Total Structure Volume (cubic yards)	Estimated Tons (1.5 tons/yd)
Plan B (-12 feet)	46,219	69,328
Plan B_4 (-9 feet)	61,888	92,832
Plan B_3 (-6 feet)	78,833	118,250
Plan B_2 (3 feet)	132,536	198,804
Plan C (3 feet)	121,670	182,504
Plan C_4 (11 feet)	169,170	253,755
Plan C_3 (21 feet)	225,243	337,865
Plan C_Kicker	86,187	129,281
Plan D (11 feet & -9 feet)	98,131	147,196
Plan D_Kicker	25,126	37,690
Plan D Power Plant (11 feet & -9 feet)	98,131	147,197
Plan D Kicker DS Dike (11 feet & 3 feet)	29,126	43,689
Plan D 50% Dike (11 feet & 3 feet)	61,628	92,442

10 Recommendations

10.1 Recommended alternative implementation

The recommended plan is Plan D with the 50%-length transverse dikes. Plan details are provided in the Appendix. For initial implementation of the alternative, construction should be limited to the kicker portion of the Plan D. The Plan D Kicker will provide the most initial benefit. In addition to the kicker, the adjacent pilot channel must be cut through the in-channel disposal to provide the authorized navigation channel clearances. The kicker should be constructed with the appropriate size rip-rap and backfill material. The structure needs a bulkhead to extend upstream and downstream, ensuring bank stability. A bulkhead is tied into bank protection typically constructed with rip-rap, which prevents bank scour. The bulkhead should extend the entire length of the kicker and be sized with the appropriate rip-rap to ensure bank stability. The upstream extended length of the bulkhead should be no less than 20 ft. The downstream extended length should be no less than 40 ft. The kicker's toe, tie back dike, and bulkhead ends must be keyed sufficiently into the bank to minimize the likelihood of structure failure. Once complete, the area behind the kicker should be used as dredge disposal. The back filling of the kicker will provide stability and a new disposal area.

Once the kicker is in place, the site should be monitored to determine the need for the additional transverse dikes. If the dikes are required, then they should be constructed in a multistaged approach (preferably three stages). It is recommended building each stage an equal dike length. Between the stages, time should be given to evaluate the effectiveness of the dikes at their current lengths before lengthening.

10.2 Future analysis

Implementation of the recommended alternatives requires careful consideration. All possible impacts, not just deposition, bed shear, and velocity changes to the reach, should be considered. This includes but is not limited to environmental or water quality issues and flood-extent changes. Furthermore, the navigation industry should evaluate the selected alternative. The selected alternative should be evaluated in a navigation study to determine navigability of the pass. Also, it may be

beneficial to determine the sediment load potential coming from the storm water ditch.

10.3 Monitoring

Prior to construction, an adaptive monitoring program should be established. Once constructed, the alternative must be monitored on a regular basis. These data could be applied for additional model validation to increase model reliability for future efforts. Proper implementation, monitoring, and further analyses will help secure the success of the implemented alternative.

Upon completion of construction, it is recommended that the kicker be inspected after flow events. The inspection frequency is simply defined by flow rather than time. For lower flows, a visual recognition might only be required, but for higher flows, bathymetric data of the structures and bed might be taken to ensure structure stability. Some consideration should be given to a range of high flood potential flows, but 100,000 ft³/sec is recommended as an initial starting point. Continued inspection is imperative for the success of the project.

In addition to inspection after flood flows, a temporal inspection program should be considered. This will provide the changes that occur to the structures, accumulated over multiple flow magnitudes. Inspection should, at a minimum, include velocity measurements along with detailed surveys of shoaling through the entire navigation pass. The inspection would help to determine if the additional portion of the alternatives are necessary. If the kicker is not sufficiently clearing the pass, then it is recommended to construct the transverse dikes.

10.4 Concerns

The first concern is the ability of the Plan D, kicker-only alternative to maintain the channel at the appropriate clearances. As mentioned, if it does not maintain the channel, then the dikes should be constructed. Second, the left bank will be under pressure from the redirection of the thalweg by the structures. This could induce shear stresses on the left bank that cause bank erosion. If bank erosion is induced, then the left bank must be armored. Bank erosion on the left bank will be one of the indicators of success for the alternative. Third, the storm water ditch was not evaluated in this effort. At this time it is unclear the amount and armoring potential of the material coming from this source. The source could affect the success of the alternative.

References

American Society of Civil Engineers. 1998. Inland navigation: Locks, dams, and channels. Ed. B. L. McCartney. *ASCE Manuals and Reports on Engineering Practice No. 94*. Reston, VA: American Society of Civil Engineers.

Berger, R. C., J. N. Tate, G. L. Brown, and G. Savant. 2010. *Adaptive hydraulics user manual, a two-dimensional modeling system developed by the Coastal and Hydraulics Laboratory*. Vicksburg, MS: U.S. Army Engineering Research and Development Center.

Derrik, D. L, T. J. Pokrefke, Jr., M. B. Boyd, J. P. Crutchfield, R. R. Henderson. 1994. *Design and development of bendway weirs for the Dogtooth Bend Reach, Mississippi River*. TR HL-94-10. Vicksburg, MS: U.S. Army Corps of Engineers, Waterways Experiment Station.

Franco, J. J. 1978. *Guidelines for the design, adjustment and operation of model for the study of river sedimentation problems*. Instruction Report H-78-1. Vicksburg, MS: U.S. Army Corps of Engineers Waterways Experiment Station.

Julien, P. Y. 2002. *River mechanics*. Cambridge, UK: Cambridge University Press.

Martin, S. K., G. Savant, and D. C. McVan. 2011. Two-dimensional numerical model of the Gulf Intracoastal Waterway near New Orleans: Case study. *Journal of Waterway, Port, Coastal, and Ocean Engineering, ASCE* 138(3): 236-245
Doi:10.1061/(ASCE)WW.1943-5460.0000119.

Parchure, T. M. 2005. *Structural methods to reduce navigation channel shoaling*. ERDC/CHL TR-05-13. Vicksburg, MS: U.S. Army Engineering Research and Development Center.

Stockstill, R. L., and J. M. Vaughan. 2009. *Numerical model study of the Tuscarawas River below Dover Dam, Ohio*. ERDC/CHL TR-09-17. Vicksburg, MS: U.S. Army Engineering Research and Development Center.

Stockstill, R. L., J. M. Vaughan, and S. K. Martin. 2010. *Numerical model of the Hoosic River Flood-Control Channel, Adams, MA*. ERDC/CHL TR-10-01. Vicksburg, MS: U.S. Army Engineering Research and Development Center.

Tate, J. N., T. C. Lackey, and T. O. McAlpin. 2010. *Seabrook fish larval transport study*. ERDC/CHL TR-10-12. Vicksburg, MS: U.S. Army Engineering Research and Development Center.

Thomas, W. A., D. M. Gee, and R. C. MacArthur. 1981. *Guidelines for the calibration and application of computer program HEC-6*. Davis, CA: U.S. Army Corps of Engineers, Hydrologic Engineering Center.

U.S. Army Corps of Engineers (USACE), Mobile District (SAM). 1988. Jackson Bar Supplement to the General Design Memorandum, Improvement of Navigation on the Lower Black Warrior-Tombigbee Waterway.

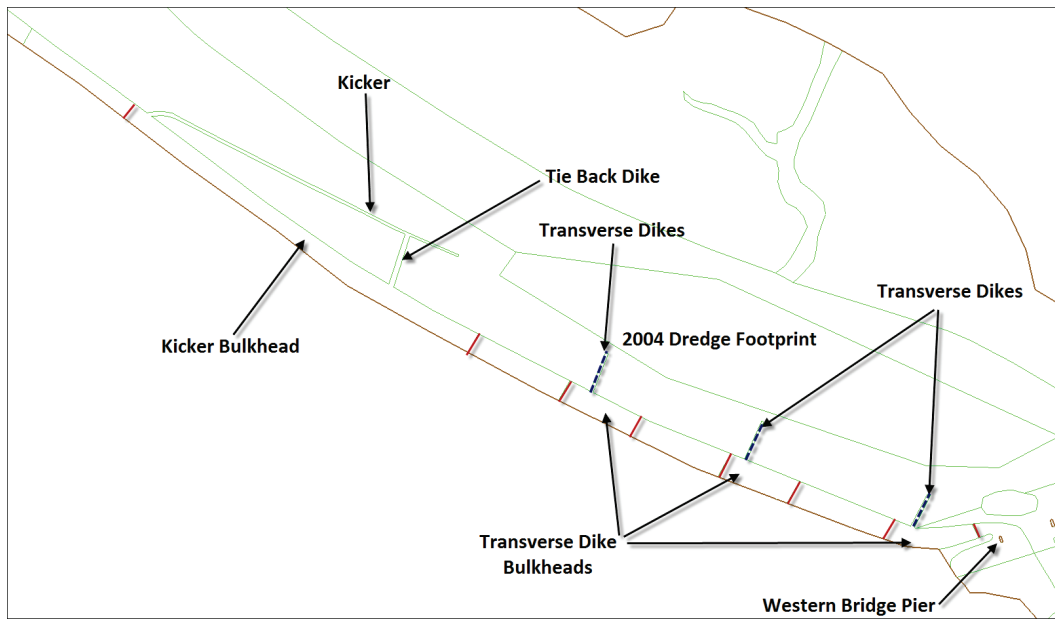
USACE. 1991. *HEC-2 user manual*. Davis, CA: U.S. Army Corps of Engineers, Hydrologic Engineering Center.

USACE. 1995. *A comparison of the one-dimensional bridge hydraulic routines from: HEC-RAS, HEC-2, and WSPRO*. Davis, CA: U.S. Army Corps of Engineers, Hydrologic Engineering Center.

Wang, S. S. Y., Y. Jia, P. J. Roche, P. E. Smith, and R. A. Schmalz. 2008. *Verification and validation of 3d free-surface flow models*. Reston, VA: American Society of Civil Engineers.

Appendix

Figure 93. Final recommended alternative, Plan D with the 50%-length transverse dikes.



1. Transverse Dikes

- 175 ft long
- 10 ft top width
- 1:2 side slopes
- Spaced 800 ft apart
- First dike upstream of bridge starts 350 ft upstream
- Finish elevation is 11 ft NGVD

2. Kicker

- Starts 2700 ft upstream of bridge
- 1500 ft long
- Tie back dike 1000 ft upstream of last most upstream dike
- Top with 10 ft
- Finish elevation 11 ft NGVD
- Tip of kicker is 350 ft off right bank
- Pilot channel adjacent to kicker

REPORT DOCUMENTATION PAGE

Form Approved
OMB No. 0704-0188

The public reporting burden for this collection of information is estimated to average 1 hour per response, including the time for reviewing instructions, searching existing data sources, gathering and maintaining the data needed, and completing and reviewing the collection of information. Send comments regarding this burden estimate or any other aspect of this collection of information, including suggestions for reducing the burden, to Department of Defense, Washington Headquarters Services, Directorate for Information Operations and Reports (0704-0188), 1215 Jefferson Davis Highway, Suite 1204, Arlington, VA 22202-4302. Respondents should be aware that notwithstanding any other provision of law, no person shall be subject to any penalty for failing to comply with a collection of information if it does not display a currently valid OMB control number.
PLEASE DO NOT RETURN YOUR FORM TO THE ABOVE ADDRESS.

1. REPORT DATE May 2015	2. REPORT TYPE Technical Report	3. DATES COVERED (From - To)			
4. TITLE AND SUBTITLE Jackson Bar Training Structure Study		5a. CONTRACT NUMBER			
		5b. GRANT NUMBER			
		5c. PROGRAM ELEMENT NUMBER			
6. AUTHOR(S) Jeremy A. Sharp, and Steve H. Scott		5d. PROJECT NUMBER			
		5e. TASK NUMBER			
		5f. WORK UNIT NUMBER			
7. PERFORMING ORGANIZATION NAME(S) AND ADDRESS(ES) Coastal and Hydraulics Laboratory U.S. Army Engineer Research and Development Center 3909 Halls Ferry Road Vicksburg, MS 39180-6199		8. PERFORMING ORGANIZATION REPORT NUMBER ERDC/CHL TR-15-4			
9. SPONSORING/MONITORING AGENCY NAME(S) AND ADDRESS(ES) U.S. Army Engineer District, Mobile 109 St. Joseph Street Mobile, AL 36602		10. SPONSOR/MONITOR'S ACRONYM(S) CESAM-EN-HH			
		11. SPONSOR/MONITOR'S REPORT NUMBER(S)			
12. DISTRIBUTION/AVAILABILITY STATEMENT Approved for public release; distribution is unlimited.					
13. SUPPLEMENTARY NOTES					
14. ABSTRACT Three proposed alternatives intended to reduce shoaling at Jackson Bar, Alabama were investigated. A two-dimensional (2-D) hydrodynamic and sediment model was used to simulate hydraulic conditions at Jackson Bar, located on the Black Warrior-Tombigbee Waterway (BWT) in the vicinity of Jackson, Alabama. Jackson Bar, a sand bar, is located on the left descending bank upstream of a railroad bridge. Located in a bend in the BWT at Jackson, AL the railroad bridge presents a navigation hazard. Annual dredging provides the clearance necessary for tows to properly align with the bridge pass. The hydrodynamic model was validated with gage data from the USGS 02470050 Tombigbee River at Steamplant near Leroy, AL gage (Leroy gage), a previously-constructed HEC-2 model, and a previously-constructed WES physical model from 1987. Three alternatives were modeled in an attempt to reduce shoaling / eliminate dredging at Jackson Bar by using one or more river training structures (bendway weirs, dikes, kickers). A three-fold screening approach was applied to determine the feasibility of each alternative. The selected alternative was a variation of Plan D that used a kicker and transverse dikes.					
15. SUBJECT TERMS Bendway wiers, Black Warrior-Tombigbee Waterway, Dikes, Numerical modeling, River, Sediment, Training works					
16. SECURITY CLASSIFICATION OF:		17. LIMITATION OF ABSTRACT	18. NUMBER OF PAGES	19a. NAME OF RESPONSIBLE PERSON	
a. REPORT U	b. ABSTRACT U	c. THIS PAGE U	UU	102	Jeremy A. Sharp
					19b. TELEPHONE NUMBER (Include area code) 601-634-4212